NITROGEN MANAGEMENT IN MAIZE-BASED SYSTEMS OF THE TANZANIAN HIGHLANDS: BALANCING FOOD AND ENVIRONMENTAL OBJECTIVES

JINSEN ZHENG

2019

A Dissertation Submitted to the Division of

Environmental Science and Technology

Graduate School of Agriculture

Kyoto University

in Partial Fulfillment of the Requirements

For the Degree of

Doctor of Philosophy

ABSTRACT

A dramatic increase in nitrogen (N) fertilizer use will accompany the agricultural intensification in Sub-Saharan Africa (SSA) to feed the growing population, yet the fate of added N is poorly understood in this region. In this dissertation, I evaluated the effects of N management practices on the N partitioning within the soil-crop system and accordingly the crop yield response, as well as on the N losses through different pathways from the maize systems of the Tanzanian highlands. Two sites (TZi, sandy Alfisols; and TZm, clayey Andosols) were included to represent the diversity in soil type. The ultimate objective was to develop appropriate N management practices that can enhance maize yield in the Tanzanian highlands while minimizing potentially adverse impacts on the environment.

First, I investigated the fluctuation of soil inorganic N and its availability to maize under different N rates (0–150 kg N ha^{-1}). Results showed that in the early season, soil mineralized N was exposed to the leaching risk due to limited crop N demand. Also, applied-N depleted fast at TZi, particularly at higher N rate, but a large fraction (~80%) was retained available to crop at TZm. Such effect of soil type largely contributed to the higher yield at TZm (up to 4.4 Mg ha^{-1}) than at TZi (up to 2.6 Mg ha^{-1}) under the same N rate. The best-fitted linear-plateau model indicated that the soil inorganic N availability (0–0.3 m) at the tasseling stage (i.e., 68–71 days after planting) significantly accounted for the final yield. Further, yield at TZi was still limited by N availability at the tasseling stage due to fast depletion of applied-N, whereas it no longer limited the yield at TZm once above 67 kg N ha^{-1}.

Next, I examined the pathway of N loss through ammonia (NH_3) volatilization with six urea-N rates (0–150 kg N ha^{-1}) and the mitigation treatments of immediate irrigation and urea deep placement. Much higher NH_3-N loss from applied N (36%–52%) was found at TZi compared to TZm (5%–22%). Sigmoid models best described the response pattern of proportional N loss to increasing N rates at both sites, and showed that simple surface urea application is not recommended at TZi, whereas TZm is inherently capable of buffering NH_3-N loss for a single application of up to 60 kg N ha^{-1}. The susceptibility of TZi soil to NH_3 loss mainly resulted from its low capacities of pH buffering and cation exchange, and high urease activity. Both mitigation treatments were effective. The inhibited rise of soil pH but not NH_4^+ concentration mainly explained the mitigated NH_3 loss, though nitrification in the irrigation treatment might also have contributed.

Then, I quantified the nitrate (NO_3^-) leaching from the critical root zone (0–0.3 m) of maize in response to increasing N rates and maize straw incorporation. The soil rewetting process, particularly at the onset of the rainy season and following N applications, was an important driver of NO_3^- loss. Nitrate loss increased exponentially with N rates, and varied inter-annually. Relating cumulative NO_3^- loss to maize yield under increasing N rates revealed a tipping point—occurrence depending on season—above which yield increment was accompanied by substantial NO_3^- loss. Straw incorporation induced net N immobilization in the early growing season, and reduced NO_3^- losses by 3.3–6.3 kg N ha^{-1}, yet no effect was observed on the cumulative NO_3^- losses or maize yields. The NO_3^- loss

reductions (equivalent to 1.2–2.7 kg N Mg^{-1} added C) were far below the net N immobilization potential of the straw decomposition (18.0–38.1 kg N Mg^{-1} added C), which was likely due to the large pieces of straw (~0.15 m) used in the field, which could have induced N limitation and biomass-N recycling in the decomposition microsites.

Further, I conducted year-round measurements to quantify the effects of fertilizer-N and straw management on the soil emissions of nitrous oxide (N_2O). Rainfall and the resulting soil moisture, rather than soil temperature, were important environmental drivers of N_2O emissions in this study. Applied-N stimulated N_2O fluxes across soil types but with different magnitudes—lower at TZi due to the dominance of nitrification in N_2O production, as compared to higher at TZm likely from promoted denitrification when WFPS was > 47%. N_2O emission increased either exponentially or linearly with N rate, depending on the year. Fractions of fertilizer-N lost as N_2O were well below the 1% emission factor of the IPCC Tier 1 method, ranging from 0.13 to 0.26% at TZi and from 0.24 to 0.42% at TZm, for the rate of 50–150 kg N ha^{-1} across years. Compared to N application alone, straw plus N did not alter maize yield, but did significantly raise N_2O emissions with a synergistic effect. Consequently, straw incorporation markedly increased the emission factor (up to 0.46% at TZi and 1.29% at TZm) as well as yield-scaled N_2O emission.

This dissertation provides some of the first in situ evaluations, including the NH_3, NO_3^-, and N_2O losses in response to N practices, and the applicability of straw to mitigate NO_3^- loss in two maize systems of the Tanzanian highlands. These results are valuable for designing the N strategies targeting higher yields with lower environmental costs for the cropland intensification across SSA.

ACKNOWLEDGEMENTS

My supervisor, Prof. Dr. Shinya Funakawa, has been the single most influential figure in my postgraduate study. He has provided continual guidance, encouragements, and the freedom to pursue my own research interests, as well as the sufficient research budget to carry them out. He also offered a position of research fellow at Kyoto University after ending my Doctoral Course, which allows me to fully concentrate on my dissertation preparation without any financial concern. This work can never be done without his kind support and patient supervision.

I would like to thank MEXT for accepting me as a Japanese Government Scholar (April 2013–March 2015) and the GSS program at Kyoto University—Programs for Leading Graduate Schools (MEXT), for the generous financial support as well as the research grant, which makes the five-year research and life here much easier and more enjoyable.

I would like to express my gratitude to Dr. Hitoshi Shinjo, associate professor of Kyoto University, and Dr. Tetsuhiro Watanabe, assistant professor of Kyoto University, for their valuable advice and conservations about research and academic life.

I am extremely grateful to the coordinators of my research in Tanzania: Dr. Method M. Kilasara, associate professor of Sokoine University of Agriculture; Mr. William N. Mmari, researcher at Uyole Agriculture Research Institute-Mbeya; Mr. Mwamkinga, director of the Mbeya Agricultural Training Institute; Mr. Boniface, village manager of Mangalali, and many other colleagues from the above-mentioned institutes/places, for their kind supports during my field trips and experiments. I also extend my appreciation to my field assistants: Mr. Jackson and Mr. Pascal for managing the sites in Mangalali village, and Messrs. William L. Msheri, Magnus Samson, Yona, Emma, and many other students from the training institute for managing the other sites at Uyole.

I am grateful to Drs. Soh Sugihara, Kazumichi Fujii, Yasumi Yagasaki, Ryosuke Kubo, Kaori Ando, Makoto Shibata, Tomohiro Nishigaki, Gedeon Csongor, Nguyen H. Lam, Vu T. Minh, and Setiari Marwanto; Mses. Haruyo Hoshino, Reiko Okuda, Kayo Matsui, Yuko Ogawa, Yuri Ichinose, Qian Ma, Xi Li, Yufang Chen; Messrs. Yutaro Tomita, Akihiro Aiba, Han Lyu, Shinichi Watanabe, Christopher MacCarthy; and many other previous and current members of Lab. of Soil Science and Terrestrial Ecosystem Management at Kyoto University; for establishing and maintaining the wonderful academic research environment. Special thanks should be expressed to Dr. Tomohiro Nishigaki, currently a researcher at Japan International Research Center for Agricultural Sciences, for his kind support during the initiation of my research. Special thanks are also given to Dr. Soh Sugihara, currently an associate professor at Tokyo University of Agriculture and Technology, for his encouragements and kind supports in revising some of my manuscripts and application documents. I am also happy and grateful to join the "basement team": Prof. Dr. Shigeru Araki, Messrs. Athuman J. Mahinda, Ajay K. Mishra, and Le D. Huy; I had one of my most productive periods for my dissertation.

Finally, my hearty thanks are due to my dear family: the greatest parents in the world, Xiaozhou Zheng and Chunjin Li; my lovely wife, Ying Qu; my dear brother and sister-in-law, Jinbing Zheng and Wen Wu; my cute nephew and niece, Muxuan Zheng and Qianyu Zheng for their never-ending care, and confidence, believing in me.

Jinsen Zheng
September 2018
Kyoto University

TABLE OF CONTENTS

LIST OF FIGURES

LIST OF TABLES

CHAPTER 1
Introduction

1.1 Food sufficiency and agricultural intensification in Sub-Saharan Africa

Sub-Saharan Africa (SSA) faces a vexing problem of feeding itself (van Ittersum et al. 2016). Since the 1960s, SSA failed to benefit from the improved crop varieties during the Green Revolution; the average cereal productivity in the region was stagnantly low as less than 1 Mg ha^{-1} (Hazell and Wood 2008). The same period (1961–2005), however, saw cereal yields rise to 3 Mg ha^{-1} in Latin America, South Asia, and Southeast Asia, 5 Mg ha^{-1} in China, and 10 Mg ha^{-1} in Europe, North America, and Japan (Sanchez 2015). By 2050, the population growth on the African continent is projected to increase approximately 2.5-fold, being the dominant contribution to the world population growth (United Nations 2017). In addition, the current level of cereal self-sufficiency is as low as approximately 80% (van Ittersum et al. 2016), meaning that 20% of the cereal consumption in this region depends on importation. The lowest crop productivity coupled with the fastest population growth will drive a substantial pressure on food security in this region.

Agricultural intensification in SSA is both desirable and inevitable (Palm et al. 2017; Sanchez 2015; Vanlauwe et al. 2014a). Increased food supply for feeding the growing population in this sub-continent has primarily depended on agricultural extensification—the expansion of cropland (Cassman et al. 2003) by clearing natural vegetation such as forest, savanna, and woodlands (Brink and Eva 2009; Gibbs et al. 2010). Agricultural intensification, improving productivity on the existing croplands, has the potential to save natural ecosystems from being converted to agriculture (Stevenson et al. 2013). Also, the improved cropland productivity is increasingly recognized as the entry point to break the vicious cycle underlying rural poverty (Vanlauwe et al. 2011; Bationo et al. 2007). Continued expansion of cropland should remain as the last choice to secure food production if we are going to conserve biodiversity and ecosystem services (e.g., carbon storage) for future generations (Chaplin-Kramer et al. 2015; Kehoe et al. 2017).

1.2 Nitrogen, its fate in cropping systems of SSA, and the potential environmental implications

A dramatic increase in fertilizer use, particularly nitrogen (N), will accompany the agricultural intensification in SSA. Nitrogen is an essential nutrient for plant growth and primary production. The depletion of soil N in SSA croplands (Sanchez 2002), due to continuous cropping without proper nutrient replenishment (Vitousek et al. 2009), has been one of the major biophysical constraints on crop yield (Mueller et al. 2012; Vanlauwe et al. 2014b). Use of fertilizer-N in this region is extremely limited, typically less than 10 kg N ha^{-1}(Vitousek et al. 2009), which also explained why the improved crop varieties failed to bring higher cereal yields to SSA farmers. Recognizing this, national government agencies and international organizations are making efforts to increase fertilizer use at least 6-fold to reach an average of 50 kg fertilizer nutrient ha^{-1} yr^{-1} (AGRA 2009; Mungai et al. 2016; Sanchez et al. 2009). Considering the low N input in current African cropland, Hickman et al. (2015) pointed out that at least 6 Tg N yr^{-1} will be needed just to reach an average application rate of 75 kg N ha^{-1} yr^{-1} for cereal production on existing agricultural land. If not carefully managed, this unprecedented amount of N input could be subject to substantial loss, which could have devastating consequences for ecosystems downstream (Galloway et al. 2003).

Unfortunately, the fate of added N is poorly understood in SSA cropping systems. Added N mostly ends up with a limited proportion in crop uptake and finally the protein in human diet (Ladha et al. 2005), particularly when the amount is in excess of crop demand; a better understanding of the response of crop yield to increasing N rate is therefore essential to define suitable N strategies for SSA croplands. The major pathways of N loss from cropping systems include volatilization of ammonia (NH_3), leaching, and denitrification to N_2 (Fig. 1.1; Robertson and Vitousek 2009), though water erosion may also have a contribution in hilly areas (Barrows and Kilmer 1963).

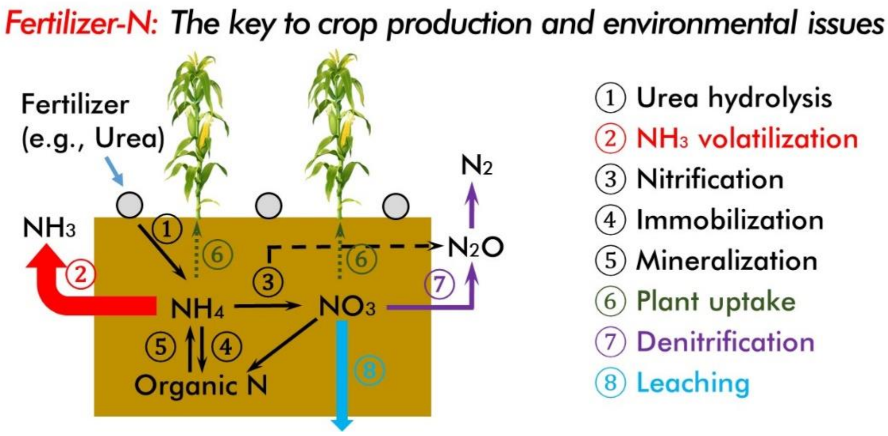

Fig. 1.1 A simplified depiction on the pathways of fertilizer-N cycling in the cropping systems; Urea is used as the example of fertilizer-N source.

Ammonia volatilization occurs at high soil pH when ammonium (NH_4^+) is present. It may account for substantial N loss of applied fertilizer-N (e.g., up to >50%) in the cropping systems (Sommer et al. 2004), particularly when urea is used as the fertilizer-N source. Release of NH_3 affects air quality (e.g., forming fine particulate matter, $PM_{2.5}$) and impacts human health (Lelieveld et al. 2015); it also contributes to N deposition, leading to soil acidification (Tian and Niu 2015), eutrophication (Bergstrom and Jansson 2006), and loss of biodiversity (Bobbink et al. 2010). Surprisingly, to date, no field measurements have been conducted in SSA croplands to examine the response pattern of NH_3 loss to increasing N rate, despite that urea heavily dominates N fertilizer consumption in this region (over 50%; IFA 2017).

Leaching is the downward movement of dissolved N in the soil profile with percolating water, which accounts for another major proportion of N loss from most upland cropping systems (Lehmann and Schroth 2003). Nitrate (NO_3^-) is generally the predominant form of leachate N in the cropping systems (van Kessel et al. 2009; Svoboda et al. 2013). Nitrate discharged to the downstream ecosystems can lead to freshwater eutrophication (Smith et al. 1999) and coastal marine ecosystem damage (Diaz and Rosenberg 2008; Howarth and Marino 2006). High-NO_3^- in the drinking water is also a health threat to children and pregnant women (Gatseva and Argirova 2008). This problem could be particularly acute in developing regions like SSA, where drinking water is generally obtained from shallow wells or streams. However, the global trends in NO_3^- research from 1960 to 2017 showed that SSA has been largely overlooked (Padilla et al. 2018). Further, the seasonal rainfall in tropics of SSA is generally characterized with uneven distribution and high rainfall intensity, which may induce higher NO_3^- leaching loss from both soil and applied fertilizer.

Denitrification is the major biological process that returns soil N to the atmospheric N_2 (Philippot et al. 2007), an environmentally benign gas. Except in flooded soils, N loss through denitrification appears to be smaller than other pathways (e.g., leaching; Robertson and Vitousek 2009). However, during the stepwise reduction to N_2, a fraction of reactive N, though generally small, can be emitted as nitrous oxide (N_2O) (Braker and Conrad 2011; Philippot et al. 2007)—a powerful greenhouse gas and the dominant ozone-depleting substance (Forster et al. 2007; Ravishankara et al. 2009). There are some other microbiological processes that can also produce N_2O (e.g., nitrification; Braker and Conrad 2011). Nonetheless, N substrate availability (e.g., NH_4^+, nitrogen oxides etc.) is a critical driving factor (Firestone and Davidson 1989), which inevitably increases after fertilizer-N addition. Unfortunately, there is a dearth of knowledge on soil emissions of N_2O from SSA croplands, which hinders our ability to predict the impact of regional agricultural intensification on the climate systems. Further, most countries across SSA have to use the Tier 1 emission factor (EF) from IPCC (2006), whereas the EF value was developed mainly based on measurements from temperate ecosystems (Bouwman et al. 2002b).

On top of the well-documented environmental and public health concerns, the above-mentioned N losses represent an additional economic cost to the smallholder farmers in SSA and could be of socioeconomic significance given their poor income (Nyamangara et al. 2003).

1.3 Factors affecting the magnitude and pathways of N loss from cropping systems of SSA

The magnitude and pathways of N loss from cropping systems are largely controlled by the N management practices associated with soil, environmental, and crop characteristics (Ladha et al. 2005), though other soil and land managements (e.g., tillage, catch crops) may also have contributions (e.g., Masvaya et al. 2017; Zhou et al. 2017).

Rate of fertilizer-N application is certainly one of the most important aspects in N management, as it directly links to the cost of input and potential yield level (thus the profitability) for smallholder farmers in SSA. Applied N rate exceeding the level that maximizes the yield may lead to an exponential increase in N loss in many reactive forms. Type of fertilizer-N can affect the pathways of N loss; NH_4^+-containing or forming fertilizers are likely to have a higher risk of N loss through NH_3 volatilization, such as urea (Sommer et al. 2004). Altering method of application (e.g., from broadcast to deep placement), however, may help to reduce the NH_3-N loss following urea application (Rochette et al. 2013; Yao et al. 2018). Further, N application at the timing of small crop demand can lead to a high risk of N loss.

Low-quality crop residues (e.g., maize straw; high C:N ratio) are recommended to be combined with fertilizer-N application as a technical basis for the Integrated Soil Fertility Management widely promoted across SSA (Kimani et al. 2003). Such a combined application recognizes the potential benefit in mitigating N leaching loss and thereby improving N synchrony (Vanlauwe et al. 2002) through altered N mineralization-immobilization turnover. However, the field verifications with leachate measurement are still lacking to confirm such benefit (Gentile et al. 2009; Sugihara et al. 2012a). Further, added residues may provide C source as energy for denitrifiers, thus stimulate the N_2O production (Abalos et al. 2012), yet the effect of combined sources (fertilizer-N plus residues) on the soil emissions of N_2O has not been reported with in situ measurements for SSA croplands.

Environmental factors (e.g., rainfall, soil moisture, soil temperature, etc.) have either direct or indirect effects on the different pathways of N loss. For example, rainfall is a critical factor driving NO_3^- leaching loss, particularly in re-fed agriculture of SSA (Mapanda et al. 2012a; Russo et al. 2017). Through controlling soil moisture content, it also affects the microbial process (e.g., nitrification or denitrification) in producing N_2O (Bateman and Baggs 2005). Further, soil moisture and temperature are both important factors influencing the microbial activity, which regulates the mineralization of soil organic matter and the biochemical transformations of N in soils.

Soil type also strongly affects the storage and N loss in soils. Soil texture is a key controller over the water holding capacity and permeability, both of which determine the movement and retention of N. Soil pH buffering capacity and cation exchange capacity (CEC) are important properties affecting the magnitude of NH_3-N loss (Haden et al. 2011; Sigunga et al. 2002). Also, soil texture, structure, and organic matter content strongly controls the soil microbial dynamics and further the microbe-mediated N dynamics (Juma 1993; Sugihara et al. 2010).

Crop N demand along the time-course of growing period could be one of the important crop characteristics in relation to N supply and loss. Small crop N demand with sufficient N supply (either through mineralization of soil organic matter or fertilizer-N addition) generally causes an unexpectedly high amount of N loss.

Many of the above-mentioned factors (e.g., soil, climate, etc.) are site-specific and vary both temporally over the years and spatially across SSA (Dewitte et al. 2013; Jalloh et al. 2012; Masvaya et al. 2017). Further, many factors (e.g., N management, soil type, and climate) may have interactions in determining N storage and loss in soils, thus making appropriate fertilizer-N recommendations more difficult. Therefore, a multiple year-site research is needed with integrated assessment on the magnitude and pathways of N cycling in the cropping systems of SSA.

1.4 A need for N management targeting higher yield with lower environmental costs in maize-based systems of the Tanzanian highlands

Careful N management will be needed during agricultural intensification in SSA as it plays a key role in addressing the triple challenge of food security, environmental degradation, and climate change (Zhang et al. 2015). Further, in developed regions like Europe, the environmental costs due to N pollution (see Section 1.2) has been reported to be higher than the value that N fertilizer added to the farm income (Sutton et al. 2011). Though currently, the sustainability may not necessarily be an immediate concern by smallholder farmers in SSA, the institutions and policies should encourage the intensification in a sustainable way. Mitigating N loss at the very first level of the source (i.e., cropping systems) is worth the effort because it can largely avoid the N cascade (Galloway et al. 2003).

Maize is a staple crop in SSA critical to food security (Ekpa et al. 2018). This is particularly true in Tanzania, where maize-based farming systems are heavily dominated (FAO 2001). Also, Tanzania is one of the nine countries that are expected to contribute half of the world's population growth from 2017 to 2050 (United Nations 2017). The first target of the agricultural intensification must be those areas with dense population and high potential for crop production (Palm et al. 2017; Vanlauwe et al. 2014a), such as highlands (Getahun 1978). Indeed, southern highlands of Tanzania are densely populated and intensively cultivated, known as the "breadbasket." To be specific, approximately 46% of the maize is produced in southern highlands, which only takes up 28% of the mainland area of this country (Bisanda et al. 1998; Rowhani et al. 2011). The pioneering research in developing sound N management in maize systems of the Tanzanian highlands would provide valuable references for the sustainable intensification of croplands across SSA.

1.5 Study objectives and dissertation organization

The ultimate goal of this study was to define the appropriate N management strategies in maize systems of the Tanzanian highlands that can enhance crop productivity while minimizing the potentially adverse impacts on the environment. To reach this, a multiple site-year experiment was conducted to evaluate the effects of N management practices on (1) the N partitioning within the soil-crop system and accordingly the crop yield response; (2) the N losses through different pathways (include NH_3 volatilization, NO_3^- leaching, and N_2O emission) from the maize systems of the Tanzanian highlands.

The dissertation is organized as follows. After this general introduction in Chapter 1, Chapter 2 describes the study sites and introduces the field set-up of an integrated soil-water-plant-air monitoring system. Chapter 3 investigates the temporal fluctuation of soil inorganic N and its availability to maize as affected by fertilizer application and soil type. Chapter 4 examines the pathways of N loss through NH_3 volatilization under six urea-N rates and the mitigation treatments of immediate irrigation and deep placement concerning two different soil types. Chapter 5 quantifies the NO_3^- leaching loss from the critical root zone of maize in response to increasing N rates and maize straw incorporation in two croplands. Chapter 6 quantifies the effects of N fertilization and straw incorporation on the soil-atmosphere exchange of N_2O in two maize fields with year-round measurements. Based on findings from Chapter 3–6, Chapter 7 provides a general discussion. Finally, Chapter 8 presents the concluding remarks.

CHAPTER 2

Description of Study Sites and the Field Monitoring System

2.1 Study area

Iringa (TZi) and Mbeya (TZm), located in the southern highlands of Tanzania (Fig. 2.1), were selected as study areas. These two areas were involved to represent the diversity in soil type (see below 2.2 Site characteristics).

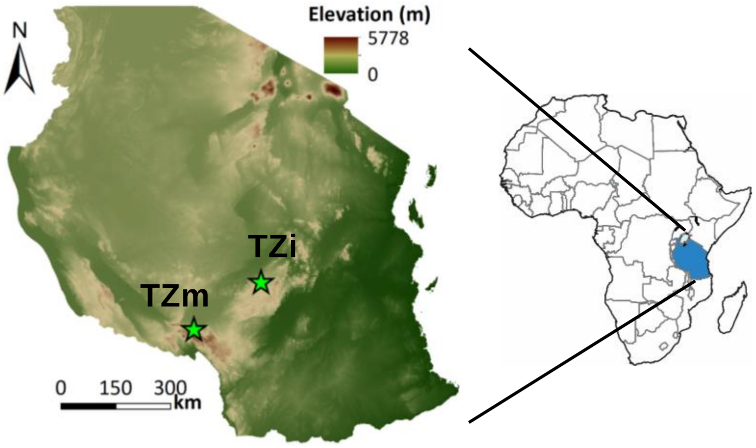

Fig. 2.1 Locations of the study areas in the southern highlands of Tanzania.

In total, four sites (two sites for each study area) were used for this study from November 2013 to November 2017. Two sites in Iringa region (TZi-1 and TZi-2) were just next to each other (within a relatively large field; 55 m × 42 m) and located in Mangalali village (07°46′ S, 35°34′ E). The other two sites in Mbeya region (TZm-1 and TZm-2; 08°55′ S, 33°31′ E) had a linear distance of approximately 1.6 km in between (Fig. 2.2). Such distance was verified to hardly alter the climate and soil conditions. TZm-1 and TZm-2 are used as experimental plots for Agriculture Research Institute-Uyole and Mbeya Agricultural Training Institute-Uyole, respectively (Fig. 2.2).

TZi-1 and TZm-1 were used for the experiment in Chapter 3 from November 2013 to September 2015, during which TZi-2 was under natural fallow, and TZm-2 was cropped to sunflower. TZi-2 and TZm-2 were used for the experiments in Chapter 4–6 from November 2015 to November 2017. It is therefore "TZi" and "TZm" in Chapter 3 refers to TZi-1 and TZm-1, whereas "ALF" in Chapter 4 and "TZi" in Chapter 5–6 refer to TZi-2, and "AND" in Chapter 4 and "TZm" in Chapter 5–6 refer to TZm-2 (see Chapter 3–6). The intensive soil sampling from two layers (0–0.15 and 0.15–0.3 m) was the main reason to change site after the first two-year experiment (November 2013–September 2015); to avoid the disturbance of such intensive sampling on the representativeness of soil inorganic N dynamics in the subsoil (0.15–0.3 m), new sites (TZi-2 and TZm-2) were used. TZi-1 and TZi-2 shared the same climate and soil properties during the experiment, and thereafter is abbreviated as TZi; the same is applied to TZm.

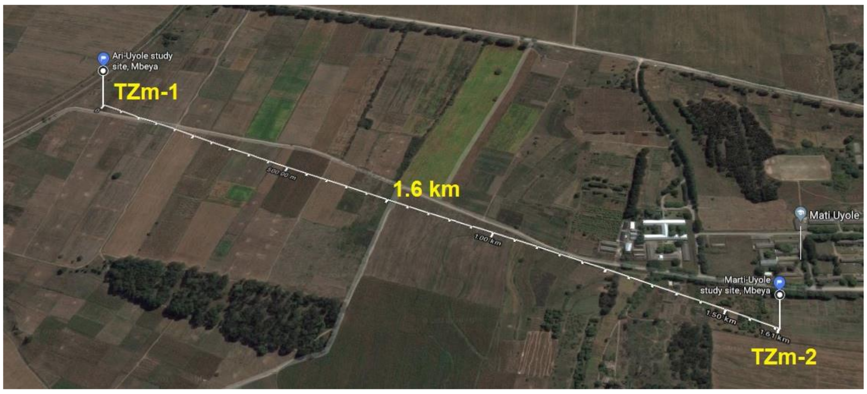

Fig. 2.2 Relative locations of TZm-1 and TZm-2 in the Mbeya region of Tanzania (modified from Google Maps).

2.2 Site characteristics

TZi has a lower elevation than that of TZm (1480 vs. 1780 m.a.s.l) and accordingly higher mean annual air temperature (23.5 vs. 17.1 °C). Mean annual precipitation is higher at TZm (860 mm) than that at TZi (560 mm), with a unimodal pattern of annual rainfall for both areas. The rainy season generally starts in late November or early December at both sites and ends in mid-April and mid-May at TZi and TZm, respectively. The soil at TZi is classified as coarse-loamy, isohyperthermic, Kanhaplic Haplustalfs, and the soil at TZm is classified as clay-loam, isothermic, Dystric Vitric Haplustands, based on the USDA system (Soil Survey Staff, 2010). Detailed descriptions of study sites and the soil characteristics at the top layer of the soil profiles are presented in Table 2.1. Before the establishment of the experimental trials in all of the four sites, maize was most commonly cropped, though in some other years, tomato (mainly at TZi) or common beans (mainly at TZm) was cropped in rotation with maize.

2.3 Field experimental set-up: an integrated soil-water-plant-air monitoring system

Figure 2.3 presents the schematic diagram and field set-up of an integrated soil-water-plant-air monitoring system for the N dynamics in the maize systems of this study. Soil samples were taken from two depths (0–0.15 m and 0.15–0.3 m) intensively to evaluate the temporal dynamics of soil inorganic N and its availability to maize. Plant samplings were also conducted at critical growth stages to investigate the crop N uptake characteristics. A semi-open static chamber method was used to measure the NH_3 volatilization, while a closed chamber method was used to quantify the flux rate of greenhouse gases including N_2O. Soil monolith lysimeters were used to collect leachate from the critical root zone

(0–0.3 m) of maize. Detailed descriptions on each compartment of this integrated system are provided in corresponding chapters (see Chapter 3–6).

Table 2.1 Description of study sites and soil characteristics at the top layer of the soil profiles (0–0.15 m for TZi and 0–0.25 m for TZm)

	TZi	TZm
Mean annual air temperature (°C)	23.5	17.1
Mean annual precipitation (mm)	560	860
Annual rainfall pattern	Unimodal	Unimodal
Elevation (m.a.s.l)	1480	1780
Soil classification	Kanhaplic Haplustalfs	Dystric Vitric Haplustands
pH (H_2O)	6.45	6.85
Total C (g kg^{-1})	3.5	17.5
Total N (g kg^{-1})	0.3	1.3
C:N ratio	12.9	13.6
CEC (cmol$_c$ kg^{-1})	1.1	17.5
Soil texture (%)		
Clay	4.7	28.4
Silt	6.9	42
Sand	88.4	29.5
Bulk density (g cm^{-3})	1.55	0.90

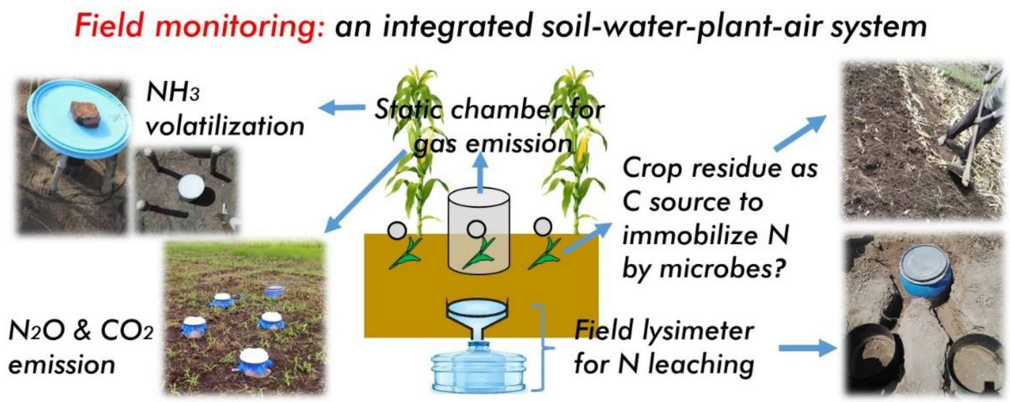

Fig. 2.3 Schematic diagram and field set-up of an integrated soil-water-plant-air monitoring system for the N dynamics in the maize systems of this dissertation.

CHAPTER 3

Nitrogen Availability to Maize as Affected by Fertilizer Application and Soil Type in the Tanzanian Highlands

Abstract

Enhancing crop production by maintaining a proper synchrony between soil nitrogen (N) and crop N demand remains a challenge, especially in under-studied tropical soils of Sub-Saharan Africa (SSA). For two consecutive cropping seasons (2013–2015), I monitored the fluctuation of soil inorganic N and its availability to maize in the Tanzanian highlands. Different urea-N rates (0–150 kg N ha^{-1}; split into two dressings) were applied to two soil types (TZi, sandy Alfisols; and TZm, clayey Andisols). Temporal dynamics of soil inorganic N were presented with a high resolution and showed that in the early growing season, soil mineralized N was exposed to the leaching risk due to small crop N demand. In the second N application (major N supply accounting for two-thirds of the total N), applied urea was more efficient in increasing soil inorganic N availability at TZm than at TZi. Such effect of soil type could be the main contributor to the higher yield at TZm (up to 4.4 Mg ha^{-1}) than that at TZi (up to 2.6 Mg ha^{-1}) under the same N rate. The best-fitted linear-plateau model indicated that the soil inorganic N availability (0–0.3 m) at the tasseling stage largely accounted for the final yield. Further, yields at TZi were still limited by N availability at the tasseling stage due to fast depletion of applied-N, whereas yields plateaued at TZm once N availability was above 67 kg N ha^{-1}. These results contribute to a better understanding of temporal patterns of soil N pools across soil types and how they affect the yield response in SSA croplands.

3.1 Introduction

Sub-Saharan Africa (SSA) struggles to be food self-sufficient (van Ittersum et al. 2016). By 2050, population growth on the African continent is projected to at least double (United Nations 2017). To maintain even the current level of cereal self-sufficiency (approximately 80%) for the increasing population, a nearly complete closure of the gap between current cropland yields and yield potential is needed (van Ittersum et al. 2016). However, SSA croplands are historically unproductive (Hazell and Wood 2008) due to continuous nutrient mining (especially nitrogen; N) from soil without proper nutrient amendments (Vitousek et al. 2009).

Increased use of fertilizer (especially N) is unequivocally a critical step in offsetting soil nutrient depletion and closing the yield gap in SSA (Dijk et al. 2012; Tamene et al. 2015). Vanlauwe et al. (2014b) argued that the appropriate use of fertilizer should be included as a fourth principle to define conservation agriculture in SSA. Indeed, regional and national efforts are underway to increase fertilizer use (AGRA 2009; Mungai et al. 2016). Increasing the use of fertilizer is also encouraged by its benefits on yield increment, doubled or even tripled together with improved seeds, as exemplified in recent studies (Sanchez et al. 2007; Nziguheba et al. 2010).

Despite the importance of increasing fertilizer input, the fate of added nutrients is largely unknown, especially N, the most yield-limiting nutrient in SSA croplands (Mafongoya et al. 2006; Wortmann et al. 2017). Applied-N can be lost from the agroecosystem through several pathways, including ammonia (NH_3) volatilization, nitrate (NO_3^-) leaching, and nitrous oxide (N_2O) emission (Lehmann and Schroth 2003; Ma et al. 2010; Butterbach-Bahl et al. 2013). Each of the pathways has significant environmental consequences such as soil acidification, eutrophication, and global warming (Galloway et al. 2003; Scudlark et al. 2005). The dominant pathways and magnitude of N loss are largely influenced by soil type and land management practices (Mapanda et al. 2012a; Russo et al. 2017; Zheng et al. 2018a), both of which vary widely across SSA croplands (Dewitte et al. 2013; Tully et al. 2016).

Various soil types—often differ greatly in soil texture, cation exchange capacity (CEC), and pH buffering capacity—can strongly affect N storage and loss in soils. Soil texture is a primary factor controlling water holding capacity (WHC) and permeability, both of which determine the movement and retention of N. Fine-textured soils with higher WHC tend to retain soil N and allow for plant or microbial uptake. Coarse-textured soils may have higher infiltration rates, leading to higher risks of NO_3^- leaching loss (Lehmann and Schroth 2003). When coupled with fertilizer type, soil pH buffering capacity and CEC can affect the magnitude of fertilizer-N loss. Both field and incubation studies (Sigunga et al. 2002; Haden et al. 2011; Zheng et al. 2018a) have shown that low pH buffering and low CEC in tropical soils resulted in substantial N losses (up to >50% of applied N) through NH_3 emission following the surface application of urea.

Soil type is also an important factor that affects the response of crop yield to increased fertilizer-N rate. Varying soil types are often associated with different agro-ecological zones in SSA. In high potential agro-ecological zones, crop yields generally increase with fertilizer input (mainly N, P, and K) to reduce the yield gap (Vanlauwe et al. 2015). However, yields may also respond poorly to NPK fertilizer input due to micronutrient deficiencies (Njoroge et al. 2017). In nutrient-poor sandy soils, much larger amounts of fertilizer-N input (e.g., organic and/or synthetic) is commonly required to attain the yield level comparable with fertile soil (Mtambanengwe and Mapfumo 2006), yet such increased yields mostly come at the cost of significantly decreased nutrient use efficiency. For example, in depleted sandy soils in Zimbabwe, the significant maize yield response (~2 Mg ha^{-1} higher than the control treatment) to chemical N input (100 kg N ha^{-1}) was only observed in the third year after repeated applications of manure at a relatively high rate (equivalent to 180 kg N ha^{-1} yr^{-1} and 30 kg P ha^{-1} yr^{-1}; Zingore et al. 2007). To achieve the sustainable intensification of African agriculture accompanied by a dramatic increase in fertilizer-N input, proper N strategies targeting different agro-ecological zones and soil resources to improve yield as well as N use efficiency are urgently needed.

Maize is the staple food for the people of SSA (Shiferaw et al. 2011; Epka et al., 2018). The highlands in East Africa are generally densely populated and intensively cultivated for production, known as the "bread basket." For example, in Tanzania, approximately 46% of the maize is produced in southern highlands, which comprises only 28% of the mainland area of this country (Bisanda et al. 1998; Rowhani et al. 2011).

The objective of this study was to investigate the fluctuation of soil inorganic N and its availability to maize in the Tanzanian highlands in two soil types and under different N application rates. Specifically, I investigated (1) the seasonal variations of soil inorganic N and how the inorganic N availability was influenced by N rate and different soil types; (2) the response of maize yield to soil inorganic N availability as affected by N rate and soil type. Finally, I provide appropriate soil-specific N strategies to increase maize yield, while minimizing the potentially adverse losses of N to the environment.

3.2 Materials and methods

3.2.1 Study sites

The study was conducted within two maize-based agro-ecological zones (Bisanda et al., 1998) in the Tanzanian highlands. One site (TZi, 1480 m.a.s.l.) is located in Mangalali village (07°46′ S, 35°34′ E) in the Iringa region. The soil is classified as coarse-loamy, isohyperthermic, Kanhaplic Haplustalfs (Soil Survey Staff, 2010). The TZi site was converted from forest to agriculture between 1960 and 1970. Since the late 1990s, maize and tomato were grown in rotation for around nine years and then followed by a continuous maize cultivation till the establishment of the current experiment in November of 2013. During the maize cultivation from 2009 to 2012, N was applied mainly as urea at a rate of ~100 kg N ha $^{-1}$ yr^{-1}. The other site (TZm, 1780 m.a.s.l.) is located in Uyole town (08°55′ S, 33°31′ E) in the Mbeya region. The soil is classified as clay-loam, isothermic, Dystric Vitric Haplustands (Soil Survey Staff, 2010). The TZm site is owned by the Uyole Agricultural Research Institute and is used as experimental fields since 1968. From 2005 onwards, the land was cropped with maize and N was applied mainly as urea at a rate between 80 and 330 kg N ha^{-1} yr^{-1} until the establishment of the current experiment in November of 2013. I sampled the topsoil (0–0.15 m) from the field in July of 2013 to evaluate the initial N concentrations, and found that the concentrations of residual N from the preceding experiment were high with large variability (98 ± 67 mg kg^{-1} [mean ± standard deviation], n = 36; range: 17–314 mg kg^{-1}).

The precipitation at TZi is 560 mm per year on average, lower than that at TZm (860 mm). The mean annual air temperature is higher at TZi (23.5 °C) than that at TZm (17.1 °C). The pattern of annual rainfall is unimodal for both sites. The rainy season generally starts in late November at both sites and ends in mid-April and mid-May at TZi and TZm, respectively. Selected soil properties for the study sites are presented in Table 3.1. Despite the similar soil pH in the topsoil between two sites, soil organic matter and CEC were substantially lower at TZi compared to those at TZm, because of lower clay content. Soil pH buffering capacity and WHC were both higher at TZm than at TZi.

Table 3.1 Selected soil physico-chemical properties from the top two layers for TZi and TZm

Site	Depth	pH	TC†	TN†	CEC‡	PBC§	WHC⁑	Soil texture (%)		
	m	(H_2O)	g kg^{-1}	g kg^{-1}	cmol$_c$ kg^{-1}	mmol OH$^-$ kg^{-1}	%	Clay	Silt	Sand
TZi	0–0.15	6.45	3.5	0.3	1.1	9.5	27.2	4.7	6.9	88.4
	0.15–0.3	5.96	1.9	0.2	0.9	NA⸸	NA	6.4	7.9	85.7
TZm	0–0.25	6.85	17.5	1.3	17.5	57.1¶	66.3¶	28.4	42.0	29.5
	0.25–0.5	7.09	9.6	0.8	22.7	NA	NA	34.6	32.9	32.5

†Total carbon (TC) and N (TN) determined by dry combustion of finely ground soils using Vario Max CHN elemental analyzer.

‡Cation exchange capacity (CEC) determined by the buffered (pH = 7) ammonium acetate saturation method.

§pH buffering capacity (PBC) determined by titratable acidity (at pH = 8.3) using a potentiometric automatic titrator following Sakurai et al. (1989).

⁑WHC = maximum water holding capacity.

⸸NA = not analyzed.

¶Samples analyzed for PBC and WHC at TZm were from 0–0.15 m depth.

3.2.2 Experimental design

The experiment was conducted from November of 2013 to June of 2015, with maize cropped consecutively for two seasons. Experimental plots were established in a randomized complete block design receiving four levels of N rate: 0, 50, 100, and 150 kg N ha^{-1}, denoted as 0–150N, respectively. Each N rate was replicated three times, and plots were 5 m × 5 m. A 1.5 m buffer strip separated each plot and block. Within each experimental plot, three maize (*Zea mays* L.; variety TMV-1 at TZi and UH6303 at TZm) seeds were planted per hole at a spacing of 0.7 m × 0.3 m, and were thinned to one plant per hole 20 days after planting (DAP), giving a population of ~48000 plants ha^{-1}. The maize varieties were recommended by the local extension services, with 6.3 and 7.5 Mg ha^{-1} being the yield potential for variety TMV-1 and UH6303, respectively (Lyimo 2005; Lyimo et al. 2014). Maize was planted in early- to mid-December at both sites and harvested in late March and mid-May at TZi and TZm, respectively (Table 3.2).

Table 3.2 Agricultural activities carried out during the study period

Activity description	TZi		TZm	
	Date	DAP	Date	DAP
The first season				
Planting and P fertilizer application	14-Dec-13	0	8-Dec-13	0
Thinning, first plant sampling (V3–4)†	3-Jan-14	20	28-Dec-13	20
First N fertilizer application	4-Jan-14	21	29-Dec-13	21
Second plant sampling (VT)	8-Feb-14	56	3-Feb-14	57
Second N fertilizer application	9-Feb-14	57	4-Feb-14	58
Third plant sampling (PM) and harvest	1-Apr-14	108	19-May-14	162
The second season				
Planting and P fertilizer application	6-Dec-14	0	18-Dec-14	0
Thinning, first plant sampling (V3–4)	26-Dec-14	20	7-Jan-15	19
First N fertilizer application	27-Dec-14	21	8-Jan-15	20
Second plant sampling (VT)	31-Jan-15	56	12-Feb-15	55
Second N fertilizer application	9-Feb-15	65	13-Feb-15	56
Third planting sampling (PM) and harvest	21-Mar-15	105	20-May-15	152

†V3–4 = maize growing stage of three-to-four leaves, VT = tasseling stage, PM = physiological maturity stage.

The farming practice recommended by the local extension services was slightly modified. The basal application of diammonium phosphate at the planting date was changed to triple super phosphate to all plots at a rate of 50 kg P ha^{-1}. This is because I hypothesized that the crop N demand is small before the first N application (see below) and indigenous N supply from mineralization of organic matter accumulated during drying season is sufficient. Nitrogen was applied by broadcasting urea (46% N, 0% P) twice during the growing season. One-third was applied 21 DAP (maize growth stage V3–4).

The remaining two-thirds was added 57 DAP (around the time of maize tasseling, VT). Weeding was carried out when necessary, and all weeded materials were removed from the plots. The schedule of agricultural activities carried out during the experimental period is presented in Table 3.2. The experiment was not irrigated.

3.2.3 Field environmental monitoring

At each site, soil moisture was monitored with CS616 sensors at 0.05, 0.2, and 0.4 m below the ground surface with two replicates for each of the two blocks (2 blocks × 2 replicates × 3 depths = 12 sensors; Campbell Scientific, Inc., USA). Soil temperature was monitored with T108 sensors (Campbell Scientific, Inc., USA) at 0.05 m depth with two of the block replicates. Air temperature was monitored using one T108 sensor at each site and precipitation was recorded by a TE525MM rain gauge (Campbell Scientific, Inc., USA). All the monitoring instruments were connected to a data logger (CR1000, Campbell Scientific, Inc., USA), which recorded data every 10 min.

Soil moisture, expressed as volumetric water content, was separately calibrated with soils sampled from each site (R^2 = 0.95 for the calibration function with n = 40 at TZi and R^2 = 0.91 with n = 77 at TZm).

3.2.4 Soil sampling and analysis

Soil sampling was carried out 21 and 29 times at TZi and TZm, respectively, during the experimental period. The soils were sampled every 10 to 14 days during the cropping season. More sampling times conducted at TZm was due to the longer rainy season at TZm than TZi. Soils were sampled from two depths (0–0.15 m and 0.15–0.3 m) using an auger (~0.04 m diameter). Based on my field observation, most of the mature maize roots (> 70%) were distributed in 0–0.2 m, which agreed with the reports by Chikowo et al. (2003) and Sugihara et al. (2012a). Therefore, sampling from the top 0.3 m soils should be sufficient to cover the major soil N source for the plant uptake. Four subsamples from the central area (4 m × 4 m) of each plot were taken and mixed as one replicate. Soil samples were air-dried and sieved through 2-mm mesh before transporting to Japan for the analysis of inorganic N (NH_4^+-N and NO_3^--N). Inorganic N was extracted from 10.0 g soil with 30.0 ml of 1M KCl for 30 min on a reciprocating shaker, and the suspension was centrifuged (2000×g, 10 min) and filtered through filter paper (No. 6, Adventec, Japan). Extracted NH_4^+-N and NO_3^--N were determined colorimetrically using the flow injection auto-analyzer (Flow Analysis Method, JIS K-0170, AQLA-700 Flow Injection Analyzer, Aqualab Inc., Japan).

After the first season harvest, soil bulk density at each site was determined by taking additional soil cores (100 cm^3 size; n = 9) for each depth at 0.07 m (representing 0–0.15 m) and 0.2 m (representing 0.15–0.3 m) from soils adjacent to the plots. With soil bulk density and soil thickness, soil inorganic N availability was determined by converting the concentration of total inorganic N (mg kg^{-1}) to an area basis (kg ha^{-1}).

3.2.5 Plant sampling and analysis

In each cropping season, aboveground plant materials were collected at three growing stages: three-to-four leaves, V3–4; tasseling, VT; and physiological maturity, PM (Table 3.2). For each sampling activity, five plants were collected randomly inside each plot (4 m × 4 m, avoiding the edge). Plant materials were immediately divided into leaf, stem, cob, and grain after sampling. Field weights of each separated plant materials were recorded before subsamples were taken for moisture correction. All subsamples were oven dried at 60 °C and homogenized using a rotating-disk mill. Total N content was determined by high-temperature combustion and subsequent gas analysis (Vario Max CHN, Elementar, Germany). Plant N uptake in each plot was calculated by $\sum_{i}^{n}(N_i \times DM_i)$, where i = categories of separated plant material (e.g., leaf, stem, cob, and grain); n = total number of category; N_i = total N content (%) determined for category i; DM_i = dry matter (kg ha^{-1}) of category i.

To estimate crop yields, maize ears remaining within the sampling area (4 m × 4 m) were collected from each replicate plot on the harvesting date. Grains were shelled from the ears, and the dry weight was estimated following the same way as other plant material (i.e., field weight × moisture correction from subsamples).

3.2.6 Calculations

Shortly (10–12 days) after N application, the increase of soil inorganic N availability ($\Delta Navail$) resulting from N application was calculated using Eq. (3.1):

$$\Delta Navail = [Navail_{-1\,DAF} - Navail_{10\text{–}12\,DAF}]_{Fertilized\,plots} - [Navail_{-1\,DAF} - Navail_{10\text{–}12\,DAF}]_{Control\,plots} \quad (3.1)$$

Where $Navail_{-1\,DAF}$ is the soil inorganic N availability one day before fertilization; and $Navail_{10\text{–}12\,DAF}$ is the soil inorganic N availability 10–12 days after fertilization. The difference in the soil inorganic N availability in the control plots is subtracted from that in the fertilized plots to account for the inherent change in the soil inorganic N availability (e.g., mineralization, immobilization, etc.). I assume no priming effect of N applications in this calculation.

3.2.7 Statistical analysis

Repeated-measures analysis of variance (ANOVA) was used to determine the effects of N rate (as the between-subjects factor), sampling time (as the within-subjects factor), and their interactions on the concentrations of NH_4^+-N and NO_3^--N. Repeated-measures ANOVA was separately run for each combination of depth, site, and season. Repeated-measures ANOVA was also used to determine the effects of N rate (as the between-subjects factor), season (treated as a within-subject factor), and their interactions on the plant N uptake at three growing stages (V3–4, VT, and PM) as well as yield at each site. Following each *F*-value testing the simple effects of N rate within each level combination of the other effects, multiple comparison of means with a least significant difference (LSD) test was conducted. All statistically significant difference was identified as $P < 0.05$ unless stated otherwise. Statistical analysis was conducted with IBM SPSS Statistics (version 24).

Both the response of plant N uptake at the VT stage and yield to soil inorganic N availability were fitted with three models: quadratic, linear-plateau, and quadratic-plateau. Model comparison was conducted using the Akaike Information Criterion (AIC) together with 'pseudo R^2', which was calculated as 1 − (residual sum of squares/total sum of squares). Model fitting and comparison were performed using the R software (version 3.3.3; http://www.r-project.org).

3.3 Results

3.3.1 Environmental factors

Rainfall amount and distribution varied inter-seasonally and across the two sites (Fig. 3.1). Higher rainfall amounts were recorded at TZm (883 mm in the first season and 707 mm in the second season) than at TZi (638 mm in the first season and 385 mm in the second season). During the rainy seasons, soil moisture contents were generally sufficient for maize growth (> −1 MPa at 0.05 m; Fig. 3.1), except for the second season at TZi, where lower precipitation (by 40% compared with the first season) and the erratic distribution resulted in several distinct dry periods (e.g., 7–15 DAP, 57–63 DAP, and 71–84 DAP in the second season; Fig. 3.1a).

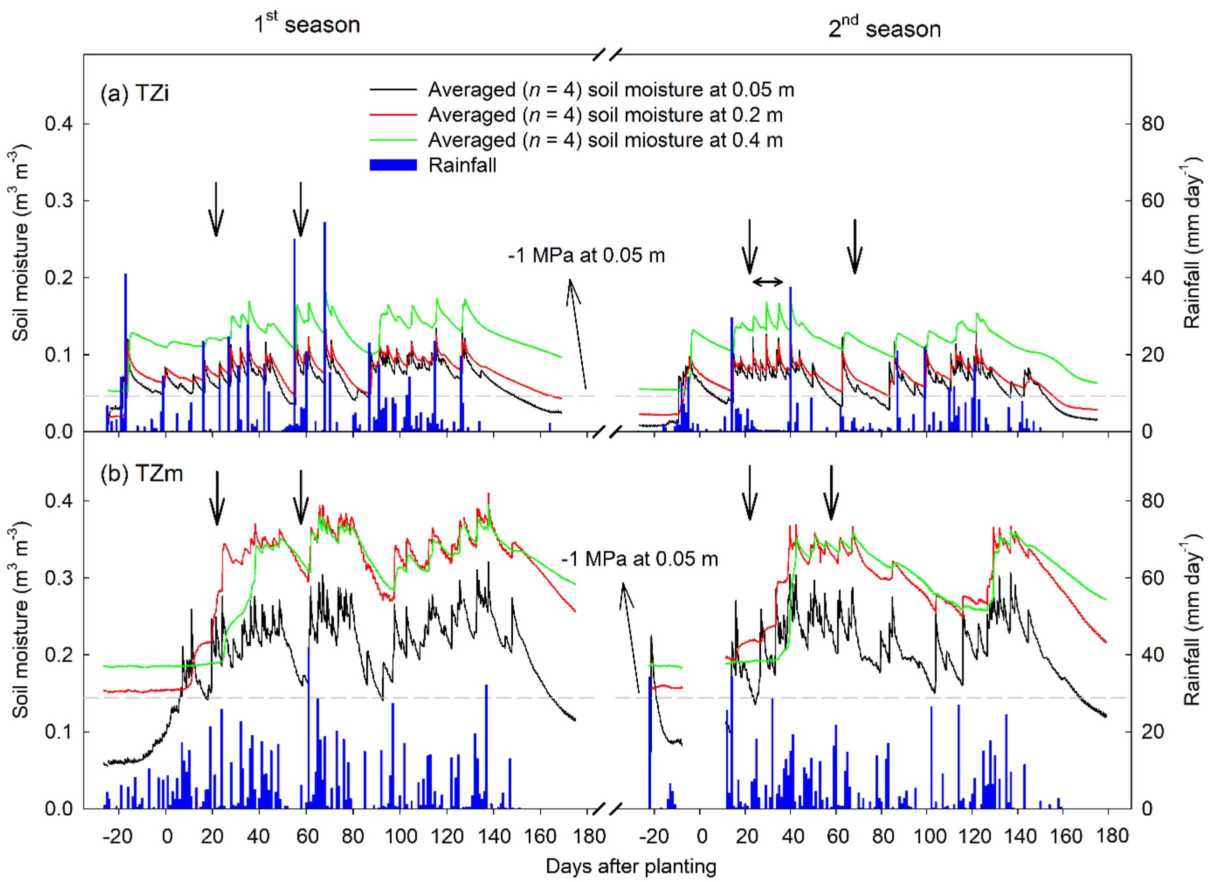

Fig. 3.1 Temporal variation in soil moisture and daily rainfall at TZi (a) and TZm (b) during the study period. The breaks of horizontal axis separate the data into two seasons: the first season (2013–2014) on the left and the second season (2014–2015) on the right. Horizontal dash lines indicate −1 MPa. Downward arrows indicate the timing of fertilizer-N applications. Double line arrow represents the period when rain gauge failed to function (25–36 DAP) in the second season at TZi.

3.3.2 Fluctuation of soil inorganic N concentrations

Soil NH_4^+-N and NO_3^--N concentrations varied both intra-seasonally (Fig. 3.2, 3.3) and inter-seasonally (Table S3.1) in the 0N treatment, and the response to N application varied with site and depth (Fig. 3.2, 3.3). Soil inorganic N concentrations were generally higher at TZm (up to 30 and 132 mg kg^{-1} for NH_4^+-N and NO_3^--N, respectively) than those at TZi (up to 12 and 9 mg kg^{-1} for NH_4^+-N and NO_3^--N, respectively).

At TZi, the variability of soil NH_4^+-N and NO_3^--N concentrations differed between the two seasons (Fig. 3.2). In the first season, both soil NH_4^+-N and NO_3^--N concentrations responded to N application (Fig. 3.2a, c, e, g). The effect of N rate on soil NO_3^--N concentrations at two depths depended on sampling time ($P < 0.05$ for the interaction N rate × sampling time; Table S3.1), while soil NH_4^+-N concentrations were significantly affected by seasonal variation ($P < 0.001$ for the sampling time, Table S3.1). The increased soil inorganic N concentration resulting from applied N, indicated by the significant difference among N treatments after N application, was retained up to 25 days (Fig. 3.2a). In the second season, no immediate response of either soil NH_4^+-N or NO_3^--N concentration to N application was observed at either depth (Fig. 3.2b, d, f, h). Soil NO_3^--N concentrations at both depths were low (< 4 mg kg^{-1}) throughout the season (Fig. 3.2b, d), and they significantly ($P < 0.05$) differed among N treatments and sampling times (Table S3.1). Soil NH_4^+-N concentrations were significantly controlled by seasonal variation ($P < 0.001$, Table S3.1) as observed in the first season. During −1–10 DAP in the second season (Fig. 3.2f, h), the increase of soil NH_4^+-N concentrations across the whole field was observed, likely due to the rapid mineralization of organic matter during the onset of rain.

At TZm, the soil NO_3^--N concentrations at the beginning of the first season (e.g., before N application) were substantially greater (44–132 mg kg^{-1} at 0–0.15 m and 13–45 mg kg^{-1} at 0.15–0.3 m) than those in the second season (1–15 mg kg^{-1} at 0–0.15 m and 0–12 mg kg^{-1} at 0.15–0.3 m). In the first season, the soil NO_3^--N concentrations showed relatively large variation among treatments at the second sampling (9 DAP in Fig. 3.3a), but not significantly different ($P > 0.1$). In both seasons, soil NO_3^--N concentrations responded to N application (Fig. 3.3). Soil NH_4^+-N concentrations generally maintained a similar level among treatments at each depth across each season (Fig. 3.3), as suggested by the simple main effect of sampling time ($P < 0.001$, Table S3.1). The increased soil NO_3^--N concentration resulting from N application was retained up to 63 days (Fig. 3.3c). At the beginning of the second season, the increase of soil NH_4^+-N concentrations (−23–−6 DAP in Fig. 3.3f, h) followed by NO_3^--N flushes (−6–10 DAP in Fig. 3.3b, d) was observed across the field.

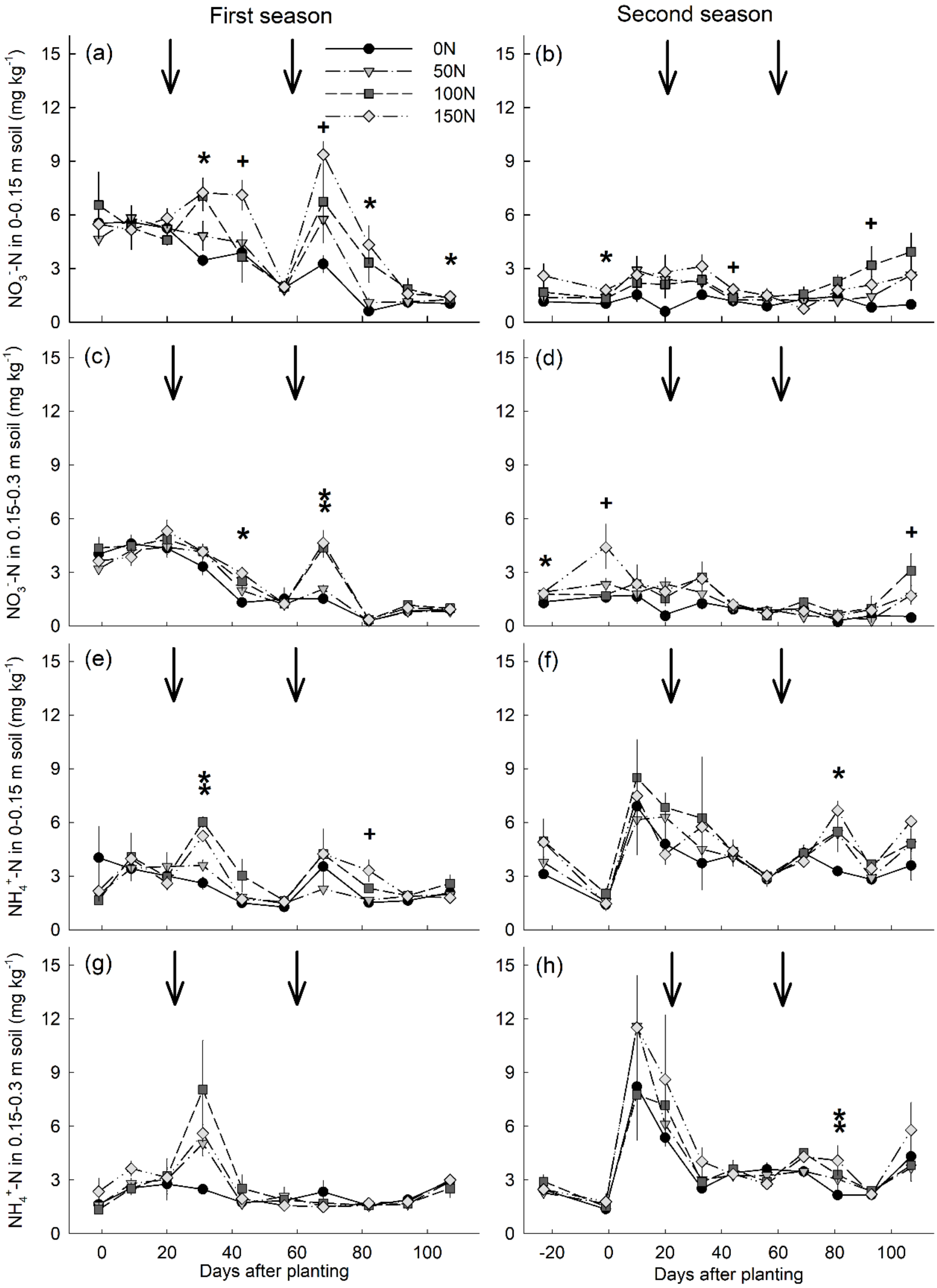

Fig. 3.2 Temporal fluctuation of soil NO_3^--N (a–d) and NH_4^+-N (e–h) concentrations (mg kg^{-1}) at TZi. Downward arrows indicate N applications as well as the plant sampling at V3–4 and VT stages. Error bars represent the standard error of the means (n = 3). +, *, and ⁑ above each sampling time indicate significant difference in means of soil inorganic N concentrations among N treatments at $P < 0.1$, $P < 0.05$, and $P < 0.01$ level.

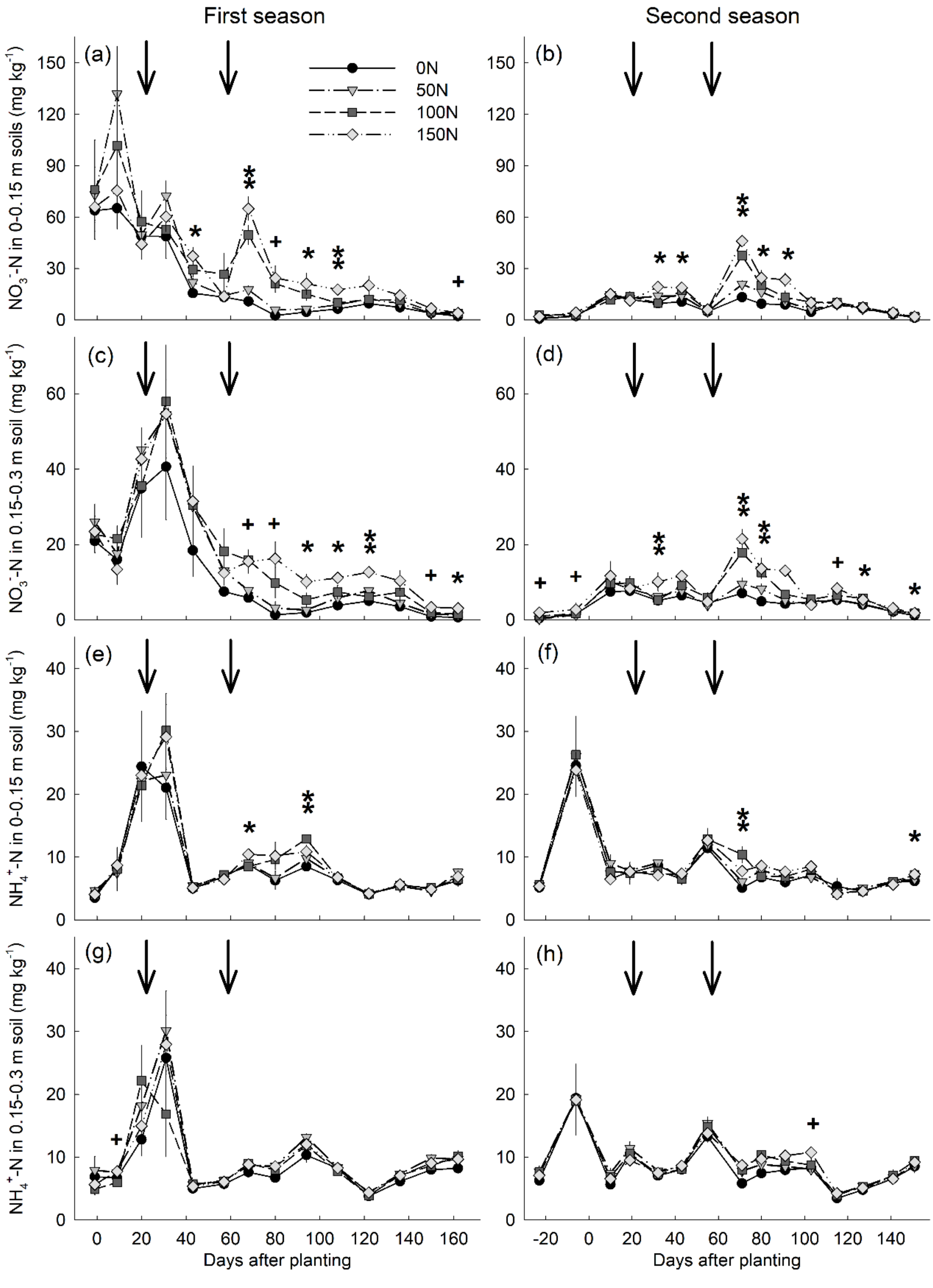

Fig. 3.3 Temporal fluctuation of soil NO_3^--N (a–d) and NH_4^+-N (e–h) concentrations (mg kg^{-1}) at TZm. Downward arrows indicate N applications as well as the plant sampling at V3–4 and VT stages. Error bars represent the standard error of the means (n = 3). +, *, and ⁑ above each sampling time indicate significant difference in means of soil inorganic N concentrations among N treatments at $P < 0.1$, $P < 0.05$, and $P < 0.01$ level.

3.3.3 Relationship between N rate and Δ*Navail* at each site

Shortly (10–12 days) after N application, Δ*Navail* (calculated using Eq. (3.1)) in 0–0.3 m increased significantly with N rate for the second N application (P = 0.017 at TZi and P = 0.003 at TZm) but not for the first N application (P = 0.612 at TZi and P = 0.709 at TZm) across sites (Fig. 3.4). For the second N application, the higher slope of the regression line at TZm (0.98) shows that applied urea increased plant-available N in soils more efficiently compared to TZi (0.20), especially at higher urea-N rates (Fig. 3.4). For example, a single application of urea with 100 kg N ha^{-1} increased ~79 kg N ha^{-1} of inorganic N in the 0–0.3 m soils at TZm, but only increased ~18 kg N ha^{-1} at TZi (Fig. 3.4). In the first season at TZm, vast ranges were observed for the Δ*Navail* (Eq. (3.1)) with the same N rate after the first N application (showed by the large standard error in Fig. 3.4b).

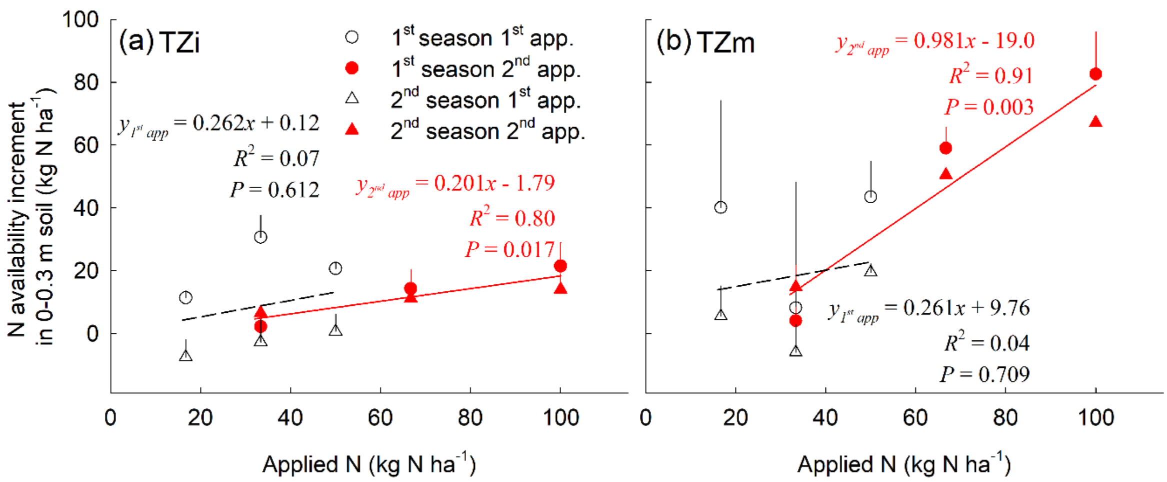

Fig. 3.4 Relationship between N application rate and Δ*Navail* (Eq. (1); N availability increment) after N application in 0–0.3 m at TZi (a) and TZm (b). Error bars represent positive standard error of the means (n = 3).

3.3.4 Plant N uptake and yield

Plant N uptake of mature maize (i.e., PM stage) varied with site and season (Table 3.3). In the plots treated with the same N rate, uptakes at TZm were 24–94 kg N ha^{-1} higher than those at TZi during the two seasons. Similarly, uptakes in the first season were 2–60 kg N ha^{-1} higher than those in the second season across two sites (Table 3.3).

The effect of N rate and season on plant N uptake was different across plant growing stages at each site. At the V3–4 stage (i.e., before N application), plant N uptake was small (< 3.5 kg N ha^{-1}) and similar across sites and seasons, though a difference (P < 0.05) was detected at TZm between the two seasons (Table 3.3). At the VT stage, significant (P < 0.001) seasonal variation of plant N uptake at each site was observed, while the effects of N rate varied with season (i.e., only significant in the first season at TZi and the second season at TZm; Table 3.3). At the PM stage, the effects of N rate were significant (*P* < 0.01) in all cases (Table 3.3).

A significant effect between season × N rate (*P* < 0.05) on the yield was observed at TZi but not TZm (Table 3.3). At TZi, yields in the first season (0.2–2.6 Mg ha^{-1}) were generally higher than those in the second season (0.2–0.3 Mg ha^{-1}), with a significant effect of the N rate on the yield only observed in the first season (Table 3.3). At TZm, higher yields in the first than the second season were observed at lower (0–50N) but not higher N rates (100–150N) (Table 3.3). With similar rainfall amount received in the first season at TZi (638 mm) and the second season at TZm (707 mm), yield at TZm (1.5–4.4 Mg ha^{-1}) was higher than that at TZi (0.2–2.6 Mg ha^{-1}) with the same N rate applied (Table 3.3).

Table 3.3 Plant N uptake (kg N ha^{-1}) at three growing stages (three-to-four leaves, V3–4; tasseling, VT; and physiological maturity, PM) and yield (Mg ha^{-1}), and the *F*-values from the results of repeated-measures ANOVA showing the effects of N application rate (N rate), seasonal variation, and their interactions on these variables

	TZi				TZm			
	V3–4	VT	PM	Yield	V3–4	VT	PM	Yield
	— kg N ha^{-1} —			Mg ha^{-1}	— kg N ha^{-1} —			Mg ha^{-1}
The first season								
0N	2.1a	8.1a	10.7a	0.18a	2.3a	21.5a	48.3a	2.9a
50N	2.0a	9.5ab	26.9b	1.2b	2.3a	25.1a	80.5a	3.9b
100N	2.0a	14.7bc	43.9c	2.0bc	2.1a	30.1a	122.1b	4.3b
150N	2.3a	17.2c	59.3c	2.6c	2.5a	25.6a	153.2b	4.3b
SED†	0.3	2.8	6.8	0.41	0.37	3.18	17.1	0.4
The second season								
0N	1.9a	2.7a	9.2a	0.18a	1.3a	5.3a	32.7a	1.5a
50N	3.0a	3.9a	15.6ab	0.34a	1.7a	8.5ab	52.3ab	2.9b
100N	3.4a	5.1a	18.5bc	0.33a	2.0a	10.5b	69.6bc	3.6bc
150N	2.7a	5.1a	24.9c	0.33a	2.0a	12.3b	93.0c	4.4c
SED	1.1	1.1	3.7	0.12	0.25	2.0	11.5	0.4
Source				*F*-values				
N rate	0.615^{ns}	8.14**	15.6**	10.5**	2.85^{ns}	3.72^{ns}	25.5***	19.2***
Season (S)	2.60^{ns}	50.8***	115***	78.9***	10.5*	249***	27.4***	20.4**
N rate × S	0.756^{ns}	2.03^{ns}	18.6***	13.4**	0.919^{ns}	1.56^{ns}	1.93^{ns}	3.43^{ns}

†SED = standard error of the difference.

Values followed by different letters within a column in each cropping season indicate significant difference at *P* < 0.05 (LSD test).

* = *P* < 0.05, ** = *P* < 0.01, *** = *P* < 0.001, ns = non-significant.

3.3.5 Plant N uptake at the VT stage and yield in response to soil inorganic N availability

The response of plant N uptake at the VT stage to soil inorganic N availability (0–0.15 m) at 31–33 DAP (i.e., after the first N application; Fig. 3.5a) and the response of yield to soil inorganic N availability (0–0.3 m) at 68–71 DAP (i.e., after the second N application; Fig. 3.5b) were all best-fitted by linear-plateau model (Table 3.4). The models suggest that 62 and 67 kg N ha^{-1} was the minimum soil inorganic N availability after N application to achieve maximum plant N uptake at the VT stage and yield, respectively (parameter *c* for linear-plateau models in Table 3.4). The maximum yield calculated from the linear-plateau model was 4.1 Mg ha^{-1}.

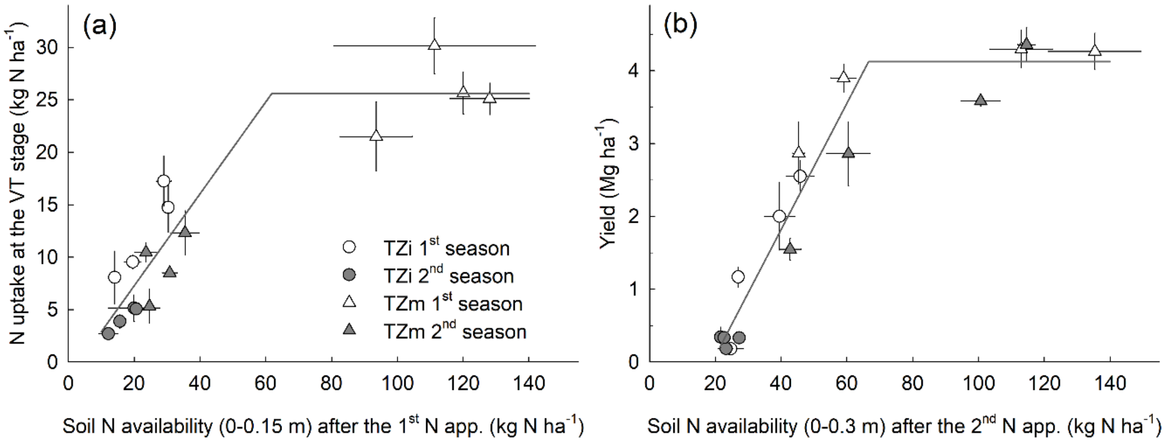

Fig. 3.5 Response of plant N uptake at the VT stage (a) and yield (b) to soil inorganic N availability after the first and second N applications (i.e., 31–33 DAP and 68–71 DAP), respectively. Error bars represent standard error of the means (n = 3).

Table 3.4 Model parameters, Akaike information criterion (AIC) and R^2 for models describing the response of plant N uptake at the VT stage and yield to soil N availability at the tasseling stage (i.e., 68–71 DAP)

Model	N uptake at VT			Yield		
	Parameter estimate	AIC	R^2	Parameter estimate	AIC	R^2
Quadratic $a + b \times N + c \times N^2$	a = –1.26 b = 0.477 c = –0.00207	88.5	0.87	a = –2.15 b = 0.124 c = –0.000582	25.6	0.93
Linear-plateau $a + b \times N$ for $N < c$; $a + b \times c$ for $N >= c$	a = –1.48 b = 0.438 c = 61.8	89.0	0.87	a = –1.65 b = 0.0867 c = 66.6	22.3	0.94
Quadratic-plateau $a + b \times N + c \times N^2$ for $N < d$; $a + b \times d + c \times d^2$ for $N >= d$	a = –2.81 b = 0.561 c = –0.00263 d = 82.3	91.0	0.87	a = –1.58 b = 0.0832 c = 2.51 × 10^{-5} d = 67.2	27.9	0.93

3.4 Discussion

3.4.1 Potential leaching loss of inorganic N in the early growing seasons

At the beginning of the rainy season, rainfall often triggers rapid mineralization of organic matter accumulated during the drying season and therefore causes the flush of inorganic N in the topsoil, known as "Birch Effect" (Birch 1964). However, the mineralized N is usually excessive and susceptible to leaching at this timing as crop N demand is small (Chikowo et al. 2004). For example, during the nitrification of soil mineralized NH_4^+ at TZi (i.e., decreasing soil NH_4^+-N concentrations during 10–20 DAP in Fig. 3.2f, h), reduction in soil inorganic N availability in 0–0.3 m (12.7 kg N ha^{-1}) was larger than the plant N uptake at V3–4 stage (2.7 kg N ha^{-1}). Similarly, during the period of NO_3^--N pulse at TZm (−6–10 DAP in Fig. 3.3b, d), N loss was estimated as 14 kg N ha^{-1} by comparing the decrease in N amount from the top 0.3 m (15.5 kg N ha^{-1}) with the plant N uptake at V3–4 stage (1.7 kg N ha^{-1}). These estimated leaching losses of N were within the ranges reported by previous studies (4.3–39 kg N ha^{-1}) across sandy and clayey soils in SSA (Kamukondiwa and Bergström 1994; Mapanda et al. 2012a). As the major driver of these potential leaching losses, the flush of inorganic N has been reported in both sandy and clayey soils in SSA (Chikowo et al. 2004; Tully et al. 2016; Russo et al. 2017) as well as other tropical regions (Wetselaar 1961). Current results support the findings of previous studies that managing indigenous N resource in the early growing season was challenging regardless of soil type, because crop roots were under-developed and N demands were too small to utilize the excessively mineralized N. Consequently, the mobile N was largely exposed to the risk of leaching.

At TZm, the substantially higher soil NO_3^--N concentrations with large variation at the beginning of the first season (Fig. 3.3a, c) compared to the second season (Fig. 3.3b, d) was attributed to the residual N from the preceding study. Such high residual soil N from the previous season could be prone to leaching loss upon sufficient rainfall in the current season (Rasouli et al. 2014; Masvaya et al. 2017). For example, during 31–43 DAP in the first season, both soil NH_4^+-N and NO_3^--N concentrations substantially dropped across all the plots and depths (Fig. 3.3a, c, e, g; equivalent to 133 kg N ha^{-1}), while the plant N uptake between V3–4 and VT was small (23 kg N ha^{-1}). Given the high precipitation (116 mm) during this period and the high initial soil moisture (> 0.21 and > 0.32 m^3 m^{-3} at 0.05 and 0.2 m, respectively, in Fig. 3.1b), leaching could be the main pathway of this N loss. Such a substantial N loss (~110 kg N ha^{-1}) largely eliminated the effect of residual N before the second N application (Fig. 3.3a, c, e, g).

3.4.2 Effects of N application and soil type on soil inorganic N

The increased soil inorganic N concentration resulting from N application, indicated by the significant difference among treatments after N application, was retained longer at TZm (up to 63 days in Fig. 3.3c) than at TZi (up to 25 days in Fig. 3.2a). The longer N retention at TZm was likely a result of a higher WHC (Table 3.1). Better N retention may also be explained by the anion exchange capacity developed by variable charge clay minerals (Ishiguro et al. 1992; Katou et al. 1996) at TZm, which can lead to NO_3^- adsorption.

For the first N application, N rate had no significant effect (P > 0.05) on $\Delta Navail$ (eq. (1)) across sites (Fig. 3.4). This could be attributed to the relatively high and variable concentrations of initial soil N (Fig. 3.2, 3.3) and the low rates of N application (17–50 kg N ha^{-1}). In the first season at TZm, the variation of initial N concentrations was largely contributed by the high residual N from the preceding experiment, which masked the effect of the first N applications (soil inorganic N availability among treatments were not significantly different following the first N application; Fig. S3.1).

For the second N application, the effect of N rate on $\Delta Navail$ (Eq.(3.1)) clearly differed between the two soils, with applied urea more efficiently increased plant-available N in soil at TZm than at TZi (Fig. 3.4). This could be mainly attributed to the higher susceptibility of the soil to NH_3 volatilization from surface-applied urea at TZi than that at TZm. Soils with coarse texture and low organic matter (i.e., TZi) are generally low in CEC and pH buffering capacity (Table 3.1), and therefore inherently weak to buffer the NH_3 loss (Ferguson et al. 1984; Corstanje et al. 2008). This is supported by the result of another research from our team, where we quantified NH_3 loss from surface-applied urea on the current two sites: under the same urea-N rate (30–100 kg N ha^{-1}, as single application), sandy Alfisols had a larger fraction of N loss as NH_3-N (36%–50% of applied N) compared to clayey Andisols (5%–20%) (Zheng et al. 2018a). Furthermore, accumulated rainfall during the 12 days after N applications did not exceed 40 mm in either season at TZi, which excluded the possibility of dominant contribution from leaching to N loss. Therefore, NH_3 volatilization should be the major pathway of N loss from urea during the short period (10–12 days) after application at TZi, which led to the low efficiency of applied urea in increasing plant-available N at TZi.

3.4.3 Plant N uptake at VT stage and yield in response to soil inorganic N availability

Plant N uptake at the VT stage did not consistently show significant difference among N treatments (Table 3.3) due to the effects of inter-seasonal variations of soil or climatic condition. In the first season at TZm, the residual N from the preceding study contributed to sufficient N supply for plant until the VT stage, as well as the relatively high yield even at 0N plots (2.9 Mg ha^{-1}). A relatively high yield (3.2 Mg ha^{-1}) and final N uptake (115 kg N ha^{-1}) resulting from sufficient indigenous soil N supply was also observed in a clayey soil in Morogoro, Tanzania (Sugihara et al. 2012a). At TZi, drought in the early crop growth period of the second season may have severely affected the yield (Table 3.3). Such climatic effects were common in sandy soils in SSA croplands. For example, both Tully et al. (2016) and Masvaya et al. (2017) reported low maize yields (in sandy soils of Tanzania and Zimbabwe) in dry season or due to drought experienced in the early growing period. Apart from these inter-seasonal variations, split N application could still be necessary as in the normal seasons a significant difference in N uptake at the VT stage among N treatments was observed (Table 3.3).

As indicated by the linear-plateau model (Fig. 3.5a), the optimal soil inorganic N availability (0–0.15 m) after the first N application (parameter c = 61.8 kg N ha^{-1} in Table 3.4) was much higher than plant N uptake at the VT stage, which may promote N leaching (e.g., 31–43 DAP at TZm in the first season; Fig. 3.3a, c, e, g). Further, high N fertilizer rates for the first application are not practical in SSA croplands. Fortunately, soil inorganic N availability after the second N application seemed more important for the final N uptake and yield (Fig. 3.5, S3.2). For example, the major N uptake (on average ~72% across sites and seasons) occurred between VT and PM. Furthermore, the second N application frequently resulted in different (P < 0.05) levels of yields while plant N uptakes at the VT stage showed insignificant differences (P > 0.05; Table 3.3).

Soil inorganic N availability in 0–0.3 m at the tasseling stage (after the second N application or 68–71 DAP) largely accounted for the final yield (Table 3.4; Fig. 3.5). This result is in line with the study conducted on sandy soils in Zimbabwe by Mtambanengwe and Mapfumo (2006). More often, relationships were set up between yield and N rate (Wang et al. 2017) or N rate plus soil available N before N application (Hartmann et al. 2015), for facilitating the determination of optimal N rate. Yet in the current study, I observed notable effects of inter-seasonal variations on the yields (i.e., residual N from the preceding study at TZm and decreased rainfall with erratic distribution at TZi). Also, the efficiency of applied urea in increasing plant-available N in soil could differ greatly between TZm and TZi (Fig. 3.4). It is therefore soil inorganic N availability after N application could integrate all these effects (direct and/or indirect) into one simple factor that significantly accounted for the final yield. The success of including all yield data in one linear-plateau model indicated the dominant control of soil inorganic N availability (0–0.3 m) at the tasseling stage over the final yield across sites and seasons.

A closer inspection on the yield–soil N response pattern (Fig. 3.5b) revealed that maize yield at TZi could still be limited by soil inorganic N availability at the tasseling stage, whereas yield at TZm may be co-limited by other nutrients (Njoroge et al. 2017) once the soil inorganic N availability was above 67 kg N ha^{-1}, considering the yield potential of the variety (Lyimo 2005). The yield plateau in the model for TZi should be interpreted with caution, as the maximum yield observed at TZi in this study was only 2.6 Mg ha^{-1}. Nevertheless, such a plateau of yields from the model fitting was supported by another experiment at TZi with higher N supply (~4 Mg ha^{-1}; see Chapter 5). Nutrient input through chemical fertilizer and/or organic resources could be indispensable in the infertile, sandy soil to ensure maize yield (Mtambanengwe and Mapfumo 2006; Masvaya et al. 2017). For example, yields at TZi from the 0N plots were below 0.2 Mg ha^{-1} due to limited soil inorganic N availability. However, maintaining high soil inorganic N availability simply by increasing urea-N rate at sandy soils like TZi could be challenging (Mtambanengwe and Mapfumo 2006) as a single N application of 100 kg ha^{-1} only increased ~18 kg ha^{-1} available N in soil (Fig. 3.4a). Such fast N depletion lowered the availability of applied N to maize, leading to the low N use efficiency (e.g., 17–23 kg grain kg^{-1} N applied at TZi vs. 29–57 kg grain kg^{-1} N applied at TZm) and insignificant ($P > 0.05$) difference in yields between the 100N and 150N treatments (the first season at TZi; Table 3.3).

3.4.4 Implications for N management in SSA croplands

Conserving the soil mineralized N in the early growing season has long been a challenge to improve N synchrony. Many approaches focus on reduced tillage (Masvaya et al. 2017) to delay net mineralization or application of low-quality organic resources (Sugihara et al. 2012a) to immobilize leachable N by microbes. The effect of reduced tillage may be too short-lived to improve the N synchrony (Chikowo et al. 2004) or even negative on maize yield (Masvaya et al. 2017). Although Gentile et al. (2008) showed in a laboratory incubation that adding a low-quality organic resource (i.e., high C:N ratio) had immobilized soil-derived N for more than 90 days, actual benefit on increasing crop yield in the field was seldom observed (Gentile et al. 2009; Chivenge et al. 2010; Sugihara et al. 2012a). Mechanistic studies and field verifications are needed to provide practical recommendations to immobilize the leachable N until mid-season for crop uptake. Nevertheless, fertilizer-N input can be reduced if mobile N can be utilized efficiently. In the second season of the current study, captured net nitrogen mineralization at the onset of rains provided ~33 and 47 kg N ha^{-1} in 0–0.3 m at TZi and TZm, respectively.

Maintaining high levels of available N in sandy soils (i.e., at TZi) and simultaneously achieving high recovery by crops is challenging (Mtambanengwe and Mapfumo 2006), as the sandy soil is more susceptible to NH_3 volatilization (e.g., from surface-applied urea in the current study) and N leaching loss. In the period of high crop N demand in sandy soils (e.g., at the tasseling stage in the current study), dissolving the urea in a water container and applied through an affordable, easy-to-construct dripping irrigation system (Postel et al. 2001; Kahimba et al. 2015) could be promising (schematic layout and examples of *in-situ* implementation of this system are provided as Fig. S3.3, S3.4 in the supplementary material). The main function of such dripping irrigation system is to increase N use efficiency (by reducing potential NH_3 loss without raising labor cost) rather than to supply water, yet in abnormally drought years/periods (e.g., 7–15 DAP in the second season at TZi) it can also serve for water supply to prevent yield failure.

At TZm, future research is required to identify the co-limiting nutrients to further improve the yield. Co-limitation of secondary nutrients or micronutrients on the yield in SSA croplands (Kihara et al. 2016) such as at TZm may be solved by applying animal manure (Zingore et al. 2007; Sileshi et al. 2016), which is unlikely to significantly increase the cost on smallholder farmers. Manure application before or at the time of planting for slower release of nutrients and side-dressing with proper urea-N rate (e.g., 75N based on Fig. 3.5) at the tasseling stage may achieve desirable yields in croplands with similar soil type to TZm.

3.5 Conclusions

In the current study, seasonal variations of soil inorganic N availability revealed the challenge of N management in the early growing season in SSA croplands: excessive soil mineralized N was susceptible to leaching loss due to limited crop N demand. Future researches should focus on how this excessive soil mineralized N can be immobilized until mid-season when crop N demand is high, and especially verification in the field that such immobilization benefits the crop yield. At higher urea-N rates (i.e., during the second application), soil type (i.e., sandy Alfisols at TZi vs. clayey Andisols at TZm) strongly affected the efficiency of applied urea in increasing plant-available N in soils. Fast depletion of applied urea-N at TZi was likely due to substantial N loss through NH_3 volatilization, as supported by the poorly pH-buffered soil with low CEC. This largely contributed to the different yield levels at two sites—lower at TZi (up to 2.6 Mg ha^{-1}) than TZm (up to 4.4 Mg ha^{-1}) under the same N rate. I also found that yield was strongly controlled by the soil inorganic N availability in 0–0.3 m at the tasseling stage (i.e., after the second N application or 68–71 DAP). Furthermore, maintaining high levels of N availability at the tasseling stage and supplying secondary nutrients or micronutrients would be the keys to further improve yields at TZi and TZm, respectively. These results contribute to a better understanding of temporal patterns of soil N pools across soil types and how they affect the yield response in SSA croplands, which is important for designing the best fertilizer-N management practices to achieve higher yield and lower environmental impact as N application rates increase.

Supplementary materials

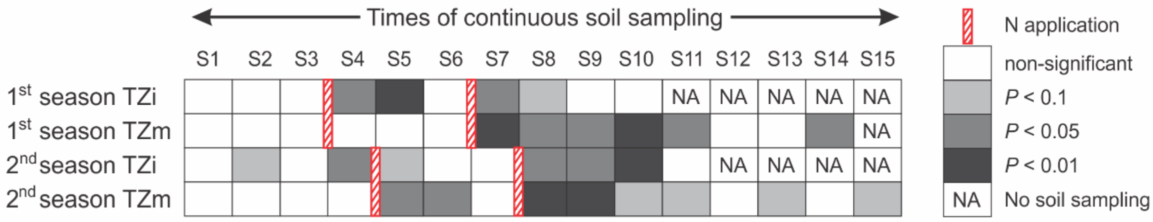

Fig. S 3.1 Results of mean comparison of soil inorganic N availability (0–0.3 m; kg N ha^{-1}) among N treatments at each sampling time.

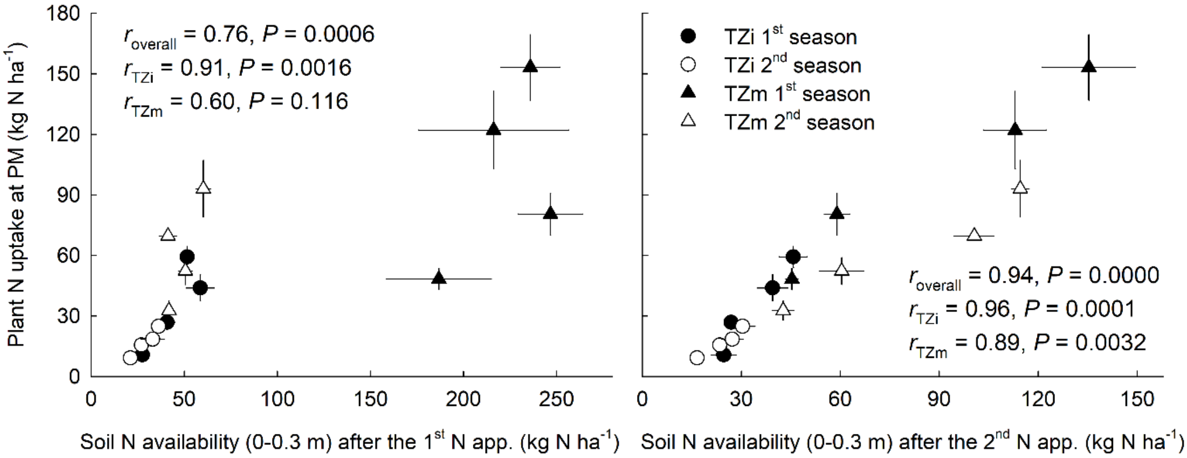

Fig. S3.2 Response of plant N uptake at the PM stage to the soil inorganic N availability (0–0.3 m) after the first and second N applications, respectively. Better correlation for the second N application may indicate that it contributed more to the total plant N uptake and consequently the yield compared with the first N application.

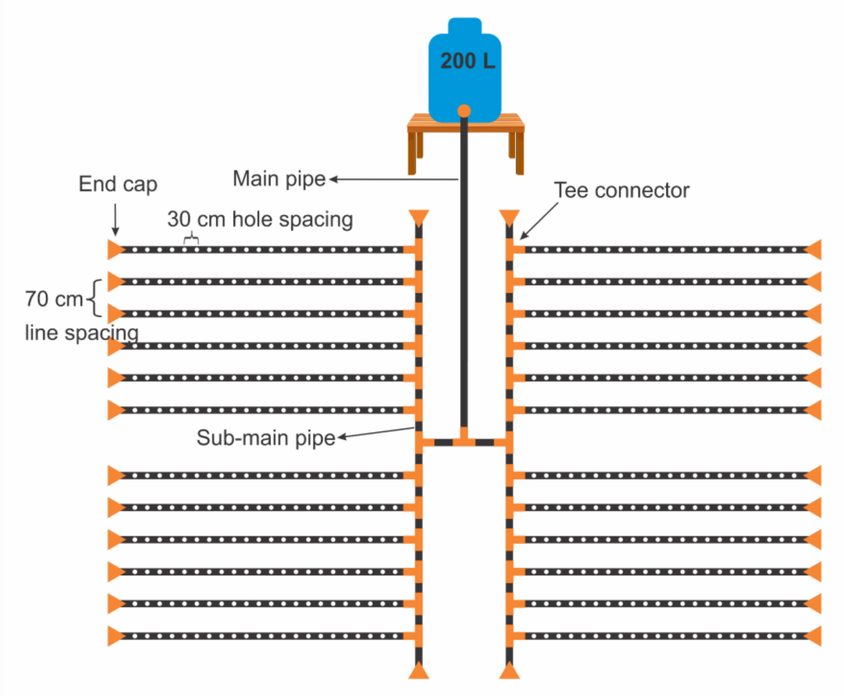

Fig. S3.3 Schematic layout of dripping irrigation (adapted from Postel et al., 2001 and Kahimba et al., 2015)

Fig. S3.4 Photographs showing examples of *in-situ* implementation of dripping irrigation in Kenya (a, b) and Tanzania (c, d). Photo credit and access: (a) L. Heng/IAEA; https://www.iaea.org/newscenter/news/more-bountiful-crops-every-drop-using-drip-irrigation-mauritius; (b) Softkenya; https://softkenya.com/kenya/drip-irrigation-in-kenya/; (c) SolutionMUS; http://www.solutionmus.org/solutionmus-in-action/locations/tanzania/; (d) Wisons.net; https://blogs.worldbank.org/taxonomy/term/17048. Accessed on 10 December 2017.

Table S3.1 Averaged values of soil NH_4^+-N and NO_3^--N concentrations (mg kg^{-1}) and the *F*-values from the results of repeated-measures ANOVA showing the effects of N application rate (N rate), sampling time, and their interactions on these variables

	TZi				TZm			
	0-15 cm		15-30 cm		0-15 cm		15-30 cm	
	NO_3^--N	NH_4^+-N	NO_3^--N	NH_4^+-N	NO_3^--N	NH_4^+-N	NO_3^--N	NH_4^+-N
The first season								
0N	3.2	2.5	2.3	2.2	21.6	8.6	11.6	8.7
50N	3.6	2.4	2.3	2.4	30.8	8.8	15.8	10.4
100N	4.2	3.0	2.9	2.7	32.9	9.6	16.9	9.1
150N	5.0	2.8	2.8	2.6	33.6	9.7	18.6	9.7
Source	*F*-values							
N rate	2.85^{ns}	2.99^{ns}	3.82^{ns}	1.76^{ns}	1.81^{ns}	1.31^{ns}	1.50^{ns}	1.57^{ns}
Sampling time (T)	35.2^{***}	7.88^{***}	83.5^{***}	13.5^{***}	44.8^{***}	39.2^{***}	45.3^{***}	28.3^{***}
N rate × T	2.59^{*}	1.21^{ns}	2.50^{*}	1.62^{ns}	1.80^{ns}	0.44^{ns}	0.54^{ns}	0.90^{ns}
The second season								
0N	1.1	3.7	1.0	3.5	7.4	7.9	4.5	8.2
50N	1.8	4.2	1.4	4.0	9.3	8.4	5.3	9.0
100N	2.1	4.9	1.7	3.9	11.3	8.6	6.8	9.1
150N	2.1	4.7	1.8	4.6	13.6	8.3	8.2	9.1
Source	*F*-values							
N rate	4.09^{*}	6.58^{*}	4.81^{*}	3.07^{ns}	7.74^{**}	0.37^{ns}	17.3^{**}	2.65^{ns}
Sampling time (T)	4.29^{*}	8.38^{**}	11.5^{***}	20.4^{***}	64.8^{***}	57.8^{***}	50.5^{***}	42.3^{***}
N rate × T	1.38^{ns}	0.46^{ns}	1.89^{ns}	0.61^{ns}	5.30^{**}	0.44^{ns}	3.89^{**}	0.32^{ns}

* = $P < 0.05$, ** = $P < 0.01$, *** = $P < 0.001$, ns = non-significant.

CHAPTER 4

Ammonia Volatilization Following Urea Application at Maize Fields in the East African Highlands with Different Soil Properties

Abstract

Use of nitrogen (N) fertilizer is underway to increase in Sub-Saharan Africa (SSA). The effect of increasing N rates on ammonia (NH_3) volatilization—a main pathway of applied-N loss in cropping systems—has not been evaluated in this region. In two soils (Alfisols, ALF; and Andisols, AND) with maize crop in the East African highlands, I measured NH_3 volatilization following urea broadcast at six rates (0–150 kg N ha^{-1}) for 17 days, using a semi-open static chamber method. Immediate irrigation and urea deep placement were tested as mitigation treatments. The underlying mechanism was assessed by monitoring soil pH and mineral N (NH_4^+ and NO_3^-) concentrations. More cumulative NH_3-N was volatilized in ALF than in AND at the same urea-N rate. Generally, higher urea-N rates increased proportional NH_3-N loss (% of applied N loss as NH_3-N). Based on well-fitted sigmoid models, simple surface urea application is not recommended for ALF, while up to 60 kg N ha^{-1} could be adopted for AND soils. The susceptibility of ALF to NH_3 loss mainly resulted from its low pH buffering capacity, low cation exchange capacity, and high urease activity. Both mitigation treatments were effective. The inhibited rise of soil pH but not NH_4^+ concentration was the main reason for the mitigated NH_3-N losses, although nitrification in the irrigation treatment might also have contributed. These results showed that in acidic soils common to SSA croplands, the proportional NH_3-N loss can be substantial even at a low urea-N rate; and that the design of mitigation treatments should consider the soil's inherent capacity to buffer NH_3 loss.

4.1 Introduction

Globally, ammonia (NH_3) volatilization from the application of synthetic nitrogen (N) fertilizers accounts for about 14% of annual NH_3-N emissions (Bouwman et al. 2002a). This N loss as emitted NH_3 causes a no-win situation between resource utilization and eco-environmental conservation. Ammonia loss from applied N results in low fertilizer-N use efficiency, posing a substantial financial cost to farmers (Pan et al. 2016). Furthermore, this N resource loss from agricultural systems turns into pollutants in the atmosphere and causes cascading effects (Galloway et al. 2003) including soil acidification, eutrophication, and declining biodiversity (e.g., Scudlark et al. 2005).

Increased use of fertilizer (especially N) is unequivocally a critical step in offsetting soil nutrient depletion and securing food production in Sub-Saharan Africa (SSA). Use of fertilizer-N in SSA is extremely limited; typically less than 10 kg N ha^{-1} yr^{-1} (Vitousek et al. 2009), which is the main cause of stagnantly low yields of cereal production in past decades. Regional and national efforts are underway to increase fertilizer use six-fold to reach an average of 50 kg mineral fertilizer ha^{-1} yr^{-1} (AGRA 2009). In trial sites of the Millennium Villages Project, the recommended application rate of N for maize (*Zea mays* L.) cultivation varied regionally up to 129 kg N ha^{-1} based on national research and extension services (Nziguheba et al. 2010). Considering the low N input in current African croplands, Hickman et al. (2015) pointed out that at least 6 Tg N yr^{-1} would be required just to reach an average application rate of 75 kg N ha^{-1} yr^{-1} for cereal production on existing agricultural land. This unprecedented amount of N input will be subject to a large amount of NH_3-N loss if not properly managed, provided that urea heavily dominates N fertilizer consumption (over 50%; IFA 2017) and topdressing of urea is the most common N management practice across SSA croplands.

Surprisingly, field measurements of NH_3 volatilization from applied fertilizer in SSA croplands are rare, and to my knowledge, the way that NH_3 loss responds to increasing rates of N application has not yet been evaluated in this region. Understanding the relationship between NH_3 volatilization and increasing N application rates is urgently needed to develop proper guidance on N management practices for local farmers. Field measurements in SSA are also essential to reducing uncertainties in the global synthetic analysis of NH_3 emissions (Pan et al. 2016; Jiang et al. 2017).

Urea is the most extensively used N fertilizer in tropical agroecosystems (IFA 2017). Its hydrolysis is known as a key process in inducing NH_3 volatilization by producing highly concentrated NH_4^+ with sharply raised pH (Black et al. 1987b). In acidic soils common to SSA croplands, pH rises during urea hydrolysis owing to proton consumption by hydrolyzed CO_3^{2-} and HCO_3^- (Ferguson et al. 1984). As the pH increases, NH_3 volatilization occurs owing to the reaction between OH^- and NH_4^+. Therefore, mitigation strategies have been developed based mainly on two goals: reducing NH_4^+ concentration and inhibiting pH rise. The former includes retarding urea hydrolysis with urease inhibitors (Cantu et al. 2017) and physical absorption of NH_4^+ by applied biochar (Subedi et al. 2015). The latter includes amendments with acidifying effects, e.g. pyrite with copper sulphate (Reddy and

Sharma 2000). Acceleration of the nitrification process by activating nitrifying bacteria can reduce both soil NH_4^+ concentration and pH (Fleisher and Hagin 1981).

The soil's inherent capacity to buffer NH_3 loss after urea application, however, is rarely involved in the design of mitigation strategy. Soils with high cation exchange capacity (CEC) and pH buffering capacity (PBC) are likely to have low NH_3 emissions even when the added amount of urea is considerable (Haden et al. 2011). Soil properties like CEC and PBC can vary extensively across soils (Haden et al. 2011), resulting in variable inherent capacity of the soil to buffer NH_3 loss. Therefore, soil-specific assessment is essential to developing a practical mitigation strategy. Some farming practices like irrigation and deep placement of urea are also well-established strategies for mitigating NH_3 volatilization (Holcomb et al. 2011; Rochette et al. 2013a); nevertheless, their performance should be tested under practical situations.

Increasing the urea application rate can be expected to change the soil NH_4^+ concentration and pH range, which is expected to affect NH_3 volatilization. Interestingly, previous studies have reported inconsistent results on the effect of urea-N rate on proportional NH_3-N loss (% of applied N loss as NH_3-N; or simply the emission factor), even within the category of acidic soil. Black et al. (1987a) reported a positive effect, Tian et al. (2001) and Rimski-Korsakov et al. (2012) indicated a negative effect, and Watson and Kilpatrick (1991) showed no clear correlation between urea application rate and proportional NH_3-N loss. As pointed out by Bouwman et al. (2002a), different factors (e.g., soil and environmental) and processes (e.g., urea hydrolysis and nitrification) interact. This is supported by a seven-year site study by Ma et al. (2010), where tremendous variation in NH_3 volatilization was observed both across years within the same soil type and across soil types within the same year.

Maize is the staple food for SSA people. Highlands in East Africa are generally densely populated and intensively cultivated for production, and are known as the "bread basket." For example, in Tanzania, about 46% of maize production is contributed by the southern highlands, which make up only 28% of the mainland area of this country (Bisanda et al. 1998).

The aim of this study was therefore to evaluate the effect of urea application rate on NH_3 volatilization in SSA croplands with different soil properties. The specific objectives were to (1) quantify the amount of NH_3 volatilization and emission factors as affected by urea application rate and soil properties; (2) determine the soil's inherent capacity to buffer NH_3 loss, above which large NH_3 losses occur; and (3) figure out effective strategies to mitigate NH_3 losses and assess the underlying mechanism in maize fields in the East African highlands.

4.2 Materials and methods

4.2.1 Site description

Field experiments were conducted at two maize fields with different soil properties in the East African highlands. One site is located in the village of Mangalali in the Iringa region of Tanzania (07°46′

S, 35°34′ E), which has an elevation of 1480 m. Maize has been cultivated by local farmers for more than five years. The soil is classified as coarse-loamy, isohyperthermic, Kanhaplic Haplustalfs (ALF). The other site is located in the town of Uyole in the Mbeya region of Tanzania (08°55′ S, 33°31′ E), which has an elevation of 1780 m. It is used as experimental maize plots inside the Mbeya Agricultural Training Institute. The soil is classified as clay-loam, isothermic, Dystric Vitric Haplustands (AND). Soil classification was performed based on the USDA system (Soil Survey Staff, 2010). Detailed properties of ALF and AND are presented in Table 4.1.

Table 4.1 Physical and biochemical properties of soil from top10 cm

Property	ALF	AND	*P* value
Sand / %	88.4	29.6	–
Silt / %	6.9	42.0	–
Clay / %	4.7	28.4	–
TC / %	0.53 ± 0.02	2.02 ± 0.02	<0.001
TN / %	0.04 ± 0.002	0.16 ± 0.001	<0.001
pH initial / 1:5 H_2O	5.66 ± 0.07	6.34 ± 0.02	<0.001
CEC / $cmol_c\ kg^{-1}$	1.3 ± 0.3	18.9 ± 0.3	<0.001
Ca^{2+} / $cmol_c\ kg^{-1}$	1.3 ± 0.05	6.1 ± 0.3	<0.001
Mg^{2+} / $cmol_c\ kg^{-1}$	0.15 ± 0.02	1.71 ± 0.15	0.008
Na^{+} / $cmol_c\ kg^{-1}$	0.02 ± 0.003	0.13 ± 0.015	0.002
K^{+} / $cmol_c\ kg^{-1}$	0.09 ± 0.005	2.12 ± 0.13	0.004
PBC / mmol OH^{-} kg^{-1}	9.5 ± 0.3	57.1 ± 0.3	<0.001
WHC / %	27.3 ± 0.1	66.3 ± 0.9	<0.001
UA_1[a] / μg N g^{-1} $hour^{-1}$	8.0 ± 0.8	4.9 ± 0.2	0.019
UA_2[a] / μg N g^{-1} $hour^{-1}$	11.0 ± 1.5	6.0 ± 0.2	0.028
UA_3[a] / μg N g^{-1} $hour^{-1}$	74.0 ± 6.4	22.2 ± 5.9	0.004

CEC cation exchange capacity, *PBC* pH buffering capacity, measured as consumption of OH^{-} at pH 8.3 (Fig. S4.1), *WHC* maximum water holding capacity.

[a] UA_1, urease activity measured at 25 °C without pH buffer; UA_2, urease activity measured at 37 °C without pH buffer; UA_3, urease activity measured at 37 °C with pH buffer.

4.2.2 Experimental design and treatments

At each site, maize (*Zea mays* L.) was grown in a field (~700 m^2) with a spacing of 0.7 m × 0.3 m, giving a population of ~48000 plants ha^{-1}. To facilitate the experimental setup and sampling process, I cleared a small area (6 m × 8 m) from the field before the start of the experiment. Ammonia volatilization was measured on this area without maize cultivation. Maize removal was not expected to affect the experiment because I focused on the NH_3 volatilization from soils applied with urea. Further, volatilized NH_3 was measured with enclosures (see the semi-open static chamber system below), which largely excluded the interaction between crop and the fertilizer inside the enclosure, leading to a negligible difference between field conditions of maize removal and maize under cultivation. Enclosures are much used in the field experiments allowing many treatments to be evaluated in the same field (Sommer et al. 2004).

For the measurement of NH_3 volatilization, a randomized complete block design was adopted for eight treatments: six urea application rates with surface broadcast (0, 30, 50, 70, 100, and 150 kg N ha^{-1}, denoted as 0N, 30N, 50N, 70N, 100N, and 150N, respectively) and two mitigation treatments with an application rate of 100 kg N ha^{-1} (irrigation of 10 mm water immediately after urea application, denoted as 100N+W; and deep placement of urea at 5 cm depth, 100N+DP). Three replicates were measured for each treatment, resulting in a total of 24 plots. Each plot was 0.5 m × 0.5 m in size. Plots were separated by a 0.5 m buffer. The plot size was designed based on the size of the chamber for NH_3 volatilization measurement (12 cm diameter cylinder; see below). According to local practices, urea is always applied after rainfall during the rainy season. I therefore applied irrigation equivalent to 5 mm rainfall to the ALF plots one day before starting the experiment. In the AND plots, the experiment was started one day after a rainfall event (22 mm).

Adjacent to the plots for NH_3 volatilization measurement, nine plots (0.5 m × 0.5 m size; separated by a 0.5 m buffer) receiving three treatments (100N, 100N+W, and 100N+DP; with three replicates) in a randomized complete block design were set up for soil sampling.

4.2.3 NH_3 volatilization measurement

A semi-open static chamber system was used for NH_3 volatilization measurement. A polyvinyl chloride cylinder of 12 cm diameter and 30 cm height was inserted about 10 cm into the soil at each plot. Two foam disks with a density of 0.026 g cm^{-3} and a thickness of 2 cm were placed horizontally inside each chamber at 10 cm and 20 cm above the soil surface, respectively. The lower disk trapped NH_3 volatilized from the soil, while the higher one prevented contamination from atmospheric NH_3. The diameter of the foam disks was made slightly larger than that of the chamber so that they would remain in place when the foam expanded against the sides of the chamber. These foam disks were soaked with acid reagents (1 M H_3PO_4 + 4% v/v glycerol) before use. A volume of 20 ml of acid reagent was verified to be sufficient to saturate the foam disk evenly but not drip from the foam or leach down the sides of the chamber. During the experimental period, the chamber was sheltered from the direct effects of rainfall and sunshine with a round PVC plate (42.5 cm in diameter) supported by four wood sticks driven into the soil. The plate was slightly inclined by adjusting the heights of the wood sticks and placed about 10 cm above the top of the chamber to allow air flow.

The foam disks were collected and replaced with freshly soaked foams 1, 3, 5, 7, 9, 12, and 17 days after urea application. Foam disks were sealed in plastic bags during transport. The trapped NH_4^+ was extracted by three sequential extractions with 100, 100, and 50 ml of 1 M KCl. Each time after adding KCl solution, the foam disk was squeezed 10 times by hand and the extract was then transferred to a 500 ml volumetric flask. The final volume of the KCl extract was then brought to 500 ml by adding 1 M KCl. To verify the reliability of this extraction method, several fourth extractions were conducted for samples from the 150N treatment, and these confirmed that the amounts of NH_4^+ remaining were negligible. The KCl extract was filtered (No. 6 filter paper, Adventec, Japan) and determined colorimetrically using a flow injection auto-analyzer (Flow Analysis Method, JIS K-0170, AQLA-700 Flow Injection Analyzer, Aqualab Inc., Japan).

4.2.4 Environmental monitoring

At each site, in the plots used for NH_3 volatilization measurement, four soil moisture probes (ECH$_2$O TE, Decagon Devices, Inc., USA) were connected to a digital data logger (Em50, Decagon Devices, Inc., USA) to monitor soil moisture and temperature at a 5 cm depth, at a frequency of every minute. One of these four sensors was inserted into the ambient field, while the other three were used for soils inside the chambers receiving the 100N, 100N+W, and 100N+DP treatments, respectively. Soil moisture expressed as volumetric water content was separately calibrated with soils sampled from each field (R^2 = 0.96 for the calibration function with n = 8 in ALF and R^2 = 0.97 with n = 5 in AND). Rainfall at each site was recorded every 10 minutes by a TE525MM rain gauge connected to a CR1000 data logger (Campbell Scientific, Inc., USA).

4.2.5 Soil sampling and analysis

In the 24 plots used for NH_3 volatilization measurement, soils were sampled from the top layer (0−10 cm) before urea application to evaluate the initial soil characteristics. Soils were air-dried and sieved through 2-mm mesh before being transported to Japan for analysis of total C (TC), total N (TN), pH (initial pH), major exchangeable cations (Ca^{2+}, Mg^{2+}, Na^+, K^+), CEC, PBC, and urease activity. Air-drying was verified to have negligible influence on the soil urease activity in this study (see Fig. S4.2 in the supplementary material).

The contents of TC and TN were determined with a CN analyzer (Vario Max CN, Elementar, Germany). Major exchangeable cations were extracted with 1 M ammonium acetate at pH 7.0. Exchangeable Ca^{2+} and Mg^{2+} were determined by atomic absorption spectroscopy and Na^+ and K^+ by flame emission spectroscopy (AA-660 instrument, Shimadzu, Japan). To determine CEC, I washed the residual soil with ethanol after ammonium acetate extraction and then extracted the remaining NH_4^+ with 10% sodium chloride. Extracted NH_4^+ was determined by steam distillation and titration. To determine PBC, titratable acidity was measured following Sakurai et al. (1989) with a potentiometric automatic titrator (COM-1600, Hiranuma Sangyo Co., Ltd., Japan). Consumption of OH^- at pH 8.3 was used to represent PBC, which is thus expressed as mmol OH^- kg^{-1} soil (Fig. S4.1). Soil urease activity was determined as the release of NH_4^+-N after 2-hour incubation following the procedure by Kandeler and Gerber (1988). Urease activity was determined at 25 °C (without pH buffer) and 37 °C (with and without pH buffer); and expressed as mg NH_4^+-N kg^{-1} soil $hour^{-1}$.

In the nine plots specially set up for soil sampling, chambers were also installed to maintain a similar condition to the plots for NH_3 measurement, but with a larger diameter (35 cm). The larger area covered allowed two subsamples to be taken from the chamber during each sampling activity. Two subsamples were mixed to reduce uncertainties caused by sampling error. Soil samplings were conducted at 0, 1, 3, 5, 7, 9, 12, and 17 days after urea application, and were analyzed for soil moisture, pH, and mineral N (NH_4^+ and NO_3^-) concentrations. To detect whether immediate irrigation can move dissolved urea and NH_4^+ down to deeper soil and thereby reduce the surface NH_4^+ concentration, I sampled only the upper 3−4 cm soil from the 100N and 100N+W treatments. This is because the vertical diffusion of urea-N and NH_4^+ are often limited to within 3 cm after surface urea application (Black et al. 1987b). For the 100N+DP treatment, in order to capture the effect of deep placement of urea on pH change, I sampled soil from the top 7 cm covering the placement depth.

Field moist soils (around 50 g for each sample) were immediately transported to the local laboratory for oven drying at 60 °C after recording the total moist weight. The dry weight of each sample was then recorded before sieving through 2-mm mesh for subsequent analysis at the laboratory in Japan. The difference in soil weight before and after oven drying, together with bulk density, was used to calculate the volumetric water content. The soil pH (1:5 soil: water ratio) was measured with a glass electrode (pH/ion meter LUQUA F-74BW, Horiba Ltd., Japan). Mineral N was extracted from 10.0 g soil (dry base) with 30.0 ml of 1 M KCl for 30 min on a reciprocating shaker, and the suspension was centrifuged (2000×g, 10 min) and filtered through filter paper (No. 6, Advantec, Japan). Extracted NH_4^+ and NO_3^- were determined colorimetrically using the same flow injection auto-analyzer (Flow Analysis Method, JIS K-0170, AQLA-700 Flow Injection Analyzer, Aqualab Inc., Japan).

4.2.6 Statistical analysis

An independent two-sample *t*-test was used to examine whether initial soil characteristics differed between the two sites. Two-way analysis of variance (ANOVA) was used to examine the effects of site and urea-N rate on cumulative NH_3-N loss, with the interaction site × block included as a between-subjects factor to reduce experimental error from source of variation. Residuals were plotted with fitted values to check the model assumptions of independence and common variance. Normality of the residuals was checked by the Shapiro-Wilk test. Levene's test was applied to statistically check equal variance across treatments. The statistically significant differences were identified as $P < 0.05$ unless stated otherwise. For three treatments (100N, 100N+W, and 100N+DP), Pearson correlation was conducted between NH_3-N loss and the soil variables of mineral N concentration, pH, and moisture content, respectively.

A linear function was fitted to cumulative NH_3-N loss with urea-N rate for ALF, while a piecewise function was fitted for AND. The breakpoint in the piecewise function was statistically estimated using the *segmented* package for the R software version 3.3.3 (http://www.r-project.org). Sigmoid (three and four parameters), exponential (growth and rise to maximum), and quadratic curves were fitted to proportional NH_3-N loss with urea-N rate at each site using the non-linear least square method (the *nls* function in R). Model comparison was conducted using the Bayesian Information Criterion (BIC) together with 'pseudo R^2', which was calculated as 1 – (residual sum of squares/total sum of squares). All statistical analyses were carried out with R (version 3.3.3).

4.3 Results

4.3.1 Soil properties and environmental factors

Significant differences ($P < 0.05$) in initial soil characteristics were observed between ALF and AND, as shown in Table 4.1. ALF was lower in TC, TN, initial pH, CEC, major cations, PBC, and water holding capacity as compared with AND, but higher in urease activity measured under all conditions (25 °C without pH buffer, 37 °C with and without pH buffer).

Rainfall distribution, temporal variation of soil moisture, and temperature at 5 cm depth in the field and inside the chambers under three treatments (100N, 100N+W, and 100N+DP) are presented in Fig. 4.1. After the experiment started, several rainfall events were recorded in ALF but not in AND plots. Large difference of soil moisture between the 100N treatment and the field was observed in ALF but not AND (Fig. 4.1). In ALF, lower soil moisture in the 100N treatment compared with that in the field was attributed to the shelters above the chamber, which prevented direct water supply from rainfall. In AND, no difference of soil moisture between the 100N treatment and the field was expected as no rainfall events occurred after starting the experiment. At both ALF and AND, soil moisture was higher in 100N+W, followed by 100N, and lower in 100N+DP. The practice of deep placement probably reduced the soil bulk density and resulted in lower volumetric water content. Averaged daily soil temperature inside the chamber was higher for ALF (22.3 °C) than for AND (17.3 °C) and was negligibly affected by the treatments. Daily maximum soil temperature was lower inside the chambers compared with that in fields in both ALF and AND.

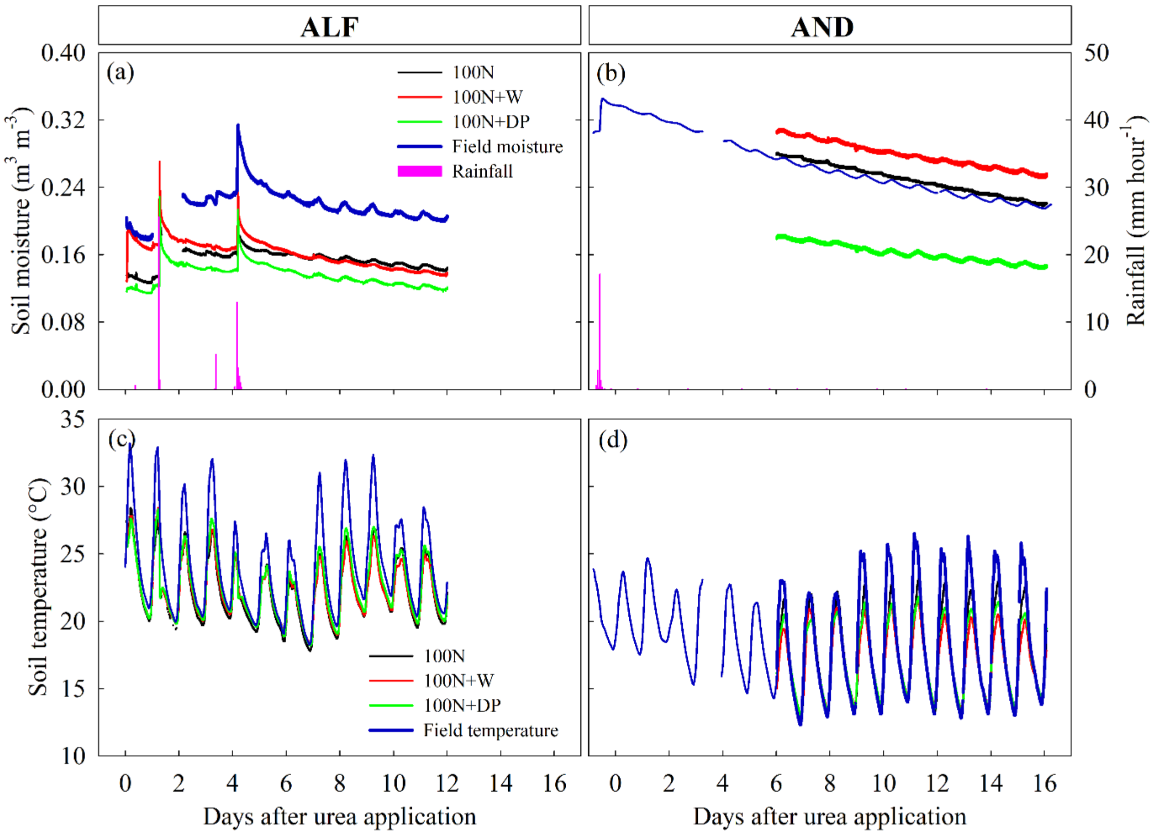

Fig. 4.1 Environmental factors including (a, b) soil moisture and (c, d) temperatures of three treatments (100N, 100N+W, and 100N+DP) and the field as well as rainfall monitored during the study period in ALF and AND, respectively. *100N* surface application of urea with 100 kg N ha^{-1}, *100N+W* irrigation of 10 mm water immediately after urea application with 100 kg N ha^{-1}, *100N+DP* deep placement of urea (100 kg N ha^{-1}) at 5 cm depth.

4.3.2 NH_3 volatilization under different urea-N rates at two croplands

NH_3-N loss between sampling dates differed by urea-N rate and sampling time during the first week after urea application at both ALF and AND (Fig. 4.2). NH_3-N loss from the 0N treatment remained low and constant across the study period at both sites. In urea-applied plots, the peak of NH_3-N loss between sampling dates occurred on sampling day 3, with the peak in ALF much higher than that in AND under the same urea-N rate (Fig. 4.2). On sampling day 3, NH_3-N loss between sampling dates contributed 73–82% and 42–55% of the cumulative NH_3-N loss in ALF and AND, respectively. NH_3-N loss between sampling dates dropped progressively to a low level after sampling day 3 in ALF, while it extended to sampling day 7 in AND.

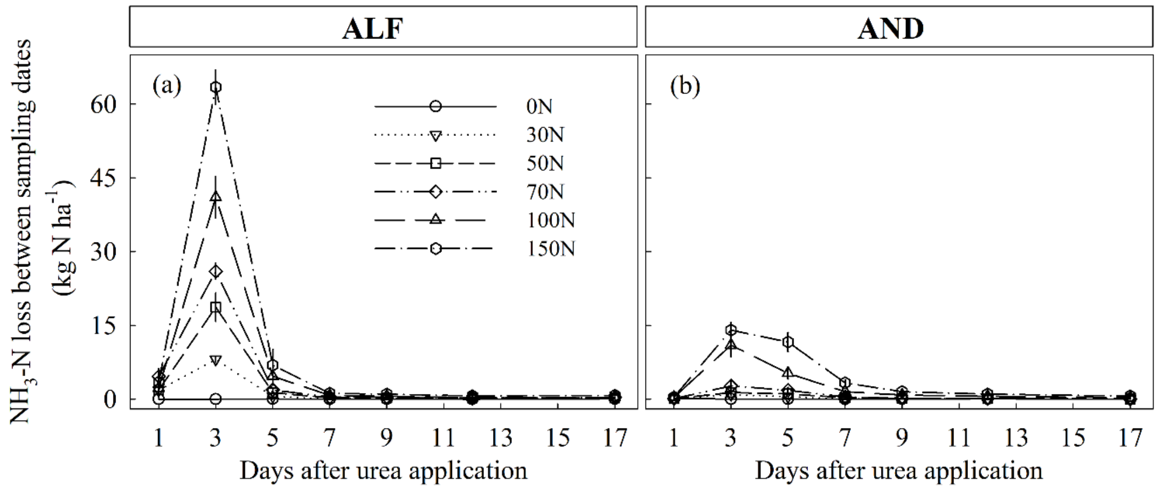

Fig. 4.2 Fluctuation of NH_3-N loss between sampling dates under different urea-N rates at (a) ALF and (b) AND. Error bars represent standard errors of the means (n = 3).

The cumulative NH_3-N loss was significantly (P < 0.001) affected by urea-N rate, and the significant interaction (P < 0.001) of urea-N rate × site resulted in consistently higher—more than double—cumulative NH_3-N loss from ALF than from AND at the same urea-N rate (Tables 4.2, S4.1). In urea-applied plots, cumulative NH_3-N loss ranged from 11.1 to 77.6 kg N ha^{-1} and from 1.9 to 32.7 kg N ha^{-1} for ALF and AND, respectively, corresponding to the range of proportional NH_3-N loss from 36.4 to 51.6% and from 5.2 to 21.6%, respectively (Table S4.1). In ALF, the first three days contributed to more than 85% of cumulative NH_3-N losses in all urea-applied plots, while it took seven days to reach a similar contribution in AND.

Table 4.2 Two-way ANOVA showing the effects of urea-N rate and site on the cumulative NH_3-N loss

Source	DF	MSq	*F*	*P*
Urea-N rate	5	2476.9	306.8	<0.001
Site	1	4381.5	542.7	<0.001
Block × Site	4	17.6	2.2	0.108
Urea-N rate × Site	5	387.1	47.9	<0.001
Residual	20	8.1		

DF degrees of freedom, *MSq* mean square

The response of cumulative NH_3-N loss to increasing urea-N rates varied across sites (Fig. 4.3a, b). A linear pattern (R^2 = 0.996, P < 0.001) with a relatively high slope (0.527) was observed in ALF (Fig. 4.3a). The intercept with urea-N rate showed that only about 5 kg N ha^{-1} could be applied without subjecting to NH_3-N loss. In AND, a piecewise pattern (R^2 = 0.96, P = 0.02) was found, with a breaking point occurring at a urea-N rate of 59 kg N ha^{-1} (Fig. 4.3b), indicating a threshold of cumulative NH_3-N loss at much higher urea-N rate.

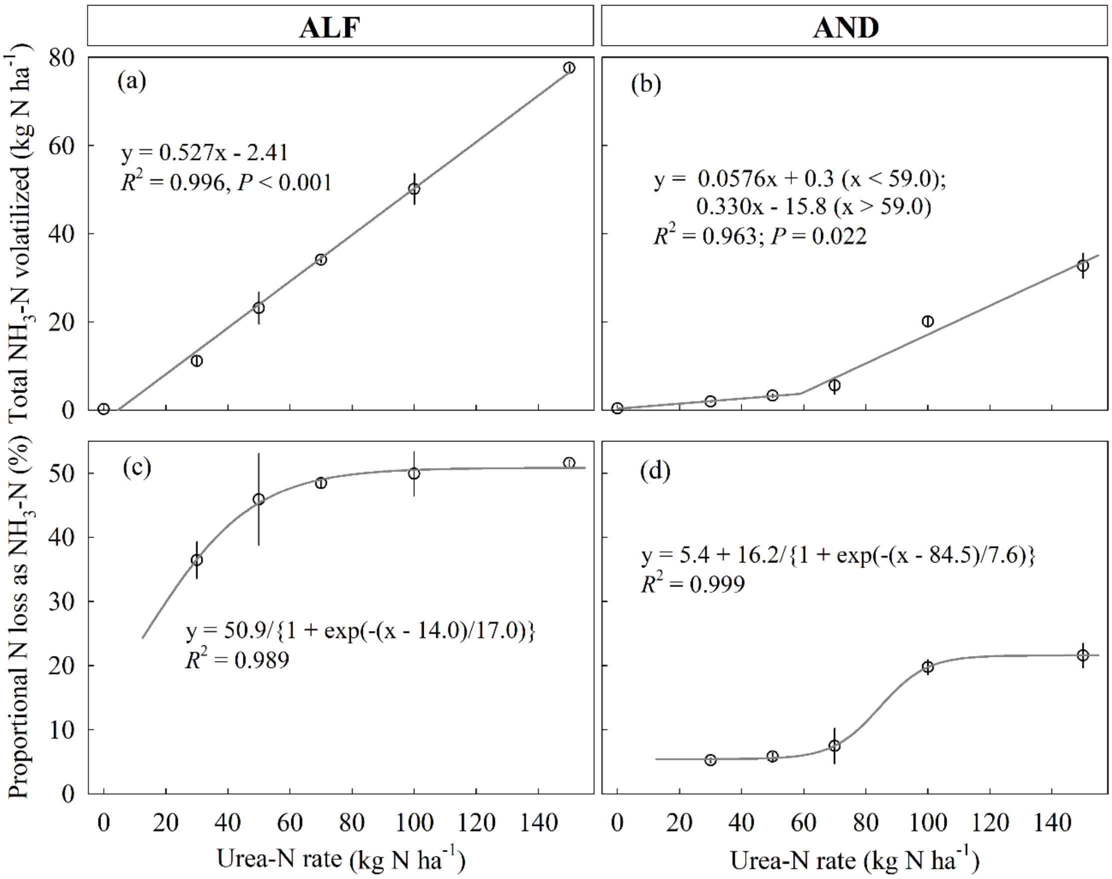

Fig. 4.3 Response pattern of (a, b) cumulative NH_3-N loss and (c, d) proportional NH_3-N loss to increasing urea-N rates in ALF and AND, respectively. Error bars represent standard errors of the means (n = 3).

In describing the response of proportional NH_3-N loss to urea-N rate, a sigmoid model with three parameters (BIC = 14.8) was equally well fitted as an exponential rise to maximum model (BIC = 12.7) for ALF (Table 4.3). A sigmoid model with four parameters (BIC = 2.2) provided a clearly better fit than any other models for AND (Table 4.3). Both well-fitted models for ALF showed a sharp increase in proportional N loss and reached a ceiling level (51%, as indicated by the parameter *a* in both models) with increasing urea-N rate (Fig. 4.3c; Table 4.3). In the sigmoid curve for AND, a “lag phase” of low proportional N loss was observed before the fast “growing phase” and the final “maximum phase” (Fig. 4.3d). The “lag phase” representing the inherent capacity of the soil to buffer NH_3-N loss was missing in ALF, while a range of urea-N rate from 0 to 60 kg N ha^{-1} could be safely adopted in AND. As indicated by the parameter *b* in sigmoid models for ALF and AND (Table 4.3), the maximum increasing rate of proportional NH_3-N loss occurred at a much lower rate of urea-N in ALF (14 kg N ha^{-1}) than in AND (84 kg N ha^{-1}).

Table 4.3 Model parameters, Bayesian information criterion (BIC), and R^2 for models describing the proportional NH_3-N loss in response to urea-N rate (u) at each site

	ALF			AND		
Model	Parameter estimates	BIC	R^2	Parameter estimates	BIC	R^2
Sigmoid with 3 parameters $a/\{1 + \exp(-(u - b)/c)\}$	a = 50.851 b = 13.993 c = 17.043	14.8	0.989	a = 23.241 b = 75.380 c = 22.454	27.6	0.922
Sigmoid with 4 parameters $y_0 + a/\{1 + \exp(-(u - b)/c)\}$	NC	–	–	y_0 = 5.397 a = 16.185 b = 84.490 c = 7.585	2.2	0.999
Exponential growth $a \times \exp(b \times u)$	a = 39.070 b = 0.00212	30.5	0.651	a = 4.550 b = 0.0109	30.8	0.796
Exponential rise to maximum $a \times \{1 - \exp(-b \times u)\}$	a = 51.318 b = 0.0421	12.7	0.994	NC	–	–
Quadratic $a + (b \times u) + (c \times u^2)$	a = 26.787 b = 0.424 c = −0.00174	24.7	0.922	a = −3.027 b = 0.224 c = -3.56×10^{-4}	30.2	0.868

NC not converged, R^2 was calculated as 1 − (residual sum of squares/total sum of squares).

4.3.3 Performance of NH_3-N loss mitigation treatments

At the two sites, both mitigation treatments (100N+W and 100N+DP) effectively reduced the cumulative NH_3-N loss (Fig. 4.4) to near-background level (the 0N treatment). At each site, cumulative NH_3-N loss from 100N+W (0.7 and 1.6 kg N ha^{-1} in ALF and AND, respectively) was slightly higher than that from 100N+DP (0.2 and 0.3 kg N ha^{-1} in ALF and AND, respectively), but not significantly different ($P > 0.9$ and $P > 0.3$ in ALF and AND, respectively).

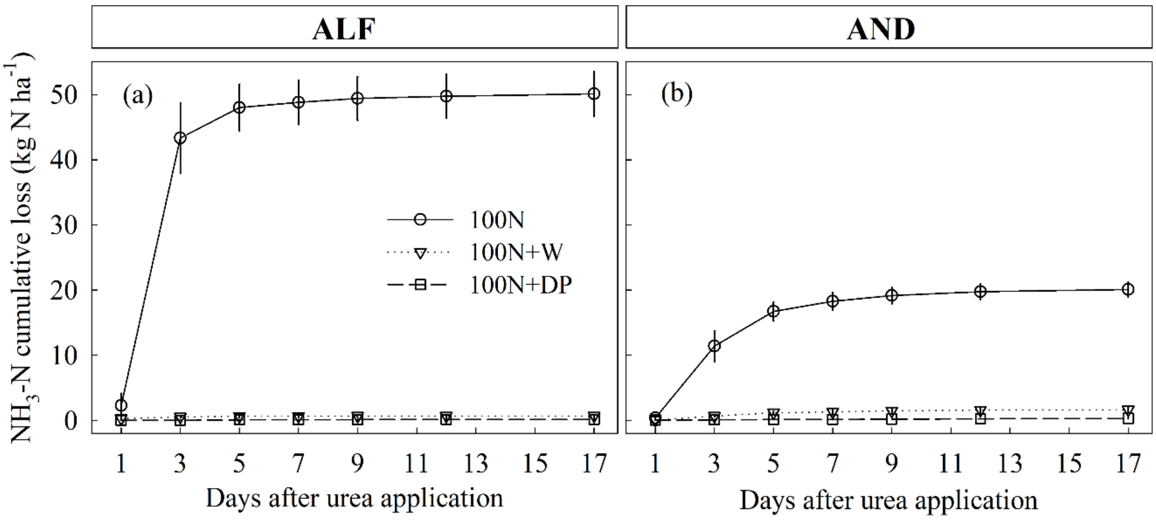

Fig. 4.4 Performance of mitigation treatments in reducing cumulative NH_3-N loss after urea application at (a) ALF and (b) AND. *100N* surface application of urea with 100 kg N ha^{-1}, *100N+W* irrigation of 10 mm water immediately after urea application with 100 kg N ha^{-1}, *100N+DP* deep placement of urea (100 kg N ha^{-1}) at 5 cm depth. Error bars represent standard errors of the means (n = 3).

4.3.4 Variation in soil mineral N, pH, and moisture

Soil NH_4^+ concentrations varied in response to treatment (100N, 100N+W, and 100N+DP) and sampling time at both ALF and AND (Fig. 4.5a, b). At each site, soil NH_4^+ concentrations in the 100N treatment peaked after urea application and were consistently higher than those in the other two treatments (100N+W and 100N+DP; Fig. 4.5a, b; Table S4.2). Soil NH_4^+ concentrations in the 100N treatment ranged from 1.5 to 140 mg N kg^{-1} in ALF, and from 44 to 428 mg N kg^{-1} in AND. At each site, the 100N+W and 100N+DP treatments resulted in similar soil NH_4^+ concentrations, ranging from 1.5 to 79 mg N kg^{-1} in ALF and from 44 to 200 mg N kg^{-1} in AND, respectively. At each site, soil NO_3^- concentrations were generally higher in the 100N+W treatment after urea application, and the variations in the other two treatments were similar (Fig. 4.5c, d). In ALF, soil NO_3^- concentrations gradually increased from 1.6 mg N kg^{-1} to a similar level (ca. 72 mg N kg^{-1}) among the three treatments (Fig. 4.5c). In AND, the range of soil NO_3^- concentrations was much larger in the 100N+W treatment (5.8–219 mg N kg^{-1}) than in the other two treatments with a similar range (5.8–130 mg N kg^{-1}; Fig. 4.5d).

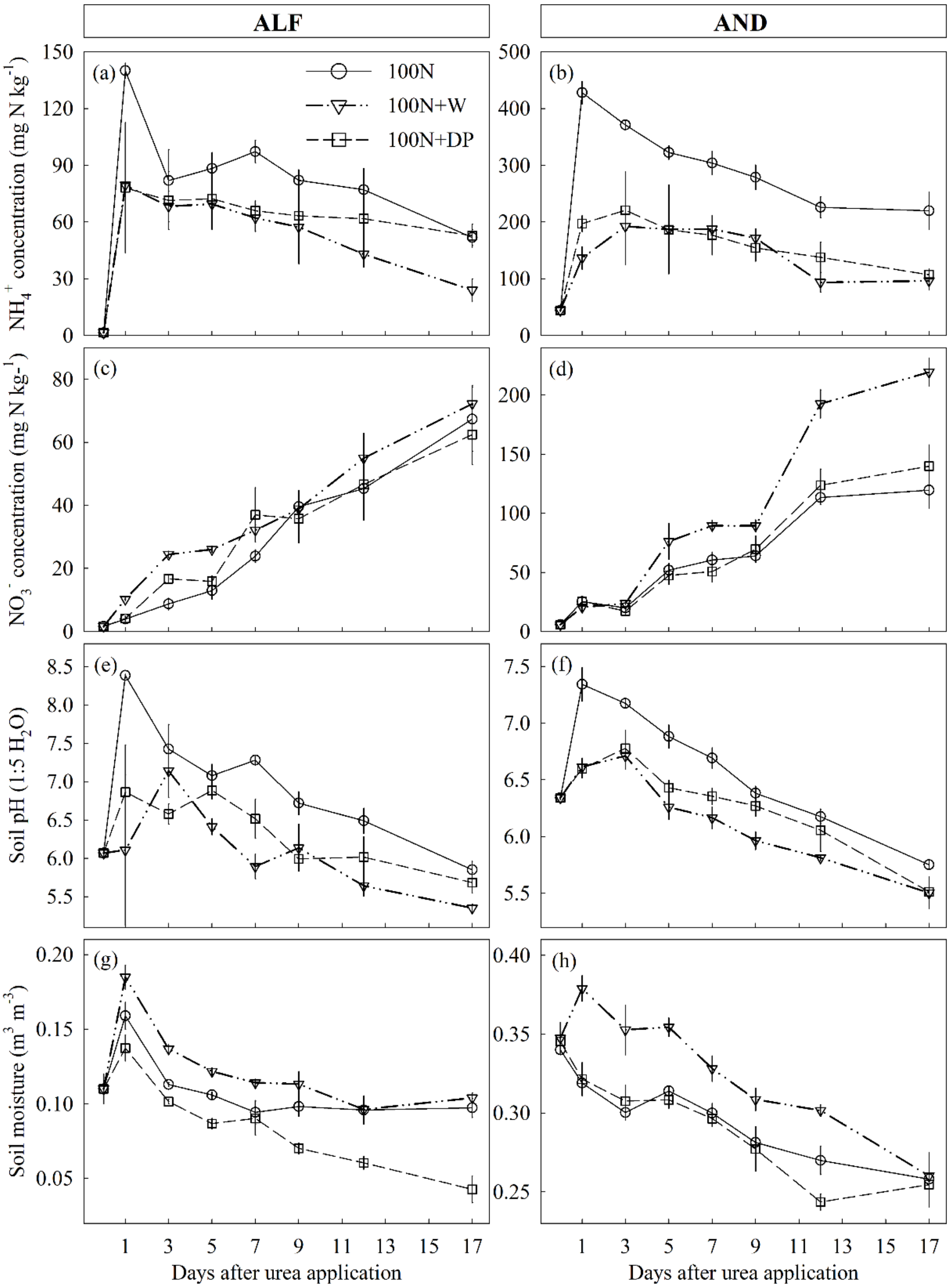

Fig. 4.5 Soil factors including (a, b) NH_4^+ concentration, (c, d) NO_3^- concentration, (e, f) pH, and (g, h) moisture content for three treatments (100N, 100N+W, and 100N+DP) monitored in ALF and AND, respectively. *100N* surface application of urea with 100 kg N ha^{-1}, *100N+W* irrigation of 10 mm water immediately after urea application with 100 kg N ha^{-1}, *100N+DP* deep placement of urea (100 kg N ha^{-1}) at 5 cm depth. Note that in the 100N and 100N+W treatments, soils were sampled from 0–3 cm, whereas in the 100N+DP treatment, soils were sampled from 0–7 cm. Error bars represent standard errors of the means (n = 3).

Soil pH followed very similar variation patterns to soil NH_4^+ concentrations in ALF and AND (Fig. 4.5e, f; Table S4.2). In ALF, pH in the 100N treatment peaked at 8.4, which was much higher than the peak in the 100N+W treatment (7.1) or 100N+DP treatment (6.9). In AND, the highest pH peak was also found in the 100N treatment (7.3), followed by those in the 100N+DP treatment (6.8) and 100N+W treatment (6.7). Soil moisture at both sites was generally higher in the 100N+W treatment and lower in the 100N+DP treatment, with soil moisture in the 100N treatment varying in between across sampling times (Fig. 4.5g, h; Table S4.2).

Soil pH and NO_3^- concentrations were most frequently correlated with NH_3-N loss between sampling dates (Table 4.4). Soil NO_3^- concentrations were negatively correlated with NH_3-N loss, with the exception of the weak correlation found in the 100N+DP treatments at both sites. Soil pH was significantly ($P < 0.1$) and positively correlated with NH_3-N loss in all the treatments that showed relatively high cumulative NH_3-N loss (the 100N treatment in ALF and 100N and 100N+W treatments in AND). Significant correlation between soil NH_4^+ concentration and NH_3-N loss was only found in the 100N treatment in AND. Soil moisture was significantly ($P < 0.05$) correlated with NH_3-N loss in the 100N treatment in ALF and in the 100N+W treatment in AND.

Table 4.4 Correlation ($n = 7$) between NH_3-N loss and soil variables of mineral N concentrations, pH, and moisture content (VWC) for treatments of 100N, 100N+W, and 100N+DP (see footnotes for the description of these treatments) during the study period

		NH_4^+ (mg kg^{-1})	NO_3^- (mg kg^{-1})	pH (1:5 H_2O)	VWC (m^3 m^{-3})
ALF	100N[a]	0.35	**−0.77**	*0.71*	0.86[b]
	100N+W[a]	−0.29	**−0.77**	0.14	0.52
	100N+DP	0.07	0.14	−0.06	−0.07
AND	100N[a]	**0.81**	−0.50	***0.98***	0.27
	100N+W[a]	0.33	**−0.76**	***0.91***	**0.81**
	100N+DP	−0.51	−0.14	−0.21	0.16

Italics, bold, and both indicate the significance of the Pearson correlation at $P < 0.1$, < 0.05, and < 0.01, respectively.

100N surface application of urea with 100 kg N ha^{-1}, *100N+W* irrigation of 10 mm water immediately after urea application with 100 kg N ha^{-1}, *100N+DP* deep placement of urea (100 kg N ha^{-1}) at 5 cm depth.

[a] Data on NH_3-N loss between sampling dates were log transformed before correlation analysis.

[b] Spearman correlation ($P = 0.006$) was applied owing to violation of the normality assumption.

4.4 Discussion

4.4.1 NH_3 volatilization in response to urea application across two croplands

ALF was much more susceptible than AND to NH_3-N loss after urea application (Fig. 4.2, 4.3; Table S4.1), as the lowest proportional NH_3-N loss from the 30N treatment in ALF (36.4%) was about 15% higher than the highest loss from the 150N treatment in AND (21.6%). This could be attributed to the different soil properties (PBC, CEC, and urease activity) and environmental factor (soil temperature) (Table 4.1; Fig. 4.1). Enhancement of the native soil PBC (i.e., by adding hydroxyl-Al polymer or acid cation exchange resin) has been shown to reduce soil surface pH and thus cumulative NH_3-N loss after urea application (Ferguson et al. 1984). A close and negative correlation between proportional NH_3-N loss and CEC ($R = -0.846$) was reported for eight arable soils applied with cattle urine (Whitehead and Raistrick 1993). Higher soil urease activity stimulates urea hydrolysis rate, raising soil pH and NH_4^+ concentrations more sharply and leading to higher NH_3-N loss (Soares et al. 2012). Furthermore, at the same study site receiving surface urea application, lower proportional N loss was recorded in the winter than in the summer (Elliot and Fox 2014), possibly because the low temperatures depressed urease activity. All the findings mentioned above suggested that ALF would be more susceptible to NH_3-N loss, as it was lower in PBC and CEC, and higher in urease activity and soil temperature. Lower initial soil pH is expected to contribute to the reduction of NH_3-N loss (He et al. 1999), yet in ALF, the weak PBC outweighed its low initial pH in reducing NH_3-N loss (Table 4.1).

The sigmoid model was found to be helpful in describing the relationship between urea-N rate and proportional NH_3-N loss in the present study. Sigmoidal curves are commonly fitted to cumulative NH_3-N loss with time (e.g., Soares et al. 2012; Subedi et al. 2015), but are seldom considered for proportional N loss with urea-N rate. This is partly due to the limited numbers of urea-N rates tested in previous studies, most of which tested two or three rates in addition to the control, as summarised in a study by Rochette et al. (2013b). Furthermore, the resolution of the lower range of urea-N rates was too low (mostly one rate under 100 kg N ha^{-1}) to be fitted with a sigmoidal curve to capture the inherent capacity of the soil to buffer NH_3-N loss. It is, however, very important for small farm holders in SSA to adopt a relatively low urea-N rate and achieve high urea-N use efficiency. The full sigmoid curve would also have been drawn for ALF provided that a lower urea-N rate (i.e., < 20 kg N ha^{-1}) had been included in the measurement.

Parameter y_0 in the sigmoid model for AND (Fig. 4.3d; Table 4.3) could be explained by the high local soil pH and NH_4^+ concentration exceeding the buffering capacity of the limited soil in contact with each urea granule (Black et al. 1987b). At lower urea-N rates, most urea diffusions from adjacent granules did not overlap, which might explain the constant proportional NH_3-N loss of the "lag phase" in AND. Such a "lag phase" might also result from CEC with pH-dependent charges. Before being saturated, more NH_4^+ would be retained by greater CEC at increasing urea-N rates, keeping the loss of NH_4^+ through NH_3 emissions proportional.

The proportional NH_3-N loss generally increased with urea-N rate in the present study (Fig. 4.3b), yet patterns with various effects of urea-N rate have been reported for acidic soils receiving surface application, including higher, similar, and lower proportional NH_3-N losses at higher urea-N rates (Black et al. 1987b; Watson and Kilpatrick 1991; Tian et al. 2001). With an increased urea-N rate, more urea granules were hydrolyzed on the same area of soil, causing higher local soil pH and NH_4^+ concentrations (Black et al. 1987b). Urea hydrolysis rate could also be stimulated by an increased substrate (urea) concentration within a certain range (Singh and Nye 1984). Both could contribute to a greater proportional NH_3-N loss at the higher urea-N rate. For studies reporting no effect of urea-N rate, a maximum level to which soil pH could rise might prevent further increase in proportional NH_3-N loss at higher urea-N rate (Watson and Kilpatrick 1991). This seems to explain the "maximum phase" in ALF (Fig. 4.3c), which started at a relatively low urea-N rate. Saturation of urease activity at higher urea-N rate (Dalal 1975), however, might explain the "maximum phase" in AND (Fig. 4.3d), as much lower urease activity (Table 4.1) and peak of pH were found in the 100N treatment (Fig. 4.5f). The relationship between urea-N rate and proportional NH_3-N loss in the present study can be described by combining the above-mentioned two patterns—greater proportional N loss and levelling out with further increasing urea-N rate—with AND exhibiting a considerable inherent capacity to buffer NH_3-N loss, which formed the "lag phase."

The only study, to my knowledge, reporting lower proportional NH_3-N loss at higher N rates (acidic soil receiving surface urea application; Tian et al. 2001), was conducted on wheat crops in the winter season. A corresponding explanation, however, was not provided. Temperature is a controlling factor for microbial activity. At low temperatures (10 °C), nitrification activity can still be high (Avrahami et al. 2003), while urease activity is likely to be depressed (Sahrawat 1984). Together, these can lead to two consequences: easier saturated urease activity, meaning comparable hydrolysis rate among different urea-N rates; and extended duration of NH_3 volatilization (Elliot and Fox 2014), which allows the nitrification process to be activated to stimulate the reduction of NH_3-N losses (Fleisher and Hagin, 1981). However, the absence of in situ measurements of soil pH and mineral N concentrations prevents a full explanation of the result.

4.4.2 Mitigation of NH_3 loss

Both the 100N+W and 100N+DP mitigation treatments performed well in the current study to reduce NH_3-N loss (Fig. 4.4). In order to assess the underlying mechanism of such reductions, soil mineral N, pH, and moisture were monitored for three treatments (100N, 100N+W, and 100N+DP) during the study period.

The effective inhibition of soil pH increase following urea hydrolysis is likely the main reason for the good performance of both mitigation treatments. The timing of depressed peaks in soil pH coincided with dropped peaks of NH_3-N loss in both mitigation treatments (Fig. 4.2, 4.5e, f), and positive correlations ($P < 0.1$) were found for those treatments with relatively large cumulative NH_3-N losses (Table 4.4). Mitigation treatments did reduce soil NH_4^+ concentrations after urea application (Fig. 4.5a, b; Table S4.2); nonetheless, NH_3-N loss in the 100N treatments simply dropped with decreased soil pH while NH_4^+ concentrations remained relatively high (i.e., after day 3; Fig. 4.2, 4.5a, b). Reduced correlations between soil NH_4^+ concentration and NH_3-N loss by mitigation treatment were found in AND but not in ALF (Table 4.4). Therefore, there may not be a response of NH_3-N loss to high NH_4^+ concentrations in the absence of favorable soil pH (i.e., pH > 7.4 in ALF and >6.8 in AND). Rochette et al. (2013b) also reported that soil pH raised above 7 was the main factor explaining the exponentially increased NH_3-N loss. The current result is further supported by the low NH_3-N loss reported in studies that NH_4^+-N fertilizer was added without inducing a rise in soil pH (Sommer et al. 2004; Zaman et al. 2008).

The nitrification process seemed to be affected by the 100N+W treatment (Fig. 4.5c, d; Table S4.2), and possibly contributed to NH_3-N loss reduction in ALF but not in AND. Close inspection of Fig. 4.5c reveals that in ALF, the 100N+W treatment resulted in a higher NO_3^- concentration in the early period of this study. During this period, substantial NH_3-N losses occurred, and therefore active nitrification might have contributed to NH_3-N loss reduction. By contrast, a higher NO_3^- concentration in AND was observed in the later period of the study (Fig. 4.5d), during which soil pH had already dropped because of NH_3 volatilization and nitrification could only further acidify the soil. Different activation timing of the nitrification process in the 100+W treatment between the two sites may result from the different initial soil moisture status. Nevertheless, activating the nitrification process before or during urea hydrolysis could help reduce NH_3-N loss (Fleisher and Hagin 1981), whereas inhibited or delayed nitrification may increase NH_3-N loss from soil after urea application (Soares et al. 2012).

Soil moisture is unlikely to explain the reduction of NH_3-N loss in the current mitigation study, although it responded to the different treatments (Table S4.2; Fig. 4.5g, h). As expected, soil moisture was higher in the 100N+W treatment and generally lower in the 100N+DP treatment (Fig. 4.5g, h), while the 100N treatment, which volatilized a substantial amount of NH_3-N (Fig. 4.4), had intermediate soil moisture content. A change in soil moisture may influence NH_3-N loss in two ways: from initially dry to adequately moist condition, it stimulates urea hydrolysis and thus increases NH_3-N loss; and from adequately moist to saturated condition, it induces downward movement of urea and NH_4^+ solution and thus reduces NH_3-N loss (Black et al. 1987a; Kissel et al. 2004). Local farming practices in which urea application is carried out when the soil is wet (after rainfall) actually increase the risk of NH_3-N loss, as Black et al. (1987a) and Sigunga et al. (2002) reported that NH_3-N loss increased with wetter soil (starting from the permanent wilting point) and reached a maximum with soil at field capacity.

4.4.3 Implications for managing NH_3 loss in SSA croplands

Approaches to mitigating NH_3-N loss have been extensively investigated (Sommer et al. 2004; Holcomb et al. 2011), including utilization of urease inhibitor, slow-release urea, and neutral or acidic N fertilizer produced at a higher cost. However, the availability of many approaches to small-farm holders in rain-fed SSA agriculture is largely limited, owing to their limited accessibility to resources and low-income levels. Knowing the soil's inherent capacity to buffer NH_3-N loss and involving it in the design of mitigation strategy are therefore critical. For instance, soils with similar properties and climatic conditions to AND in this study are likely to buffer NH_3-N loss inherently when a considerable amount of urea-N is applied. A single application of up to 60 kg N ha^{-1} urea is quite sufficient to improve the yield. In contrast, soils with similar properties and climatic conditions to ALF in this study should avoid surface application of urea, even at a low rate, such as 30 kg N ha^{-1}.

The rain-fed cropping system is dominant in SSA agriculture, and irrigation is rare owing to the lack of water resources and accessible facilities. In soils with a small inherent capacity to buffer NH_3-N loss, I recommend that local farmers determine the timing of urea application based on weather forecast or personal experience, ensuring that rain falls soon after urea application or even applying the urea during a rainfall event. To my knowledge, however, local farmers prefer to apply urea after rainfall, which actually increases the risk of NH_3-N loss, as previously discussed.

Deep placement of urea could require high labor costs in SSA croplands where only manpower is usually available. Dripping pipes (drilled with equally distributed holes) can be buried at around 5 cm soil depth and connected to a bucket at a relatively higher elevation. Urea can then be dissolved in the bucket before application. Such a simple drip system is easy to construct and is recommended to achieve the same performance as deep placement.

4.5 Conclusions

To my knowledge, this is the first study to report the effect of urea-N rate on the proportional NH_3-N loss in SSA croplands. In two soils (ALF and AND) cropped to maize in the East African highlands, ALF was found to be much more susceptible than AND to NH_3 loss after surface urea application, mainly owing to the different soil properties (PBC, CEC, and urease activity) and environmental factor (soil temperature). ALF had no inherent capacity to buffer NH_3 loss, so surface urea application is not recommended, while up to 60 kg N ha^{-1} could be applied in AND without inducing substantial proportional NH_3-N loss. Mitigation of NH_3 loss through irrigation and urea deep placement all performed well, mainly owing to their effective inhibition of soil pH rise following urea hydrolysis; the contribution from the nitrification process in the irrigation treatment could also be a factor. Suitable strategies (i.e., rain forecast-based urea application and simple drip system) are recommended based on the results of the current mitigation treatments. These results highlight that in acidic soils common to SSA croplands, the proportional NH_3-N loss can be substantial even at a low urea-N rate, and that soil's inherent capacity to buffer NH_3 loss should be involved in forming N management practices. Future research needs to better understand the underlying mechanisms of NH_3 volatilization from applied N fertilizer for designing effective mitigation strategies targeting different agro-ecological zones.

Supplementary materials

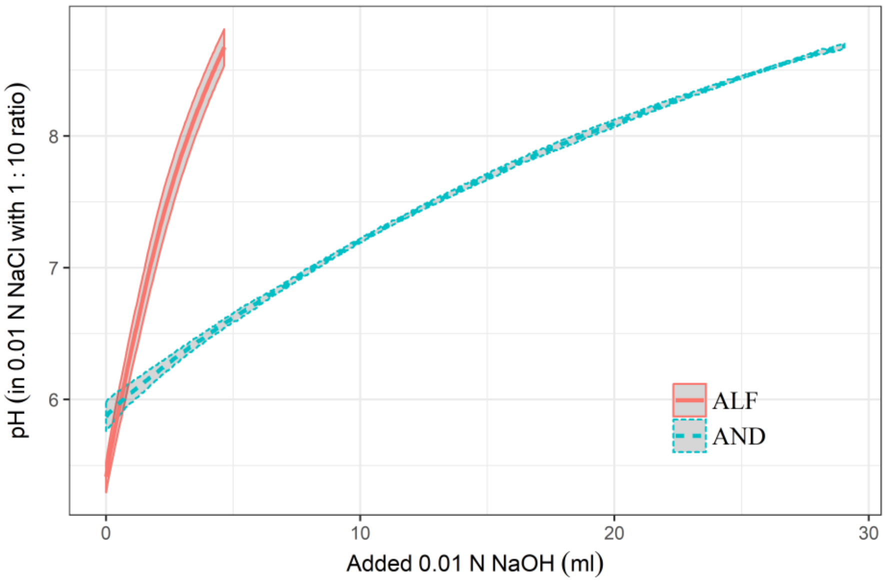

Fig. S4.1 Titratable acidity to represent the pH buffering capacity of soils at ALF (*n* = 6) and AND (*n* = 3). Shaded area indicates 1 standard deviation.

Experimental description for Fig. S4.1:

Titratable acidity was measured using a potentiometric automatic titrator (COM-1600, Hiranuma Sangyo Co., Ltd., Japan) following Sakurai et al. (1989) with a slight modification. Briefly, weight 4.0 g of air-dried soil < 2 mm into a 100 ml glass beaker and added 40 ml 0.01 mol L^{-1} NaCl solution as supporting electrolyte. After pre-equilibrium by magnetic stirring for 2 min, NaOH solution with a concentration of 0.01 mol L^{-1} was added at a rate of 0.05 ml min^{-1} with continuous magnetic stirring. Measurements for the ALF soil include six replicates randomly sampled across the experimental field, while three replicates were included for the AND soil.

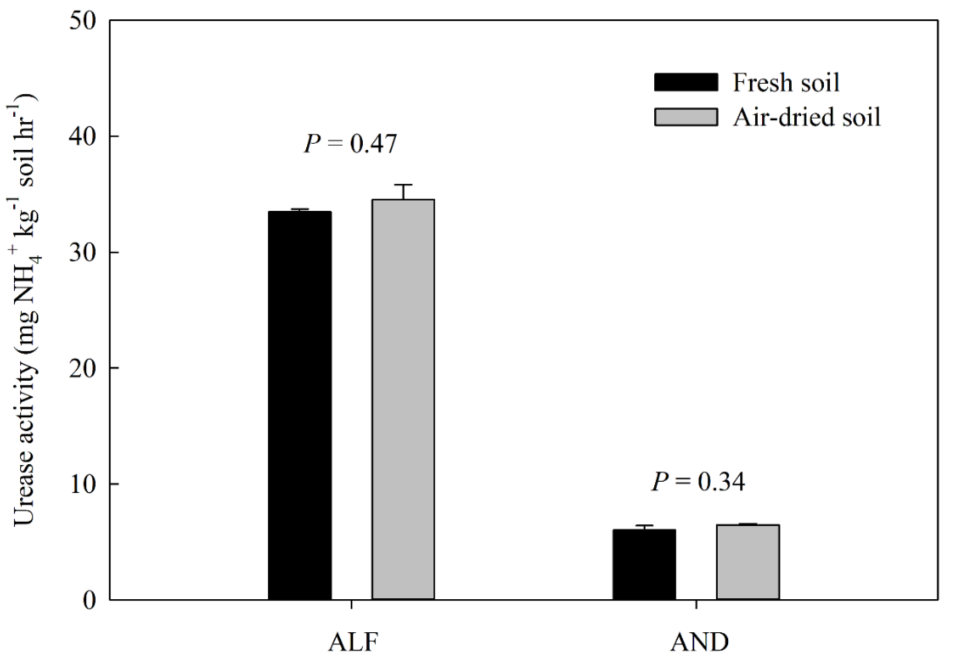

Fig. S4.2 Effect of air-drying on the soil urease activity of the field-moist soil samples from ALF and AND. Error bar represents standard error of the means (n = 3). P values are from t-test.

Experimental description for Fig. S4.2:

The fresh soils were sampled at the beginning of the fourth maize cropping season (early December of 2016; the season following the NH_3 volatilization study) from fields where the NH_3 volatilization study was conducted. The soils contained relatively low initial moisture content, with 2% for ALF and 5% for AND. The fresh soils (sieved through 2 mm mesh) from each study site were divided into two groups undergoing two treatments respectively: one group of samples remained in the fridge (4 ℃) as fresh samples, the other group of samples were air-dried at 25 ℃ for about two weeks till a constant weight. Two group samples were then analyzed for soil urease activity at the same time. Soil urease activity was determined as the release of NH_4^+-N after 2-hour incubation at 37 ℃ with a borate buffer at pH 10.0, following the procedure by Kandeler and Gerber (1998). This result that no significant effect of air-drying of fresh soils on the soil urease activity agreed with the findings by Zantua and Bremner (1975).

Table S4.1 Mean values (± standard error, n = 3) of cumulative NH_3-N loss and corresponding proportional NH_3-N loss (EF, meaning emission factor)

	ALF		AND	
	Cumulative loss (kg N ha^{-1})	EF (%)	Cumulative loss (kg N ha^{-1})	EF (%)
0N	0.2 ± 0.10 a	–	0.3 ± 0.04 a	–
30N	11.1 ± 0.9 b	36.4 ± 2.9 a	1.9 ± 0.1 ab	5.2 ± 0.3 a
50N	23.1 ± 3.6 c	45.9 ± 7.1 a	3.2 ± 0.3 ab	5.8 ± 0.6 a
70N	34.1 ± 0.6 d	48.5 ± 0.8 a	5.6 ± 1.9 b	7.5 ± 2.7 a
100N	50.1 ± 3.4 e	49.9 ± 3.4 a	20.1 ± 1.1 c	19.7 ± 1.1 b
150N	77.6 ± 0.7 f	51.6 ± 0.5 a	32.7 ± 2.8 d	21.6 ± 1.9 b

Values followed by the different letter (column) indicate significant different (Tukey contrast, P < 0.05).

Table S4.2 Mean values (± standard error, n = 24) of soil mineral N concentrations, pH, and moisture content (VWC) for treatments of 100N, 100N+W, and 100N+DP (see footnotes for the description of these treatments)

		NH_4^+ (mg kg^{-1})	NO_3^- (mg kg^{-1})	pH (1:5 H_2O)	VWC (m^3 m^{-3})
ALF	100N	77.5 ± 8.1	25.4 ± 4.8	6.904 ± 0.167	0.109 ± 0.005
	100N+W	50.7 ± 5.8	32.6 ± 4.6	6.088 ± 0.156	0.123 ± 0.006
	100N+DP	58.4 ± 6.6	27.6 ± 4.5	6.323 ± 0.118	0.087 ± 0.006
AND	100N	274.0 ± 23.5	57.5 ± 8.4	6.591 ± 0.106	0.298 ± 0.006
	100N+W	138.2 ± 16.0	89.4 ± 15.7	6.173 ± 0.083	0.329 ± 0.008
	100N+DP	153.4 ± 14.2	60.3 ± 9.9	6.294 ± 0.081	0.294 ± 0.007

100N surface application of urea with 100 kg N ha^{-1}, *100N+W* irrigation of 10 mm water immediately after urea application with 100 kg N ha^{-1}, *100N+DP* deep placement of urea (100 kg N ha^{-1}) at 5 cm depth.

CHAPTER 5

Nitrate Leaching from Critical Root Zone of Maize in Two Tropical Highlands of Tanzania: Effects of Fertilizer-Nitrogen Rate and Straw Incorporation

Abstract

In addition to environmental and public health concerns, nitrate (NO_3^-) leaching from agriculture represents an additional economic cost to smallholder farmers in Sub-Saharan Africa. Little field leachate data, however, are available for the cropping systems in this region, where efforts are underway to increase fertilizer (especially nitrogen, N) use to secure food production. During 2015–2017, I monitored NO_3^- leaching from the critical root zone (0–0.3 m) of maize in the tropical highlands of Tanzania, using repacked soil monolith lysimeters. Four urea-N rates (0, 50, 100, and 150 kg N ha^{-1}; split into two dressings) and two combined applications (maize straw with 50 and 150 kg N ha^{-1}) were evaluated in two soil types (sandy Alfisols and clayey Andisols). The soil rewetting process, particularly at the onset of the rainy season and following N applications, was a critical driver of NO_3^- loss. Nitrate loss increased exponentially with increasing N rates, yet inter-annual variation was observed in response to the inter-annual variation in rainfall and the preceding fallow management. Relating cumulative NO_3^- loss to maize yield under increasing N rates revealed a tipping point—occurrence depending on season—above which yield increments were accompanied by substantial NO_3^- loss. Straw incorporation induced net N immobilization in the early growing season, and reduced NO_3^- losses by 3.3–6.3 kg N ha^{-1}, but no effect was observed on the cumulative NO_3^- losses or maize yields. The NO_3^- loss reductions (equivalent to 1.2–2.7 kg N Mg^{-1} added C) were far below the potential of net N immobilization by the decomposition of straw (18.0–38.1 kg N Mg^{-1} added C). This was likely caused by large pieces of straw (~0.15 m) used in the field, which could have induced N limitations and biomass-N recycling in the decomposition microsites. These results showed the potential to enhance maize yield without inducing substantial N leaching loss by adopting the proper N rate in the tropical highlands of Tanzania, and highlighted that temporary immobilization of leachable N by using large pieces of straw (~0.15 m) in the field was inefficient for the improvement of N synchrony and benefits to yield.

5.1 Introduction

Sub-Saharan Africa (SSA) struggles to be food self-sufficient (van Ittersum et al. 2016) as rapid growth of the population is projected (United Nations 2017); however, the croplands have been historically unproductive (Hazell and Wood 2008). The stagnantly low yields of cereal production (~1 Mg cereal ha^{-1}) are mainly caused by the continuous mining of soil nutrients (especially nitrogen, N) without proper return (Sanchez 2002), which is driving a growing recognition and efforts to increase fertilizer use in this region (AGRA 2009; Vanlauwe et al. 2014b).

To offset soil N depletion and secure food production, the amount of N input to SSA croplands would be substantial with the increase in fertilizer use. As pointed out by Hickman et al. (2015), at least 6 Tg N yr^{-1} would be required just to reach an average application rate of 75 kg N ha^{-1} yr^{-1} for cereal productions on existing agricultural lands in SSA. This unprecedented input of N to croplands would increase N availability and cycling and subsequently nitrate (NO_3^-) leaching from agroecosystems (Galloway et al. 2008), particularly in tropics of SSA that experience seasonal rainfall with high intensity.

Nitrate leaching from agriculture can have environmental and public health consequences (Qin et al. 2010; Han et al. 2016). Enrichment of NO_3^- in the ground and surface waters can cause algae blooms, induce hypoxia, and consequently kill fishes (Diaz and Rosenberg 2008). High-nitrate levels in drinking water pose a serious health threat to children and pregnant women (Gatseva and Argirova 2008; Water Quality Association 2014). Such health risk can be particularly acute in developing regions like SSA, where drinking water is generally obtained from shallow wells or streams. Further, NO_3^- leaching could be of socioeconomic significance for the smallholder African farming systems given the poor income of local farmers (Nyamangara et al. 2003).

The increase in fertilizer use can be expected to increase NO_3^- leaching, yet the quantity and pattern may change with varying environmental and soil factors (e.g., rainfall, soil type, etc.) and management factors (e.g., cultivation-fallow sequence, organic residue input, etc.). Higher rainfall amounts increase drainage volume and likely flush more NO_3^- from the plant root zone (Russo et al. 2017). By contrast, clayey soils tend to have a higher water-holding capacity and retain NO_3^- available to plant and microbes for a longer time; therefore, it may reduce the NO_3^- leaching (Tully et al. 2016; Zheng et al. 2018b). Fallow management preceding cultivation often increases N availability for both crop uptake and leaching loss (Maroko et al. 1998; Hartemink et al. 2000). Compared with chemical fertilizer, organic inputs in the field release N slower (Palm et al. 2001) or may temporarily immobilize soil mineral N (Recous et al. 1995); depending on its quality, it may potentially contribute to reduced leaching loss. Overall, factors influencing the drainage volume and the NO_3^- concentrations in the leachate can alter NO_3^- leaching loss. However, little field data are available for NO_3^- leaching from SSA croplands. Based on a recent review by Russo et al. (2017), only six studies measured NO_3^- concentrations in the leachate water, even less than those conducted in individual research farms in central California. Field measurements are therefore urgently needed to predict the NO_3^- leaching loss from farms and guide farmers as N application rate increases across SSA.

Combined use of low-quality organic residues and chemical fertilizer, as the technical basis and one of the major components in Integrated Soil Fertility Management, has been widely promoted across SSA (Kimani et al. 2003). Vanlauwe et al. (2001) formulated an attractive direct hypothesis on the combination of these two types of resources, stating that temporary immobilization of mineral N and subsequent release because of microbial decomposition of residues (added as a source of carbon, C) may reduce N leaching loss and improve N synchrony. Indeed, reduced N leaching loss through immobilization has been proved through laboratory incubations (Sakala et al. 2000). However, such a hypothesis has not been effectively verified by field leachate measurements, and it is still uncertain how such improved N synchrony, if verified, can benefit the final yield. In tropical areas having distinct dry and wet seasons, soil mineralized N at the beginning of the rainy season can be excessive (>40 kg N ha^{-1}) and prone to leaching loss (Sugihara et al. 2012a; Zheng et al., 2018b). If low-quality residues can be used to temporarily immobilized this potentially leachable N from soil for subsequent crop uptake, both fertilizer-N input from farmers and N leaching loss can be reduced.

The use of lysimeters is an established method for measuring the downward movement of water and nutrients through the soil profile (Goss and Ehlers 2009). Various types of lysimeters have been extensively used and each has its advantages and disadvantages (Fares et al. 2009). For example, suction cup lysimeters provide access to deeper soil layers and higher sampling frequency (Tully et al. 2013; Russo et al. 2017). However, soil water flux cannot be directly measured, and the existence of preferential flow may largely affect the representativeness of the sample concentrations (Wang et al. 2012). In contrast, soil monolith lysimeters (either intact or repacked) measure water and NO_3^- fluxes more directly (Fan et al. 2017), yet the installation process is quite labor-demanding. Soil monolith lysimeters are simple to manage because no tension is applied for each sampling, and therefore have been employed by some studies in Zimbabwe (Nyamangara et al. 2003; Mapanda et al. 2012a).

Clarifying the characteristics, rates, and driving factors of NO_3^- leaching is the pre-requisite for proposing effective mitigation strategies. This study aimed to evaluate the effects of increasing fertilizer-N rates and maize straw incorporation on NO_3^- leaching from the critical root zone (0–0.3 m) of maize in the tropical highlands of Tanzania, using repacked soil monolith lysimeters. The specific objectives of this study were to (1) investigate the temporal dynamics of NO_3^- losses; (2) quantify the cumulative NO_3^- loss amount; and (3) examine the relationship between yields and cumulative NO_3^- losses, as affected by increasing N rates and straw incorporation. Finally, I verified the potential benefit of improved N synchrony and maize yield because of modified mineralization-immobilization turnover by straw incorporation and determined if a suitable N strategy could be identified to achieve high yield and low leaching loss.

5.2 Materials and methods

5.2.1 Study sites

The study was conducted at two maize-based systems with different soil types in the southern highlands of Tanzania. One site, TZi, is located in Mangalali village (07°46′ S, 35°34′ E; 1480 m a.s.l.) of the Iringa region. The soil is classified as coarse-loamy, isohyperthermic, Kanhaplic Haplustalfs (Soil Survey Staff 2010). TZi had been under natural fallow for two years before the start of the experiment. Before natural fallow, maize had been continuously cultivated by local farmers for more than five years. The other site, TZm, is located in Uyole town (08°55′ S, 33°31′ E; 1780 m a.s.l.) of the Mbeya region. The soil is classified as clay-loam, isothermic, Dystric Vitric Haplustands (Soil Survey Staff 2010). TZm was located within the Mbeya Agricultural Training Institute-Uyole for use as experimental plots, and sunflowers were cultivated in the preceding season. TZi receives 560 mm of precipitation per year on average, lower than that at TZm (860 mm). Annual daily average temperature was higher at TZi (23.5 °C) than that at TZm (17.1 °C). The pattern of annual rainfall is unimodal for both sites. The rainy season generally starts from late November for both sites, and ends in mid-April and mid-May at TZi and TZm, respectively. Selected properties for the soil profiles of the study sites are presented in Table S5.1. Despite the similar soil pH and C:N ratio in the topsoils between two sites, soil organic matter and CEC were substantially lower at TZi compared to those at TZm, because of the low clay content. Water-holding capacity was higher at TZm than at TZi at the 0–0.15 m and 0.15–0.3 m depths, respectively.

5.2.2 Experimental design

From November 2015 to June 2017, maize was cultivated consecutively for two seasons. Experimental plots were established in a completely randomized block design for six treatments: four levels of N rate: 0, 50, 100, and 150 kg N ha^{-1}, denoted as 0–150N, respectively, and two more treatments combining the N application and maize straw incorporation—50N+S (50 kg N ha^{-1} plus ca. 2 Mg C ha^{-1}) and 150N+S (150 kg N ha^{-1} plus ca. 2 Mg C ha^{-1}). Each treatment was replicated three times. A 1.5 m buffer was set up to separate each plot (plot size: 5 m × 5 m) and block. Within each plot, three maize (*Zea mays* L.; variety: TMV-1 for TZi and UH6303 for TZm) seeds were sowed per hole at a spacing of 0.7 m × 0.3 m, and were thinned to one plant per hole 20 days after sowing (DAS), giving a population of ~ 48000 plants ha^{-1}. Maize was planted in early- to mid-December at both sites, and harvested in late March and mid-May at TZi and TZm, respectively. Because of heavy rainfall, seeding on Dec-14-2015 failed to germinate at TZi and re-sowing was conducted on January 1, 2016.

Maize straws were chopped into ~0.15-m pieces and incorporated into 0–0.15 m soil using a hand hoe. The date of straw incorporation and its quality (i.e., C and N content and C:N ratio) are presented in Table S5.2. Based on local farming practices, N application, by broadcasting urea, was split into two times (Zheng et al. 2018b). One-third of the total amount was applied 21 DAS (three- to four-leaf stage of maize growth). The remaining two-thirds was added 57 DAS (around the time of maize tasseling). Weeding was carried out when necessary, and all weeded materials were removed from the plots. Phosphorus (P) was added to all plots as a basal application with 50 kg P ha^{-1}, using triple superphosphate.

5.2.3 Lysimeter installation and leachate collection

To avoid the effects of installation disturbance, I installed lysimeters more than three months before the start of the experiment. Gravity-drained lysimeters (Fig. S5.1) made of plastic (0.4 m inner diameter and 0.4 m height) were installed in the edge of the treatment plot. Four lysimeter replicates were installed for the treatment plots covering two out of the three blocks, with two replicates in a plot connecting to the same storage tank (Fig. S5.1) to reduce the heavy work load. A hole was excavated without disturbing the surrounding soil for the installation of each lysimeter and the excavated soil was carefully backfilled for each lysimeter with minimal changes to the original soil horizon and bulk density. A 0.05-m gap between the soil surface and the top of the casing (Fig. S5.1) was left to prevent the surface water exchange. Based on my field observations on maize root distribution (>70% in the top 0.2 m soil, which was supported by Sugihara et al. (2012a) who reported 74–86% were distributed in 0–0.15 m), 0–0.3 m was defined as the critical root zone in this study. Furthermore, results from Mtambanengwe and Mapfumo (2006) and Zheng et al. (2018b) all indicated that 0–0.3 m soil dominated the N supply for plant uptake, which also supported the current definition for the critical root zone. One maize plant was grown at the center of each lysimeter (Fig. S5.1). Fertilizer applications and weeding in the lysimeters were managed precisely the same as those in the plots, and an accurate rate of added C and N from straw to each lysimeter is presented in Table S5.2. During land preparation for maize planting in 2016/17, 0–0.15 m soil in the lysimeter was replaced with that from the corresponding treatment plot.

Each sampling bottle (Fig. S5.1) was checked every week during the rainy season, whereas during the dry season, no leaching occurred because of negligible rainfall. Sampling frequency was increased if heavy rainfall occurred, to avoid the overflow of leachate in the sampling bottle (~6 L volume). During each sampling, leachate volume was recorded before taking a 30 ml subsample. The excess leachate in the sampling bottle was then removed to avoid disturbing the next sampling. Microbiological evolution was inhibited by adding $CuBr_2$ solution (0.1–1 mg Cu L^{-1}) to each sampling bottle (Fujii et al., 2009; Shibata et al., 2017). The leachates collected in situ were filtered through 0.45 µm filters (Hydrophilic cellulose acetate membranes, Sartorius Stedim Biotec GmbH, Germany), and preserved at 4 °C until analysis.

5.2.4 Data collection and sample analysis

Rainfall was recorded every 10 min by a TE525MM rain gauge connected to a CR1000 data logger (Campbell Scientific, Inc., USA). To estimate yield, maize ears inside the plots (4 m × 4 m, avoiding the edge) were collected and grains were shelled from the ears. Weights of shelled grains were recorded before subsamples were taken for moisture correction. Subsamples of the grains were oven-dried at 60 °C to a constant weight. Nitrate concentration in the filtered leachate sample was determined by high-performance liquid chromatography with a Shim-pack IC-A1 column and a CDD-10A conductivity detector (Shimadzu Inc., Japan). Though other N compositions (ammonium-N and dissolved organic N) were also determined, NO_3^- was the focus of this study because it greatly dominated the contribution to the total N losses (Fig. S5.2). This is in agreement with most of the reports for agricultural systems (van Kessel et al. 2009).

5.2.5 Calculations and statistical analysis

The mass loss of NO_3^- for each individual lysimeter for each sampling interval was derived by multiplying the manually recorded drainage volume with the measured NO_3^- concentration in the leachate of the respective lysimeter. Then, the arithmetic mean of NO_3^- loss was calculated for each sampling interval, as well as each season from the four lysimeter replicates.

The NO_3^- leaching ratio (NLR, %) for each cropping season was calculated as:

$$NLR = \frac{L_F - L_C}{N_{applied}} \times 100\%$$

Where L_F and L_C represent cumulative NO_3^- leaching loss (kg N ha^{-1}) in the N-applied and control treatment (0N plots), respectively, and $N_{applied}$ is the total amount of N applied (kg N ha^{-1}). In the straw incorporated treatments, $N_{applied}$ includes the N source from the maize straw (Table S5.2).

The effects of N rates on maize yield, NO_3^- concentration in the leachate, and cumulative NO_3^- loss (refering to each season in this study) were determined by one-way ANOVA. Following each *F*-value, multiple comparison of means with an LSD test (equal variance assumed) or a Dunnett's T3 test (equal variance not assumed) was conducted. The effects of straw incorporation on maize yield, NO_3^- concentration in the leachate, and cumulative NO_3^- loss were assessed by *t*-tests. All statistically significant differences were identified as $P < 0.05$ unless stated otherwise. Statistical analysis was conducted with IBM SPSS Statistics (version 24).

5.3 Results

5.3.1 Rainfall and water drainage

Cumulative rainfall and accordingly the water drainage in the 2015/16 season were higher than those in the 2016/17 season at each site (Fig. 5.1). The rainfall in the 2015/16 season was ~200 mm higher than the mean annual rainfall at each site. At TZi, water drainage was, on average, 355 mm and 110 mm in the 2015/16 and 2016/17 season, respectively, accounting for 46.9% of cumulative rainfall (based on the 2015/16 data only because data from the 2016/17 season were not available). At TZm, water drainage was, on average, 416 mm and 257 mm, accounting for 37.0% and 43.9% of cumulative rainfall in the 2015/16 and 2016/17 season, respectively. At TZm, the cumulative rainfall in the 2016/17 season may be lower than the actual value because of missing data during 0–25 DAS (Fig. 5.1b), which could have overestimated the ratio of drainage to rainfall. Prolonged dry periods were observed during the growing season at each site (i.e., 53–88 DAS in the 2015/16 season at TZi, 53–74 DAS in the 2016/17 season at TZm), during which no leaching occurred. Cumulative drainage among treatments was similar, except for the 2015/16 season at TZm, where a difference ($P < 0.05$) was observed (Table S5.3).

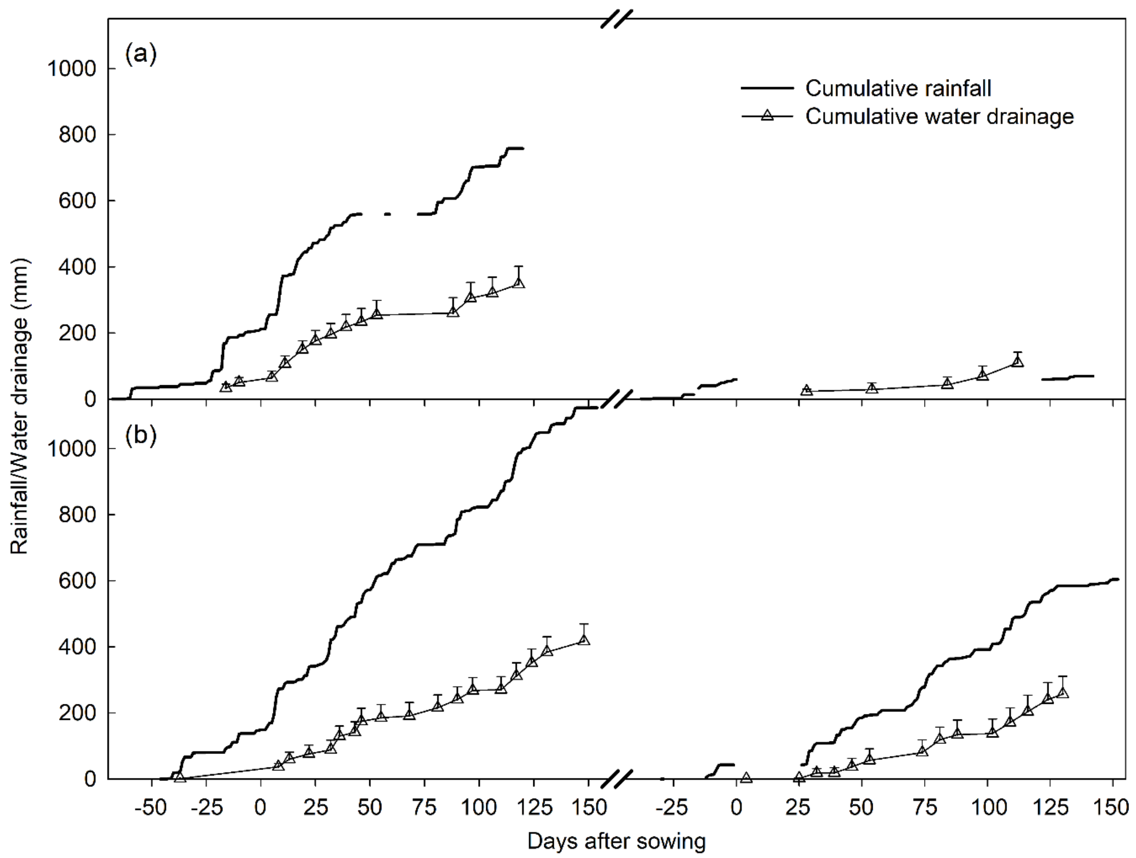

Fig. 5.1 Cumulative rainfall and water drainage at TZi (a) and TZm (b). The breaks in the horizontal axis separate the data into two seasons: the first season (2015/16) on the left and the second season (2016/17) on the right. The breaks in the lines representing cumulative rainfall indicate missing rainfall data because of the malfunction of a rain gauge. Error bars represent standard deviation of the water drainage.

5.3.2 Nitrate concentrations in leachate

During the study period, the average NO_3^--N concentration increased with increasing N rates (7–20 mg N L^{-1} for 0–150N at TZi and 5–8 mg N L^{-1} for 0–150N at TZm), though statistical significance ($P < 0.05$) was only found at TZi (Fig. 5.2). The range of the NO_3^- concentration in the third and fourth quantiles also increased at higher N rates at both sites (Fig. 5.2). Straw incorporation did not alter the distribution or the averaged value of NO_3^- concentrations (Fig. 5.2).

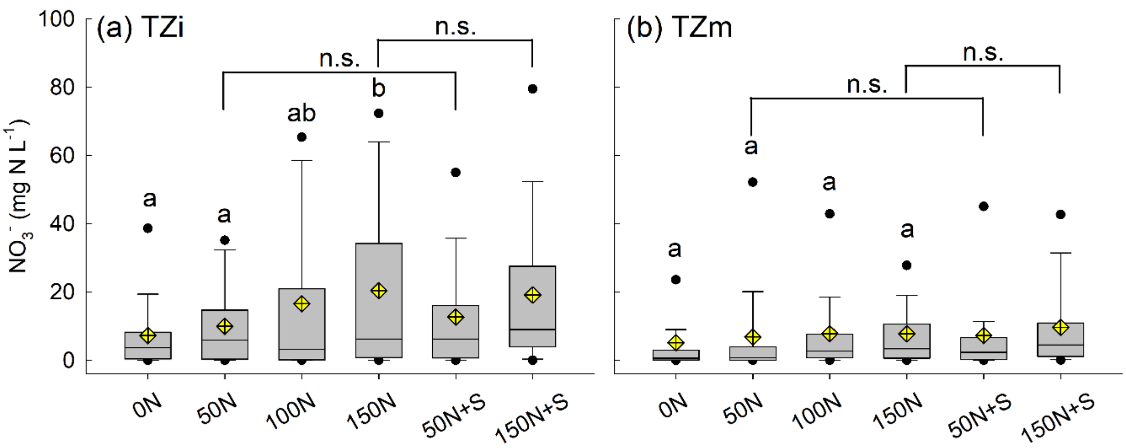

Fig. 5.2 Box-whisker plots showing the distribution of NO_3^- concentrations and their averages (crossed diamonds) for different treatments during the study period from November 2015 to May 2017 at TZi (a) and TZm (b). Only the 5th and 95th percentiles are plotted as outliers. Different letters above boxes indicate significant differences among N rates at the $P < 0.05$ level by either the LSD test (equal variance assumed) or Dunnett's T3 test (equal variance not assumed). n.s. indicates non significance ($P > 0.05$) by *t*-test.

5.3.3 Temporal dynamics of NO_3^- loss between sampling dates

The NO_3^- loss between sampling dates in this study (Fig. 5. 3) nearly represents the weekly flux of NO_3^-. As mentioned in Section 5.2.3, the leachate was sampled weekly, except in some cases with heavy rainfall events, when additional samplings were conducted to avoid overflow of the leachate in the sampling bottles. In the following sub-sections, temporal dynamics of NO_3^- loss between sampling dates were separately described under various N rates (Section 5.3.3.1) and with or without straw incorporation (Section 5.3.3.2).

5.3.3.1 Under various N rates

The NO_3^- losses varied seasonally and in response to the application of N fertilizer at each site (Fig. 5.3a, b). Throughout the study period, NO_3^--N losses in the 0N treatment ranged from <0.5 to 14.6 kg N ha^{-1} at TZi and from <0.1 to 9.6 kg N ha^{-1} at TZm, with the highest NO_3^- losses always occurring at the beginning of the cropping season. The response of NO_3^- losses to N application showed a delayed pattern; the increase in NO_3^- losses was often observed at one or two samplings, rather than immediately after the N applications (Fig. 5.3a, b). Coupled with the second N application, a prolonged dry period followed by sufficient rainfall resulted in notable pulses of NO_3^- losses at TZi for the 2015/16 season (up to 27.6 kg N ha^{-1} observed at 96 DAS; Fig. 5.3a), which explained 41.5–70.5% of the difference in the treatments (Fig. S5.3). Similar phenomena were also observed at TZm for the 2016/17 season (up to 14.8 and 5.2 kg N ha^{-1} observed at 32 and 81 DAS, respectively; Fig. 5.3b). Among treatments with various N rates, the highest peak of NO_3^- loss at TZi (i.e., 27.6 kg N ha^{-1} from the 150N treatment) was nearly twice as large as that at TZm (i.e., 14.6 kg N ha^{-1}).

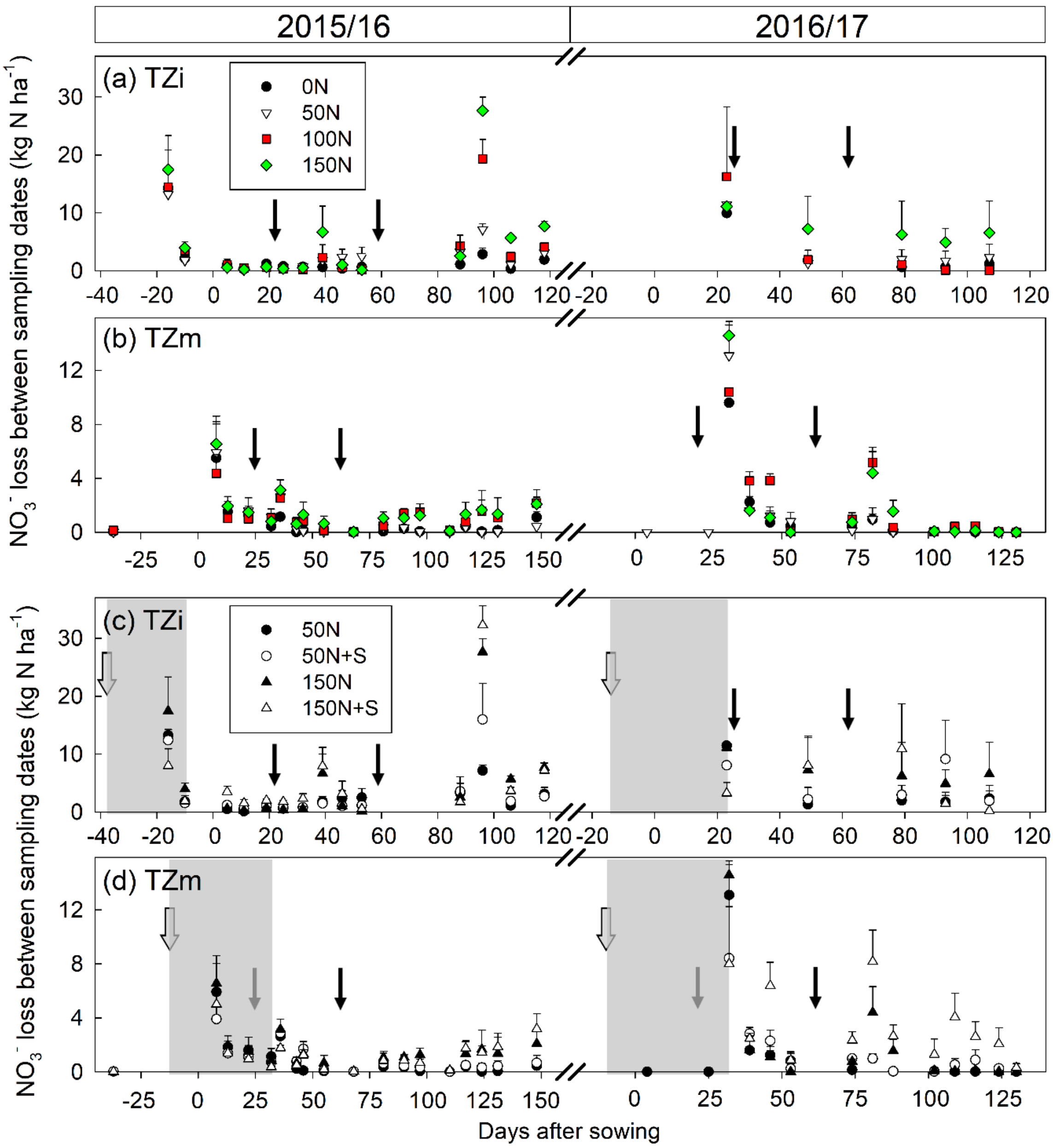

Fig. 5.3 Temporal dynamics of NO_3^- loss between sampling dates under various N rates (a, b) and with/without straw incorporation (c, d) at TZi and TZm, respectively. Panels (a and c; b and d) were separated for better visualization of the effects of N rate and straw incorporation, respectively. The breaks in the horizontal axis separate the data into two seasons: the first season (2015/16) on the left and the second season (2016/17) on the right. Thin black downward arrows indicate the timing of N application across all panels (a–d). Thick gray downward arrows indicate the timing of crop residue incorporation in c and d panels. Error bars represent standard error of the means.

5.3.3.2 With and without straw incorporation

Across sites and seasons, the NO_3^- losses in the straw applied plots (i.e., 50N+S and 150N+S) were lower at the beginning yet higher at the later period of the cropping season compared to the non-straw applied plots (i.e., 50N and 150N) (Fig. 5.3c, d). The lower NO_3^- losses at the beginning of the cropping season were caused by N immobilization during residue decomposition. The immobilization lasted for 28 and 38 d at TZi (for the 2015/16 and 2016/17 season, respectively), and 44 and 43 d at TZm (for the 2015/16 and 2016/17 season, respectively). During these immobilization periods, the NO_3^- losses were reduced by 6.3 and 5.6 kg N ha^{-1}, on average, at TZi for the 2015/16 and 2016/17 season, respectively, and 3.3 and 5.6 kg N ha^{-1}, on average, at TZm for the 2015/16 and 2016/17 season, respectively, compared to that of the non-straw applied plots. These NO_3^- loss reductions (3.3–6.3 kg N ha^{-1}) were equivalent to 30.5–50.2% of NO_3^- losses during the same periods in the non-straw applied plots.

5.3.4 Cumulative NO_3^- loss and NLR

The cumulative NO_3^- loss increased significantly ($P < 0.05$, except for the 2016/17 year at TZi) at higher N rates, showing an exponential growth pattern ($y = a \cdot e^{b \cdot x}$) across sites and seasons (Fig. 5.4). Cumulative NO_3^- losses were higher in the 2015/16 season (28.2–74.0 kg N ha^{-1} at TZi and 12.4–26.5 kg N ha^{-1} at TZm) than those in the 2016/17 season (6.3–24.1 kg N ha^{-1} at TZi and 6.1–24.3 kg N ha^{-1} at TZm); the inter-annual variation of cumulative NO_3^- loss was particularly substantial at TZi (Fig. 5.4a). Across sites and seasons, straw incorporation did not significantly alter the cumulative NO_3^- losses (Fig. 5.5).

At both sites, inter-annual variations in NLR was substantial and even greater than the variations among treatments (Table 5.1). At TZi, NLR was much higher in the 2015/16 season (20.7–30.5%) than that in the 2016/17 season (5.1–13.6%). At TZm, NLR was higher in the 2016/17 season (9.1–15.6%) than that in the 2015/16 season (2.7–9.4%).

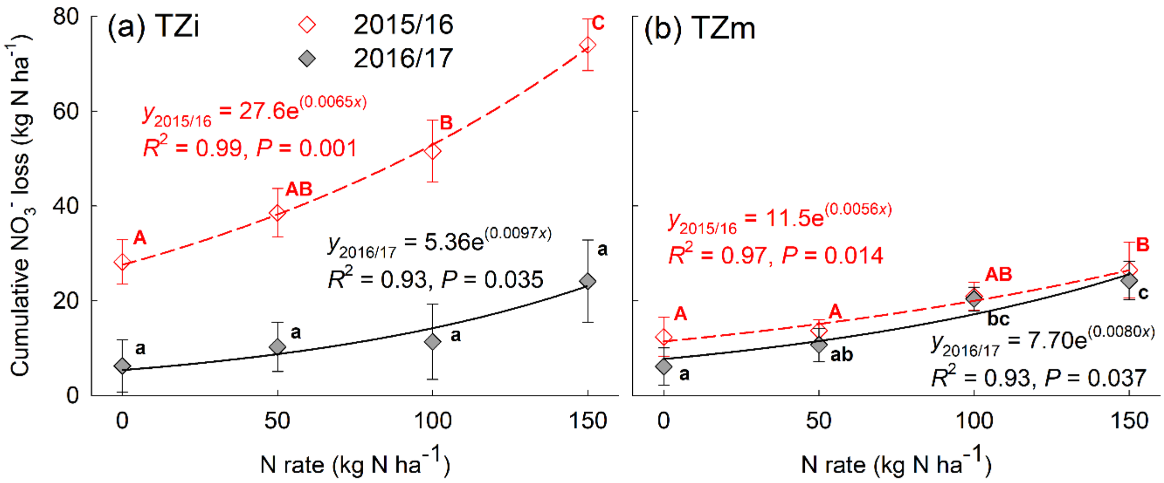

Fig. 5.4 Relationship between N rates and cumulative NO_3^- losses at TZi (a) and TZm (b). Error bars indicate standard error of the means. Different capital letters and lowercase letters indicate significant differences at the $P < 0.05$ level by LSD test in the 2015/16 and 2016/17 season, respectively.

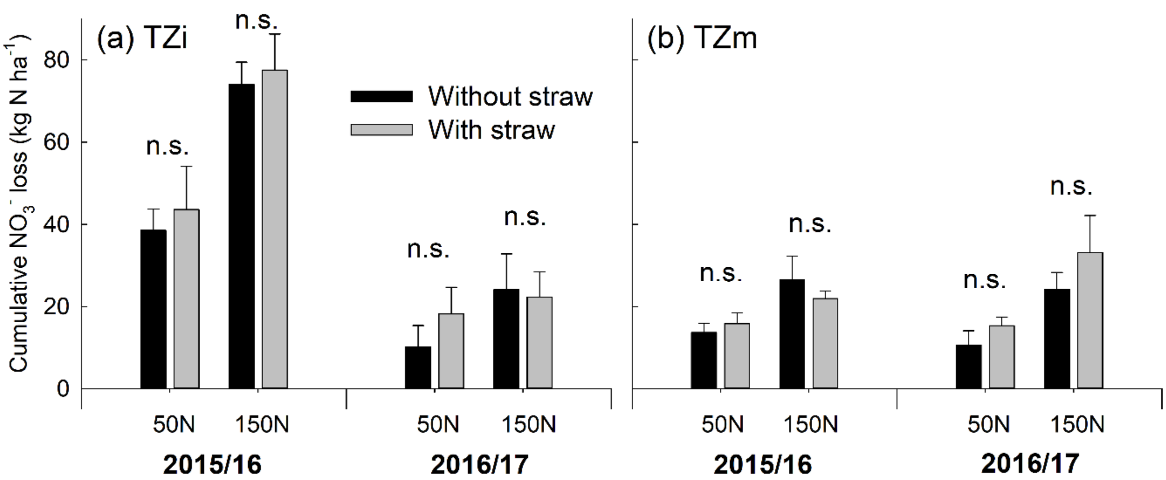

Fig. 5.5 Effect of residue incorporation on the cumulative NO_3^- loss at TZi (a) and TZm (b). Error bars represent standard error of the means. n.s. indicates non-significant difference ($P > 0.05$) by *t*-test.

Table 5.1 Nitrate leaching ratio (NLR, %) at TZi and TZm

Treatment	TZi		TZm	
	2015/16	2016/17	2015/16	2016/17
50N	20.7	8.0	2.7	9.1
100N	23.4	5.1	8.5	14.3
150N	30.5	11.9	9.4	12.1
50N+S	22.3	13.6	5.5	12.6
150N+S	29.1	8.5	5.9	15.6

5.3.5 Maize yield and its relationship with cumulative NO_3^- loss

At each site, maize yields were interactively affected by N rate and cropping season (Table 5.2). Maize yield was significantly (P < 0.05) enhanced with increasing N rate, and the yield in the 2016/17 season (2.0–3.9 Mg ha^{-1} at TZi and 1.8–4.1 Mg ha^{-1} at TZm) was higher than that in the 2015/16 season (0.8–3.1 Mg ha^{-1} at TZi and 1.1–3.9 Mg ha^{-1} at TZm) under the same N rate. Maize yields were not significantly (P > 0.05) affected by straw incorporation across sites and seasons (Table 5.2).

With only fertilizer-N applied, two distinct patterns—depending on season—were observed for the relationship between maize yields and the cumulative NO_3^- losses at each site (Fig. 5.6). In the 2015/16 season, yields tended to increase linearly with cumulative NO_3^- losses (red hollow circles in Fig. 5.6a, b), with the slope of the linear relationship greater at TZi than that at TZm (Fig. 5.6). In the 2016/17 season, the relationship at each site showed a non-linear pattern with a potential tipping point (black hollow triangles in Fig. 5.6a, b), which could be determined at the N rate where the maximum difference between scaled values of yields and NO_3^- losses occurred (Fig. S5.4). Straw incorporation did not show a clear benefit to higher yield with lower NO_3^- loss (Fig. 5.6). In some cases (i.e., 150N vs. 150N+S in the 2015/16 season and 50N vs. 50N+S in the 2016/17 season at TZi), straw incorporation decreased the yield, though not significantly (Table 5.2).

Table 5.2 Maize grain yield (Mg ha^{-1}) at two sites as affected by fertilizer-N rate and straw incorporation for each study year

	TZi		TZm	
	2015/16	2016/17	2015/16	2016/17
Effect of N rate†				
0N	0.8a	2.0a	1.1a	1.8a
50N	1.3a	3.6b	1.7ab	3.6b
100N	1.8ab	3.9b	2.3b	4.0b
150N	3.1b	3.7b	3.9c	4.1b
SED§	0.6	0.6	0.4	0.4
F-value	5.01*	4.01*	13.8**	12.6**
Effect of straw incorporation‡				
50N	1.3a	3.6a	1.7a	3.6a
50N+S	1.9a	2.8a	1.9a	3.5a
SED	0.6	1.1	0.4	0.5
150N	3.1a	3.7a	3.9a	4.1a
150N+S	2.1a	3.7a	3.8a	4.3a
SED	0.7	0.6	1.0	0.8

†Effect of N rate on the grain yield assessed by one-way ANOVA. Mean values (n =3) followed by different letters indicate a significant difference (P < 0.05) by LSD test following the F-value (* = P < 0.05, ** P < 0.01).

§SED = standard error of the difference.

‡Effect of straw incorporation on the grain yield assessed by t-test. Mean values (n =3) followed by the same letter indicate non-significant differences (P > 0.05).

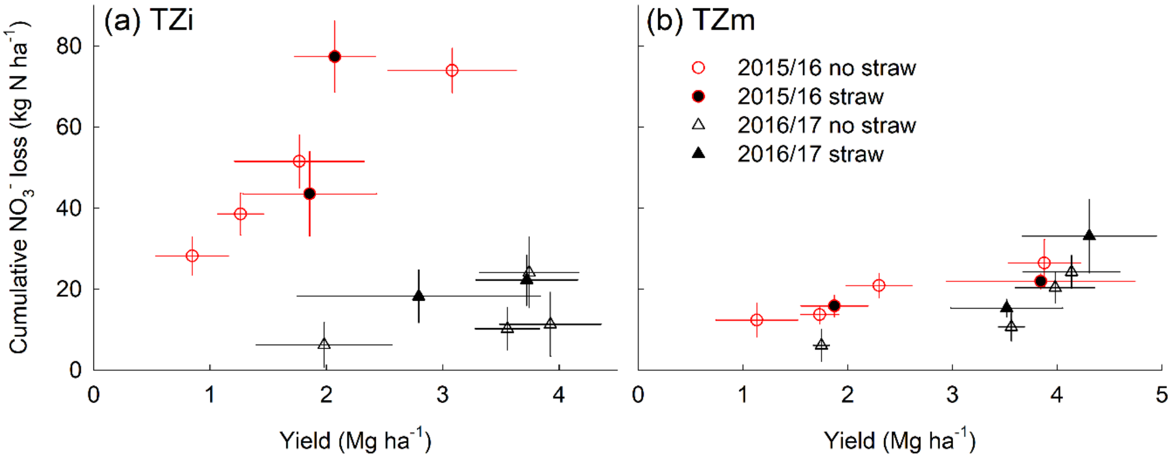

Fig. 5.6 Relationship between maize yields and cumulative NO_3^- losses at TZi (a) and TZm (b). Error bars represent standard error of the means.

5.4 Discussion

5.4.1 Drainage and lysimeter performance

Drainage was dependent on rainfall amount and soil type. The lower ratio of drainage to rainfall at TZm (37%) than that at TZi (47%) was mainly due to the higher water-holding capacity of soils at TZm (Table S5.1). These ratios were higher than those (13–30%) reported in a study in Zimbabwe (Mapanda et al. 2012a), primarily because the leachates were collected from a much deeper depth of soil (1.1 m) compared to the current study (0.3 m).

Repacked soil monolith lysimeters generally performed well in the current study; in most cases the variation of NO_3^- fluxes among the four replicates that received the same treatment was small (Fig. 5.3). In contrast, in a study using suction cup lysimeters, a large ranges of NO_3^- concentrations across replicate plots were observed, often exceeding by an order of magnitude (Russo et al. 2017). Compared to suction cup lysimeters, monolith lysimeters can capture the total drainage and therefore provide a more precise estimate of the average concentration of leachate. The small sampling area of suction cup lysimeters may fail to intersect macrospores and misrepresent nutrient concentrations (Fares et al. 2009; Wang et al. 2012).

5.4.2 Nitrate leaching

5.4.2.1 Features of temporal dynamics

The first peak of NO_3^- loss between sampling dates always occurred at the beginning of the cropping season when sufficient rainfall occurred (Fig. 5.3a, b), which was caused mainly by the rapid mineralization and nitrification of organic matter accumulated during the drying season, often known as the “birch effect” (Birch, 1964). The pulse of soil NO_3^- concentration at the beginning of the cropping season in tropical croplands has been frequently reported (Chikowo et al. 2004; Tully et al. 2016; Zheng et al. 2018b), yet few studies have documented the direct evidence of leaching loss. This result confirmed the challenge in managing the indigenous N resource in the early season, when NO_3^- leaching (up to 18 kg N ha^{-1}) occurred as mineralized N well exceeded the crop N demand (Chikowo et al. 2004; Zheng et al. 2018b). Conserving this leachable N through temporary immobilization is beneficial to improving N synchrony between soil supply and crop uptake.

The soil rewetting process following N applications could contribute to notable pulses of NO_3^- losses (i.e., 96 DAS at TZi in the 2015/16 season and 84 DAS at TZm at the 2016/17 season; Fig. 5.3a, b), which increased the challenge of improving N management. Dry soil conditions shortly after N addition possibly impeded plant N uptake (e.g., 75 DAS at TZi, soil water content dropped to 0.027 m^3 m^{-3}, equivalent to <-3 MPa) and resulted in high mineral N in the surface soil (0–0.3 m) that was prone to the leaching once sufficient rain fell. Further, the rewetting of dry soil could stimulate the N mineralization by the birch effect, as mentioned above.

5.4.2.2 Effect of N rate

The response of NO_3^- leaching to increasing N rates exhibited an exponential growth pattern in the current study (Fig. 5.4), similar to those observed in temperate and sub-tropical croplands (Svoboda et al. 2013; Cui et al. 2018). Very few studies have evaluated the effect of various fertilizer-N rates on NO_3^- leaching from SSA croplands, most of which only included one or two N rates in addition to the control treatments (Kamukondiwa and Bergström 1994; Nyamangara et al. 2003; Kimetu et al. 2006; Mapanda et al. 2012a). The only study including four N rates to date, however, reported no correlation between N application and NO_3^- leaching (Russo et al. 2017), which could be partly caused by the use of a different type of lysimeter (ceramic suction cup) compared with that in this study (monolith lysimeter). Magnitudes of the cumulative NO_3^- loss in the current study (6.3–74.0 and 6.1–26.5 kg N ha^{-1} at TZi and TZm respectively) were comparable with previous reports (4.3–56.3 and 2.5–20.0 kg N ha^{-1} in sandy and clayey soils, respectively; Nyamangara et al. 2003; Mapanda et al. 2012a) considering the N application rates.

5.4.2.3 Effect of straw incorporation

Decomposition of incorporated straw induced net N immobilization because of a high C:N ratio (60–206) of the straw (Table S5.2) in the early cropping season, and reduced NO_3^- leaching by 3.3–6.3 kg N ha^{-1} during the immobilization period compared to non-straw applied plots (Fig. 5.3c, d). With a similar amount of maize straw incorporated (2.5 Mg C ha^{-1}), Sugihara et al. (2012a) observed an increase of microbial biomass N (MBN) by 11–21 kg N ha^{-1} compared with that of control plots. This increased MBN pool was higher than the reductions of NO_3^- leaching (3.3–6.3 kg N ha^{-1}) in the current study, which likely occurred because of higher mineral N content in their soil making more N available in the decomposition sites for microbial assimilation compared with that of ours (Zheng et al. 2018b). Further, the newly synthesized biomass may also have come from N already present in the straw (Ocio et al. 1991), indicating that the increased MBN pool may not truly represent the potentially leachable N derived from soil.

The reductions of NO_3^- leaching in the current study were far below the potential of net N immobilization by the decomposition of straw considering its amount and quality. To make the current results more comparable with other field and laboratory incubation studies, I calculated the maximum net N immobilization per unit C added, equivalent to 1.2–2.7 kg N Mg^{-1} added C. This is comparable with a field lysimeter study in Nigeria (~3 kg N Mg^{-1} added C; calculated from Vanlauwe et al. 2002), but much lower than those from the laboratory incubations (represent the net N immobilization potential under non-limiting N conditions) (Fig. 5.7). According to the regression line in Fig. 5.7, the net N immobilization potential for the various C:N ratios of straws used in the current study should be 18.0–38.1 kg N Mg^{-1} added C. The large gap between field and incubation studies could be primarily attributed to the different particle size of straw and mixture ratio of straw to soil (~0.15 m chopped straw incorporated into only the top 0.15 m vs. finely ground straw fully mixed with soil) (Angers and Recous 1997). The large size of straw pieces reduced the surface area exposed to soil and therefore microbes for decomposition (Kumar and Goh 1999). A small contact area could have stimulated the N-limitation and re-cycling of microbial biomass N in the decomposition sites (Iqbal et al. 2013), leading to a small proportion of N derived from soil being assimilated by microbes. Such N-limitation and recycling of biomass-N during decomposition dwarfed the effects of varying C:N ratios of straw, soil type, and climatic conditions (i.e., rainfall and soil temperature), and resulted in small and similar values of maximum net N immobilization between two seasons and across sites in the current study (Fig. 5.7). Further, the environmental conditions in the field (e.g., soil moisture) was changing all the time, whereas they were mostly controlled and maximized for the microbial activity in the laboratory incubation. This could also contribute to the different results obtained under field and laboratory conditions (Fig. 5.7).

Straw incorporation likely failed to improve N synchrony. Re-mineralization of immobilized N induced higher NO_3^- leaching in the later growing season compared with non-straw applied plots (Fig. 5.3c, d), and largely offset the reduced NO_3^- leaching in the early growing season (Fig. 5.5). Such an offset could be expected in the 150N+S vs. 150N treatments because the N supply could have exceeded the crop N demand. However, it was unexpected and different from my hypothesis that cumulative NO_3^- loss in the 50N+S treatment was not lower than that in the 50N treatment. This might indicate that higher crop N uptake in the later growing season did not occur to improve N synchrony. Some of the re-mineralized N could be out of reach by the maize roots due to a homogeneous distribution of straws to the lysimeter with a radius of 0.2 m, while the horizontal extension of root rarely exceeded a radius of 0.1 m. In short, these results supported the direct hypothesis by Vanlauwe et al. (2001) regarding the aspect of reduced N leaching, but not improved N synchrony.

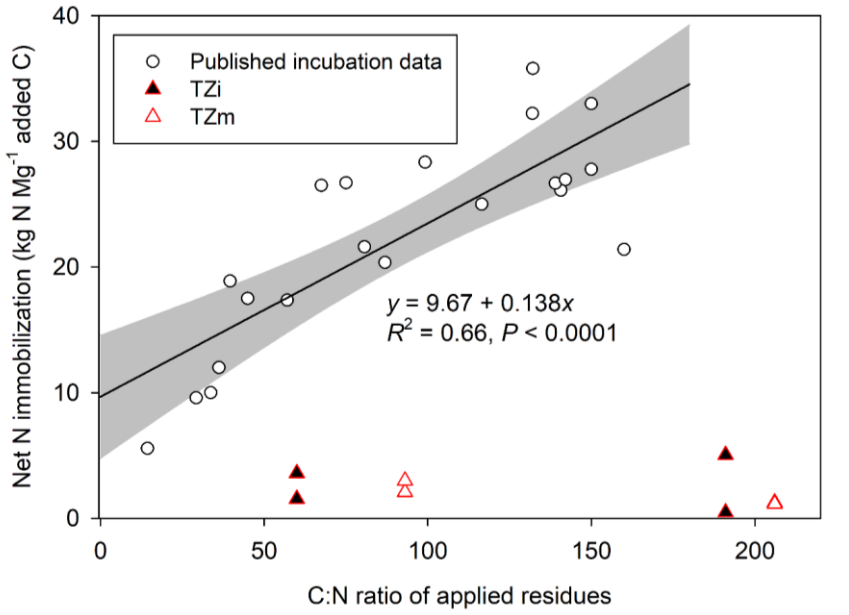

Fig. 5.7 Comparison between actual net N immobilization in this study and net N immobilization potential from published incubation studies. The grey areas indicate the 95% confidence intervals for the curve fitting. References used for generating the data in this figure include: Amougou et al (2010); Corbeels et al (2000); Henriksen and Breland (1999a, 199b); Iqbal et al (2013); Nicolardot et al (2001); Recous et al (1995); Sakala et al (2000); Trinsoutrot et al (2000); Muhammad et al (2011).

5.4.2.4 Inter-annual variation

In the 0N treatment, cumulative NO_3^- loss in the 2015/16 season was approximately four and two times as large as those in the 2016/17 season at TZi and TZm, respectively (Fig. 5.4). Such inter-annual variations was primarily due to the variations in precipitation, and consequently, in drainage (Fig. 5.1). The preceding 2 yr natural fallow might also have had a significant contribution at TZi. Water percolation is the driving force of NO_3^- movement within soils. Heavy rainfall can increase the flushing of NO_3^- and result in higher leaching (Russo et al. 2017). It is, therefore, inter-annual variations of water input (i.e., precipitation, irrigation) commonly resulted in different cumulative N losses between years (Mapanda et al. 2012a; Outram et al. 2016; Fan et al. 2017; Fu et al. 2017). Fallow management can alter N availability for the post-fallow crop, and thus, leachable N pool size (Hartemink et al. 2000; Chikowo et al. 2004), which could be one of the main reasons for the considerably high cumulative NO_3^- loss in the 0N treatment at TZi during the 2015/16 season. For example, a sandy clay loam soil in the Kenyan highland following 17 months of natural fallow was reported to increase the amount of N in light and intermediate fractions (≤ 1.37 g cm^{-3}) by 41 kg N ha^{-1} (0–0.15 m) compared to continuous maize monoculture cultivation (Maroko et al. 1998). The higher water-holding capacity (Table S5.1) could contribute to the lower inter-annual variation of cumulative NO_3^- loss at TZm than at TZi (Fig. 5.4), likely because of the buffered effect of variation in precipitation.

Nitrate leaching ratios were less responsive to treatments but depended more on seasons (Table 5.1). At TZi, the high NLR in the 2015/16 season (21–31%) is consistent with the study on a sandy soil in Zimbabwe (24–40%) by Nyamangara et al. (2003), possibly contributed by sufficient rainfall coupled with preceding fallow. Such high N leaching loss from applied fertilizer-N could be of socioeconomic significance to low-income smallholder African farmers (Nyamangara et al. 2003). Furthermore, it may suggest that soil fertility recovery by natural fallow should be adopted with caution in tropical regions experiencing distinct dry and wet seasons. At TZm, the lower NLR together with lower yield in the 2015/16 season (Tables 5.1, 5.2) compared with the 2016/17 season may suggest that applied N was also lost through other pathways, such as ammonia volatilization. Ammonia loss may have accounted for >5% of applied N at TZm (Zheng et al. 2018a) because the N applications were not immediately followed by sufficient rainfall (<3 mm within approximately 2 d after fertilization).

The NLR measured in the current study (3–31%) were well within the ranges reported by previous research across SSA croplands (5–35% as summarized by Russo et al., 2017). However, they were generally higher than most of the recently reported ranges in Chinese croplands (<5%; e.g., Xing and Zhu 2000; Gao et al. 2016; Yang et al. 2017), where much higher N rates (commonly 165–495 kg N ha^{-1}) were applied. More field experiments across agro-ecological zones and involvement of smallholder farmers are needed to develop an integrated soil-crop system management for higher yield with lower environmental costs (Chen et al. 2014; Cui et al. 2018), which still has a long way to go in SSA.

5.4.3 Relationship between maize yield and cumulative NO_3^- loss

Sustainable intensification of agriculture requires high productivity with low environmental costs. With increasing N rates, the linear relationship (in the 2015/16 season) between yields and cumulative NO_3^- losses indicated that greater yield was achieved at the expense of more NO_3^- loss, with higher expense observed at TZi as suggested by the greater slope compared with that at TZm (slopes of red hollow circles in Fig. 5.6a, b; not fitted). However, the non-linear pattern with a potential tipping point for the relationship in the 2016/17 season indicated that yield could be increased without inducing substantial NO_3^- loss by adopting a proper N rate (Fig. S5.4). Different relationships were likely attributed to the inter-annual variation of climatic (i.e., rainfall amount and pattern) and land management (i.e., preceding fallow at TZi) factors (Yang et al. 2017). Nevertheless, to confirm the potential of achieving higher yield with lower NO_3^- loss, long-term field experiments are needed to better characterize the relationship between yields and NO_3^- leaching losses with the input of various N rates.

Straw incorporation did not contribute to higher yield with lower N loss (Fig. 5.6). The large pieces of crop residue used under the field conditions could largely reduce its capacity of N immobilization and leaching mitigation. The temporarily immobilized N pool was therefore too small

(3.3–6.3 kg N ha^{-1}) to improve the N synchrony and benefit the maize yield. This may explain why the positive interactive effects of combined application of low-quality residue and fertilizer-N on the yields seldom occurred (Chivenge et al. 2010; Sugihara et al. 2012a). Nonetheless, to evaluate the applicability of crop residues in SSA croplands, C loss mitigation by crop residues (Sugihara et al. 2012b), and the effect on greenhouse gases emission (i.e., CO_2 and N_2O; Zhou et al. 2017) should be thoroughly considered.

5.5 Conclusions

During a two-year study, I examined the effect of increasing N rates and straw incorporation on NO_3^- leaching from the critical root zone (0–0.3 m) of maize in two tropical highlands of Tanzania, using repacked monolith lysimeters. The soil rewetting process, particularly at the onset of the rainy season and following N applications, was a critical driver of NO_3^- loss. Higher N rates increased cumulative NO_3^- loss exponentially, with considerable inter-annual variation observed that corresponded with the variation in rainfall amounts and preceding fallow management. Depending on season, a tipping point was observed in the relationship between cumulative NO_3^- loss and maize yield, above which yield increment was accompanied by substantial NO_3^- loss. Straw incorporation induced net N immobilization in the early growing season, and reduced NO_3^- loss by 3.3–6.3 kg N ha^{-1}, but no effect was observed on the cumulative NO_3^- losses or maize yields. The reduction in NO_3^- loss (equivalent to 1.2–2.7 kg N Mg^{-1} added C) were far below the potential of net N immobilization by the decomposition of straw (18.0–38.1 kg N Mg^{-1} added C), which was likely due to the large pieces of straw (~0.15 m) used in the field. These results showed the potential to enhance maize yield without inducing substantial N leaching loss by adopting the proper N rate in the tropical highlands of Tanzania, although future research, including long-term monitoring are required to better characterize the relationship between yield and NO_3^- loss by accounting for the inter-annual variation (e.g., climate, crop growing condition, etc.). Also, these results showed that temporary immobilization of leachable N by using large pieces of straw (~0.15 m) in the field was inefficient in improving N synchrony and benefiting yield.

Supplementary materials

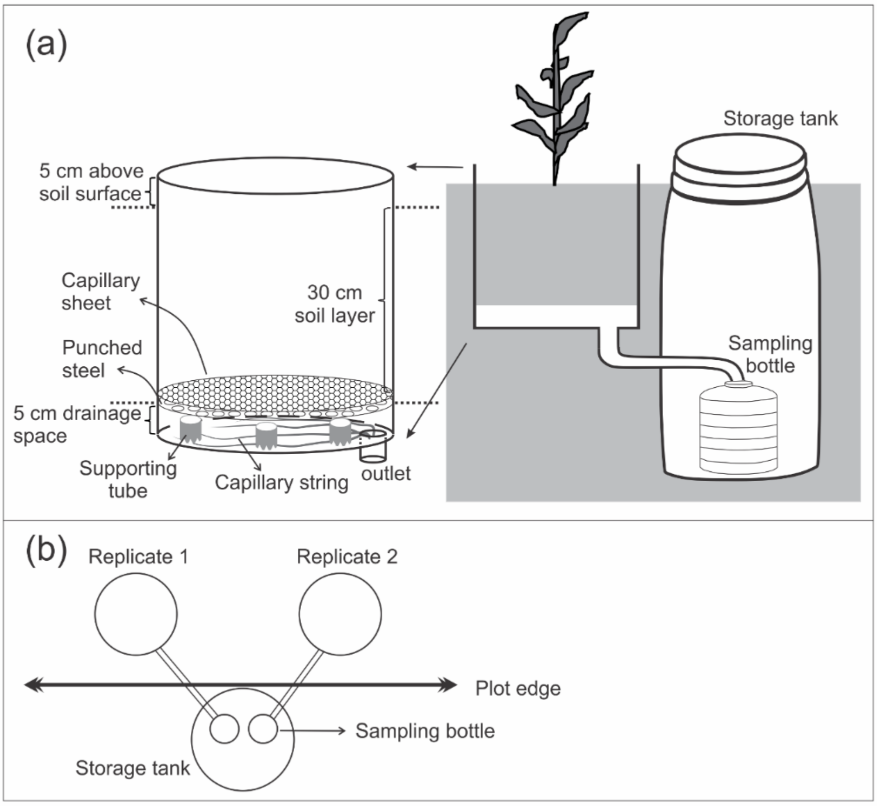

Fig. S5.1 Illustration of lysimeter installation. Lysimeter design and vertical-cut view of lysimeter installation (a), and top-down view of lysimeter installation for two lysimeter replicates connecting to the same storage tank (b).

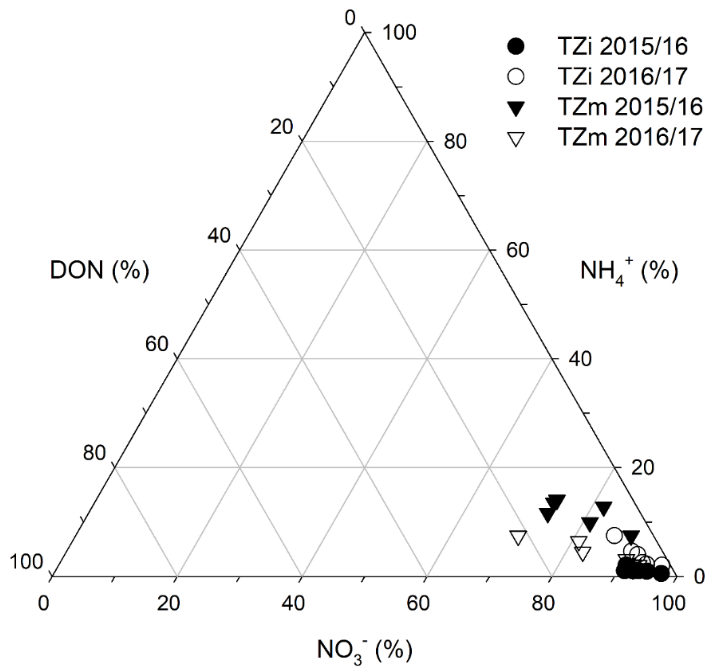

Fig. S5.2 Contribution of N compositions to the cumulative TDN loss.

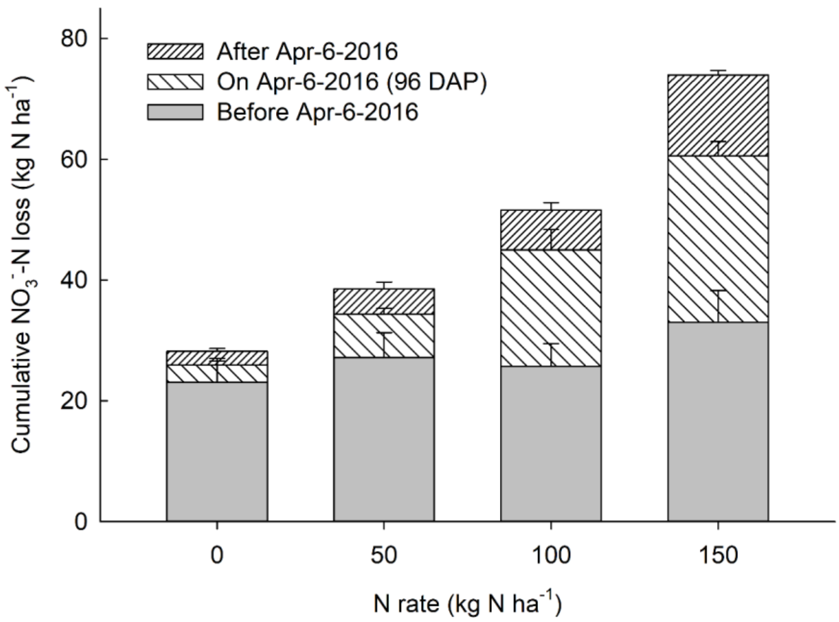

Fig. S5.3 An example showing the treatment effect of different N rates was dominantly contributed by a single leaching event at TZi during the 2015/16 season. Error bars represent standard error of the means.

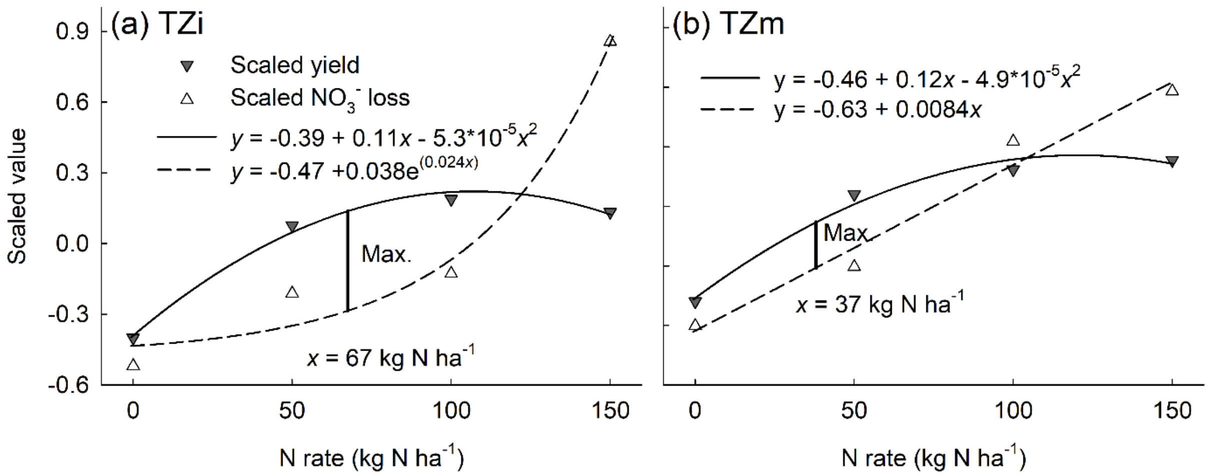

Fig. S5.4 Scaled maize yields and scaled cumulative NO_3^- losses vs. N application rates during the 2016/17 period for TZi (a) and TZm (b). Scaled data = (data at each N rate – Mean data)/Mean data, where data refers to maize yield or cumulative NO_3^- loss.

Table S5.1 Selected soil physico-chemical properties of profiles for TZi and TZm

Site	Depth	pH	TC†	TN†	C:N	CEC‡	WHC‡	Soil texture (%)		
		(H_2O)	g kg^{-1}	g kg^{-1}	ratio	cmol$_c$ kg^{-1}	%	Clay	Silt	Sand
TZi	0–15	6.45	3.5	0.3	12.9	1.1	27.2	4.7	6.9	88.4
	15–30	5.96	1.9	0.2	9.6	0.9	27.6	6.4	7.9	85.7
	30–42	5.66	2.1	0.2	8.3	1.7	ND§	13.2	8.8	78.0
	42–60	5.29	1.8	0.3	6.9	3.3	ND	16.9	8.8	74.3
	60–75+	5.07	1.5	0.2	6.7	3.7	ND	16.7	7.3	76.0
TZm	0-25	6.85	17.5	1.3	13.6	17.5	66.3‡	28.4	42.0	29.5
	25-50	7.09	9.6	0.8	12.5	22.7	62.0‡	34.6	32.9	32.5
	50–70	6.90	7.6	0.6	12.2	16.2	ND	23.5	38.1	38.3
	70–115+	Pumice layer								

†Total carbon (TC) and N (TN) determined by dry combustion of finely ground soils using Vario Max CHN elemental analyzer.

‡Cation exchange capacity (CEC) determined by the ammonium acetate saturation method.

‡WHC = maximum water holding capacity. For TZm, WHC determined for 0–0.15 m and 0.15–0.3 m layers.

§ND = not determined.

Table S5.2 Application date, DAS (days after sowing), averaged content (n = 2) of total carbon (TC), total N (TN), and C:N ratio of applied straws and the equivalent amount of added C and N to each lysimeter

	Season	Date	DAS	TC† %	TN† %	C:N ratio	Added C Mg C ha^{-1}	Added N kg N ha^{-1}
TZi	2015/16	Nov-24-2015	–38§	45	0.36	191	2.3	18.9
	2016/17	Nov-24-2016	–15	43	0.73	60	2.2	38.2
TZm	2015/16	Nov-28-2015	–12	46	0.22	206	2.7	13.1
	2016/17	Dec-3-2016	–11	43	0.46	93	2.2	23.3

§Due to heavy rainfall, seeding on Dec-14-2015 failed to germinate at TZi and re-sowing was conducted on Jan-1-2016, leading to much earlier date of straw incorporation.

†TC and TN determined by dry combustion of finely ground soils using Vario Max CHN elemental analyzer.

Table S5.3 Averaged (n = 4) cumulative drainage (mm) for each treatment

Treatment	TZi		TZm	
	2015/16	2016/17	2015/16	2016/17
0N	348a	114a	412bc	207a
50N	365a	113a	369ab	254a
100N	312a	96a	481d	271a
150N	344a	96a	357a	260a
50N+S	361a	115a	432cd	295a
150N+S	403a	123a	447cd	254a
SED[†]	25.4	24.2	24.2	39.9
F-value	2.76^{ns}	0.43^{ns}	7.45^{*}	1.18^{ns}

[†]SED = standard error of mean difference

Mean values followed by different letter indicate significant different at $P < 0.05$ level (LSD test).

* = $P < 0.05$, ns = not significant.

CHAPTER 6

Soil-Atmosphere Exchange of Nitrous Oxide in Two Tanzanian Croplands: Effects of Nitrogen and Straw management

Abstract

Cropland intensification is needed to meet the demand for food in Sub-Saharan Africa (SSA). This process requires a dramatic increase in resource inputs, including nitrogen (N) fertilizer and organic residues (e.g., straw), which alter the soil-atmosphere exchange of nitrous oxide (N_2O). The dearth of N_2O emission data for SSA croplands, however, has largely constrained our ability to define regional N_2O flux and mitigation opportunities. In two soils cropped to maize in Tanzania (TZi, sandy Alfisols; TZm, clayey Andisols), year-round measurements were conducted consecutively for 2 years to quantify N_2O emissions in response to increasing N rates and in combination with maize straw incorporation. Rainfall and the resulting soil moisture, rather than soil temperature, were important environmental drivers of N_2O emissions in these fields. Applied N stimulated N_2O fluxes across soil types but with different magnitudes—lower at TZi because of the dominance of nitrification in N_2O production and higher at TZm likely from promoted denitrification when the water-filled pore space was >47%. N_2O emission increased exponentially or linearly with N rate, depending on the year. The direct N_2O emission factors were well below the 1% of the IPCC Tier 1 method, ranging from 0.13–0.26% at TZi and 0.24–0.42% at TZm, for a N rate of 50–150 kg N ha^{-1} during the study. Compared with N application alone, straw plus N did not significantly alter maize yield, but did raise N_2O emissions with a synergistic effect. Consequently, straw incorporation markedly increased the emission factor (up to 0.46% at TZi and 1.29% at TZm) as well as yield-scaled N_2O emissions. These results suggest that linear and exponential emission responses can occur in SSA croplands, and challenge the suitability of combining straw with fertilizer-N as a “climate-smart” practice in this region.

6.1 Introduction

As a potent greenhouse gas and the leading cause of stratospheric ozone depletion (Forster et al. 2007; Ravishankara et al. 2009), nitrous oxide (N_2O) has received increasing attention in recent years (Butterbach-Bahl et al. 2013). Agricultural soils account for ~41% of global anthropogenic emissions of N_2O (~4.3 Tg N_2O-N yr^{-1}, as estimated for 2010; Reay et al. 2012) and thus have a crucial role in achieving climate stabilization targets (Frank et al. 2018). Accelerated use of synthetic nitrogen (N) fertilizers has been identified as the primary contributor to the rapid increase in atmospheric N_2O since 1960 (Davidson 2009). Apparently, agricultural intensification with increased fertilizer-N input, particularly for crop production, holds one of the keys to mitigation opportunities (Adviento-Borbe et al. 2007; Burney, et al. 2010; Reay et al. 2012).

To meet the demand for cereal crops among the growing population (van Ittersum et al. 2016), Sub-Saharan Africa (SSA) must undertake cropland intensification with dramatic increases in resource input, particularly fertilizer-N. The low level of fertilizer-N use, together with the nutrient-depleted soils common to SSA croplands, contributes to the stagnantly low yield of cereal production in the past decades (Vitousek et al. 2009). Regional and national efforts are therefore underway to increase fertilizer use (AGRA 2009; Vanlauwe et al. 2014b) to offset soil nutrient depletion and secure crop production. However, fertilizer-N addition to the croplands will inevitably increase soil emissions of N_2O.

Unfortunately, there is an absence of knowledge on soil emissions of N_2O from SSA croplands (Kim et al. 2016; Rosenstock et al. 2016). The paucity of field measurements of N_2O fluxes presents uncertainties in estimating the current and future agricultural N_2O emissions (Reay et al. 2012), This largely constrains our ability to understand the impact of regional agricultural intensification on the climate system as well as to design effective and targeted mitigation strategies. For most countries in SSA, the estimates of national greenhouse gas inventories are left with using Tier 1 emission factors (EFs) from the IPCC (2006), which were developed based on measurements conducted for the most part in temperate ecosystems (Bouwman et al. 2002).

Soil N_2O is produced mainly through the microbiological process of nitrification and denitrification (Braker and Conrad 2011), both of which are regulated by factors at the "distal" level including climate (e.g., rainfall, temperature) and soil type and at the "proximal" level including availability of carbon (C), N, and O_2 (Firestone and Davidson 1989). With O_2, N_2O can be produced as a byproduct during the oxidation of ammonium (NH_4^+) to nitrate (NO_3^-) via nitrite (NO_2^-) (Braker and Conrad 2011), although an alternative pathway, nitrifier denitrification, may also be a significant source of N_2O (Wrage-Mönnig et al. 2018). By contrast, denitrification produces N_2O as an obligatory intermediate during the stepwise reduction of NO_3^- or NO_2^- to N_2, which is an anaerobic respiration process requiring C as the energy source (Braker and Conrad 2011). Fertilizer-N additions can therefore provide N substrate for microbial production of N_2O. Rainfall and accordingly soil moisture, coupled with soil texture, can control the gas diffusion—including O_2—among soil pores (Firestone and Davidson 1989), and subsequently the dominance of the different microbial processes in producing N_2O (Bateman and Baggs 2005). The response pattern of N_2O to increasing N rates, although not common in SSA croplands (very few exceptions such as Hickman et al. 2015), could be of great help to better predict regional and site-specific N_2O emissions under cropland intensification.

Combined application of low-quality organic residues (e.g., straw with a high C:N ratio) and fertilizer-N has been widely promoted across SSA as the technical basis of Integrated Soil Fertility Management (Kimani et al. 2003), yet how such practices affect the soil N_2O emissions remains to be evaluated in this region. Straw may play multiple roles in mediating soil N_2O emissions (Chen et al. 2013). For example, straw with a low C:N ratio can mineralize N for microbial N_2O production (Baggs et al. 2006; Millar et al. 2004). By contrast, straw with a high C:N ratio may stimulate microbial N assimilation and reduce N_2O production (Wu et al. 2012). In addition, straw may serve as an energy provider for denitrifiers, and enhance N_2O production through denitrification (Abalos et al. 2012). These may partly explain the inconsistent results on the effects of the combined input of straw and fertilizer-N on soil N_2O emissions in temperate croplands (e.g., Abalos et al. 2012; Wu et al. 2012). Returning straw to the soil is a common practice to sequester C and improve soil quality worldwide (Kumar and Goh 1999); its combination with fertilizer-N may also have the potential to reduce NO_3^- leaching and improve N synchrony (Gentile et al. 2009; Sugihara et al. 2012a). However, these potential benefits could be compromised if soil N_2O emissions are enhanced as a result of straw incorporation.

A better understanding of the effects of N and straw management on N_2O emissions is needed to identify mitigation strategies for SSA croplands. To evaluate the response of N_2O emissions to N application rate and the effect of a combined application of straw and fertilizer-N on soil N_2O emissions in maize-based systems of the Tanzanian highlands, a field experiment was conducted in two Tanzanian croplands with different soil type. The specific objectives of this study were to (i) investigate the seasonal variability of N_2O fluxes; (ii) quantify the annual N_2O emissions and the EFs; and (iii) examine the relationship between N_2O emissions and maize yield, as affected by increasing N rates and the combined input of fertilizer-N and maize straw.

6.2 Materials and methods

6.2.1 Characteristics of study sites

The study was conducted at two maize fields with different soil types in the southern highlands of Tanzania. One site, TZi, is located in Mangalali village (07°46′ S, 35°34′ E; 1480 m a.s.l.) of the Iringa region. The soil is classified as coarse-loamy, isohyperthermic, Kanhaplic Haplustalfs (Soil Survey Staff, 2010). TZi had been under natural fallow for 2 years before the start of the experiment. Before natural fallow, maize had been continuously cultivated by local farmers for more than 5 years with annual N input at a rate of ~100 kg N ha^{-1} mainly as urea. The other site, TZm, is located in Uyole town (08°55′ S, 33°31′ E; 1780 m a.s.l.) of the Mbeya region. The soil is classified as clay-loam, isothermic, Dystric Vitric Haplustands (Soil Survey Staff, 2010). TZm is located within the Mbeya Agricultural Training Institute-Uyole and is used as experimental plots. Maize and common beans were grown in rotation from 2003 to 2011, followed by sunflower for 2 years until the establishment of this trial in November 2015. Nitrogen was applied mainly as urea at a rate between 80 and 100 kg N ha^{-1} yr^{-1} for maize and sunflower cultivation. TZi receives 560 mm of precipitation per year on average, lower than that at TZm (860 mm). The annual daily average temperature was higher at TZi (23.5 °C) relative to that at TZm (17.1 °C). The pattern of annual rainfall is unimodal for both sites. The rainy season (and accordingly the growing season) generally begins in late November for both sites, and ends in mid-April and mid-May at TZi and TZm, respectively. Selected properties for the soil profiles of study sites are presented in Table S6.1. Despite the similar soil pH and C:N ratio in topsoil between the two sites, soil organic matter and CEC were substantially lower at TZi as compared with those characteristics at TZm, because of the low clay content in the former soil. Water-holding capacity was higher at TZm than at TZi at depths of 0–0.15 m and 0.15–0.3 m.

6.2.2 Experimental design

From November 2015 to June 2017, maize was cultivated consecutively for two seasons at both sites. Experimental plots were established in a fully randomized block design for six treatments consisting of four levels of N rate—0, 50, 100, and 150 kg N ha^{-1}, denoted as 0, 50, 100, and150N, respectively—and two more treatments combining the N application and maize straw incorporation, denoted as 50N+S (50 kg N ha^{-1} plus ~2 Mg C ha^{-1}) and 150N+S (150 kg N ha^{-1} plus ~2 Mg C ha^{-1}). Each treatment was replicated three times. A 1.5-m buffer separated each plot (plot size: 5 m × 5 m) and block. Within each plot, three maize (*Zea mays* L.; variety: TMV-1 for TZi and UH6303 for TZm) seeds were sown per hole at a spacing of 0.7 m × 0.3 m and were thinned to one plant per hole 20 days after sowing (DAS), giving a population of ~48000 plants ha^{-1}. Maize was planted in early- to mid-December at both sites, and harvested in early April and mid-May at TZi and TZm, respectively. Because of heavy rainfall, seeding on Dec-14-2015 failed to germinate at TZi and re-sowing was conducted on Jan-1-2016.

Maize straw was chopped into ~0.15-m pieces and incorporated into the soil at a depth of 0–0.15 m using a hand hoe. Date of straw incorporation and its quality (i.e., C and N content and the C:N ratio) are presented in Table S6.2. Fertilizer-N application, by broadcasting urea, was split into two times following the local extension advice (Zheng et al. 2018b). One-third of the total amount was applied 21 DAS (three- to four-leaf stage of maize growth). The remaining two-thirds was applied 57 DAS (around the time of maize tasseling). Weeding was carried out when necessary, and all weeded materials were removed from the plots. Phosphorus (P) was added to all plots as basal application with 50 kg P ha^{-1}, using triple superphosphate.

6.2.3 N_2O flux measurements

Soil-atmosphere N_2O fluxes were measured using a static chamber method over a 2-year period from December 2015 to November of 2017. Gas samples were collected every 10–14 days during the rainy season and approximately monthly during the dry season, with intensified samplings conducted during the two weeks following each N application (e.g., 1, 2, 4, 6, 8, and 11 days after fertilization). Throughout the experimental period, 53 and 55 measurements were made at TZi and TZm, respectively. Four opaque PVC chambers (diameter, 25.5 cm; height, 30 cm) were inserted into the soil to a depth of 15 cm in each replicate plot and remained in the same location during each year. The average of four measurements was used per treatment plot. Chambers were placed between maize rows where no plants were growing. Chambers were inserted ~2 weeks before the first measurement to avoid the potential influence of installation disturbance. Chambers were re-installed in the second year during land preparation and straw incorporation. Possible effects of root mortality and activity on N_2O fluxes (Keller et al. 2000; Sey et al. 2009; Smith and Tiedje 1979) were excluded by removing living root biomass during the installation process as well as by applying the trenching method (Shinjo et al. 2006). Briefly, the bottom of each chamber was covered by a fine plastic mesh to support the soil inside and to maintain the same soil moisture condition as outside the chamber. A plastic sheet then can be used to block the root respiration during each measurement (see the procedure in detail below). Fertilizer applications for the chambers were managed identically to those in the plots, and the accurate rate of added C and N from straw to chambers is shown in Table S6.2.

For each measurement, I first removed the PVC chamber, covered its bottom with a plastic sheet, and returned it to the hole. After that, the chamber was closed with a lid fitted with a sampling port (butyl rubber septum) and made airtight. Using a polypropylene syringe adapted with a three-way stopcock, I took 20-ml gas samples at 0 min and 40 min and transferred the samples to pre-evacuated 10 ml screw top glass vials (SVG-10 Gas-Chro Vials, Nichiden-rika Glass Co., Ltd., Japan). Before removing the plastic sheet and returning the chamber to the original condition, each chamber height above the soil surface was measured by a ruler at three different positions along the inner edge of the PVC pipe for the estimation of headspace volume. The air temperature inside the chamber was measured by a CS215 probe (Campbell Scientific, Inc., USA) connected to a CR1000 data logger (Campbell Scientific, Inc.). To minimize the effects of diurnal variation in gas emission, samples were taken at the same time of day (8:00–11:00 AM) at each site.

The gas samples were analyzed with a gas chromatograph (GC-2014, Shimadzu Inc., Kyoto, Japan) equipped with a ^{63}Ni electron capture detector operated at 349 °C. The carrier gas was argon containing 5% CH_4 (Kindgas, Japan) at a flow rate of 30 ml min^{-1}. A reference gas containing 990 ppbv N_2O in N_2 (Kindgas) was injected after every fourth sample of chamber air to guarantee a precise calibration. A volume of 0.5 ml from each sample was manually injected into the gas chromatograph with a Pressure-Lok gas syringe (Series A-2, VICI Precision Sampling, Inc., USA). Before the separation of the N_2O peak on a packed Porapak Q column (80–100 mesh; length, 4 m; 3-mm i.d.) at 75 °C, CO_2 and water vapor from the sample were removed by pre-columns filled with Ascarite (Sigma-Aldrich, USA) and $Mg(ClO_4)_2$ (Wako Pure Chemical Industries, Ltd., Japan), respectively, to avoid the interference with N_2O analysis. Pre-columns were replaced approximately every month. Flux rates were calculated according to Equation 6.1:

$$F_{N_2O} = \left(\Delta c \times V_{ch} \times P \times MW_{N_2O\text{-}N} \times 10^{-2}\right)/(R \times T \times A_{ch}), \quad (6.1)$$

where F_{N_2O} = N_2O flux (µg N_2O-N m^{-2} h^{-1}), Δc = average rate of change in the mixing ratio of N_2O in the chamber air (ppbv h^{-1}), V_{ch} = chamber volume (cm^3), P = pressure (atm); $MW_{N_2O\text{-}N}$ = molecular weight of N_2O-N (28.0134 g mol^{-1}), R = gas constant (0.08206 L atm K^{-1} mol^{-1}), T = temperature (K), and A_{ch} = chamber base area (cm^2).

6.2.4 Auxiliary measurements

Soil temperature at a depth of 5 cm was monitored with T108 sensors (Campbell Scientific, Inc.) with two replicates for plots with and without straw incorporation. Air temperature was monitored using one T108 sensor at each site, and precipitation was recorded with a TE525MM rain gauge (Campbell Scientific, Inc.). All monitoring instruments were connected to the same data logger (CR1000, Campbell Scientific, Inc.), which recorded data every 10 min. For almost every gas sampling event, soil samples from 0–15 cm were collected using an auger (~4-cm diameter) at four different positions in the vicinity of chambers to determine the gravimetric water content. To indicate O_2 availability, water-filled pore space (WFPS) was calculated using the measured bulk density, soil particle density (Table S6.1), and gravimetric water content at each site according to Equation 6.2:

$$\text{WFPS} = \frac{\text{volumetric water content}}{\text{soil total porosity}} = \frac{\text{gravimetric water content} \times \text{bulk density}}{1 - \frac{\text{bulk density}}{\text{soil particle density}}}, \quad (6.2)$$

6.2.5 Yield estimation

To estimate yield, maize ears inside the plots (4 m × 4 m, avoiding the edge) were collected and grains were shelled from the ears. Weights of the shelled grains were recorded before subsamples were taken for moisture correction. Subsamples of the grains were oven-dried at 60 °C to a constant weight. Grain yield in the current study was expressed on a dry weight basis.

6.2.6 Data analysis and statistics

Daily fluxes (g N_2O-N ha^{-1} day^{-1}) were estimated based on chamber measurements, assuming no diurnal variation in emissions. Cumulative emissions for each treatment plot were estimated by linear interpolation of daily fluxes between sampling events over the measurement period. For 2015/16 and 2016/17, the measurement period covered 347 and 341 days at TZi, and 303 and 329 days at TZm, respectively. Average daily flux (g N_2O-N ha^{-1} day^{-1}) was calculated by dividing the cumulative emission by the measurement period (number of days). To estimate the annual emission covering 365 days, I summed the N_2O emissions from growing and non-growing seasons. The non-growing seasons were not fully covered by the measurements, and the emissions were therefore estimated as follow:

$$\text{Emission estimate}_{\text{Non-growing}} = \frac{\text{Cumulative emission}_{\text{Non-growing}}}{\text{Measurement period}_{\text{Non-growing}}} \times \text{Total period}_{\text{Non-growing}}, \quad (6.3)$$

To calculate the EF, the difference between annual emissions from the 0N treatment and those from treatment was divided by the amount of fertilizer-N added in the latter treatment.

Chamber measurements of N_2O flux (μg N m^{-2} h^{-1}) were related to soil and environmental variables using Spearman correlation. One-way analysis of variance (ANOVA) was used to assess the effects of N rate on average daily flux and maize yield. After determination of an *F*-value, multiple comparisons of the means with an LSD test were conducted. An independent *t*-test was used to evaluate the effect of straw incorporation on average daily flux and maize yield. Statistically significant differences were identified as $P < 0.05$ unless stated otherwise. Statistical analysis was conducted with IBM SPSS Statistics (version 24).

The average daily fluxes at different N rates were fitted to an exponential or linear curve. The relation of delta annual N_2O emission to delta yield (where delta refers to the difference between treatment and control plots) was fitted with three models: exponential, linear, and quadrative. Model comparison was conducted using corrected Akaike's information criterion (AIC_c) together with 'pseudo R^2', which was calculated as 1 − (residual sum of squares / total sum of squares). Model fitting and comparisons were performed using R software (version 3.3.3; http://www.r-project.org).

6.3 Results

6.3.1 Environmental factors

Temporal variations in rainfall, air temperature, soil temperature at a depth of 5 cm at two sites are presented in Fig. 6.1a and Fig. 6.2a. The rainfall in 2015/16 was 758 and 1123 mm at TZi and TZm, respectively, about 200 mm higher than the mean annual rainfall at each site. By contrast, 2016/17 was a drier year according to local farmers at TZi (the data logger was out of function for most of the time in 2016/17; Fig. 6.1a) and a much lower rainfall amount (664 mm) recorded at TZm. Daily average air temperatures showed narrow ranges during the rainy seasons (19–25 °C at TZi and 16–21°C at TZm). Similarly, soil temperature at a 5-cm depth did not vary substantially (21–32 °C at TZi and 17–27°C at TZm), with negligible effect of straw incorporation observed during the rainy season (Figs. 6.1a, 6.2a).

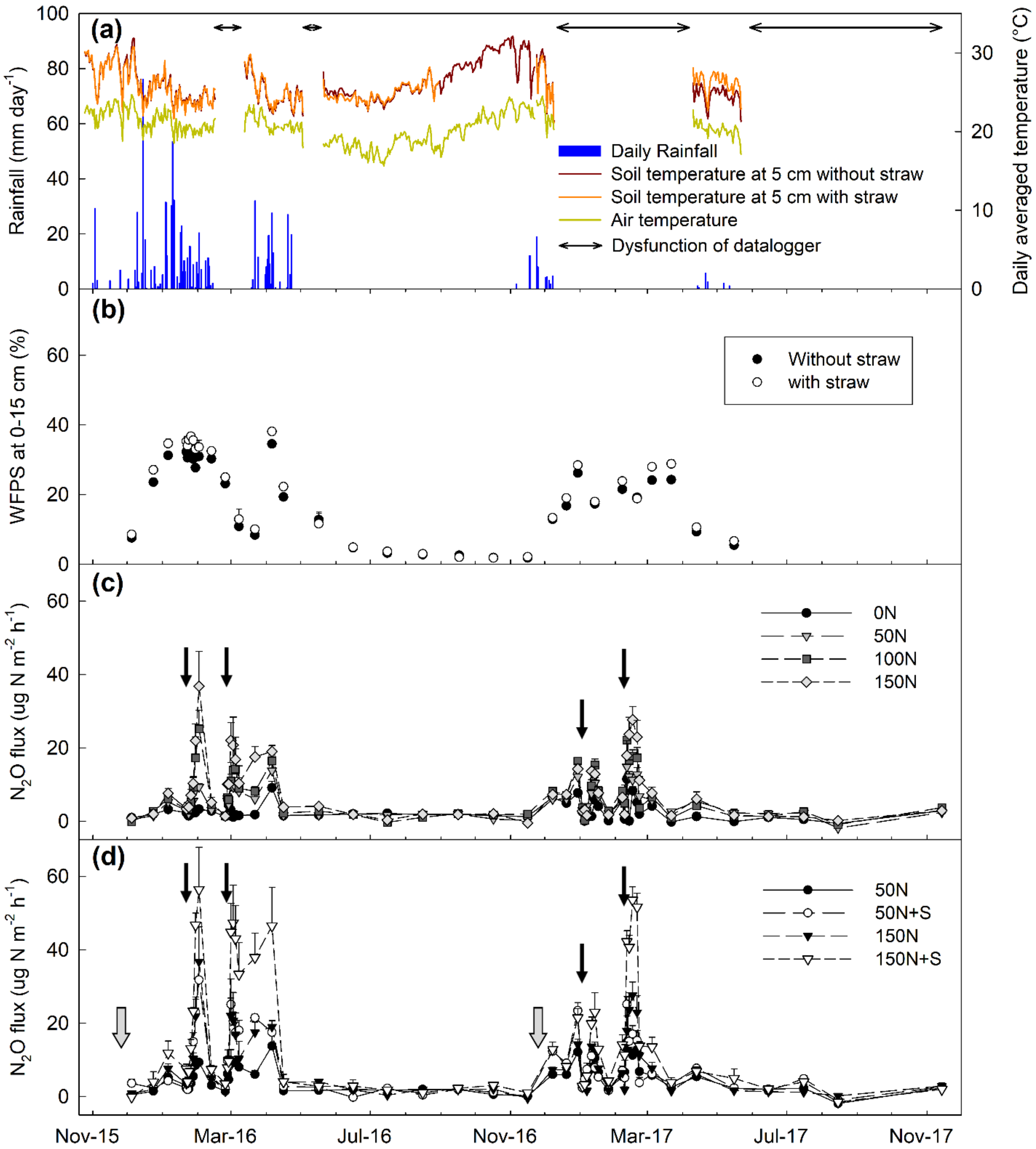

Fig. 6.1 Temporal variations in rainfall and soil and air temperature (a), in WFPS at 0–15 cm (b), and in N_2O flux under different treatments (c, d) at TZi. Gray arrows indicate the timing of straw incorporations, and black arrows indicate the timing of N applications. Error bars in (b–d) represent standard errors.

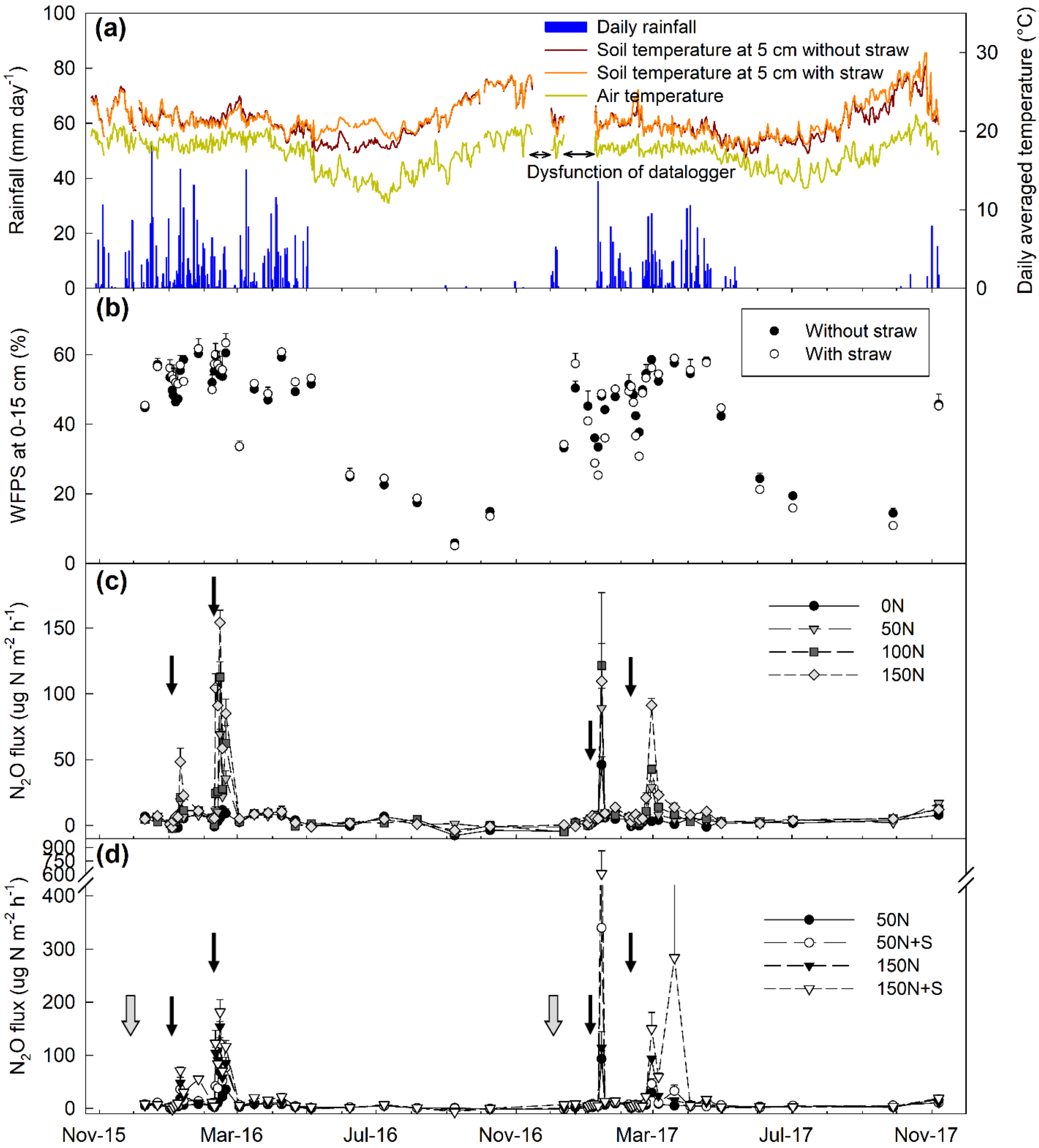

Fig. 6.2 Temporal variations in rainfall and soil and air temperature (a), in WFPS at 0–15 cm (b), and in N_2O flux under different treatments (c, d) at TZm. Gray arrows indicate the timing of straw incorporations, and black arrows indicate the timing of N applications. Error bars in (b–d) represent standard errors.

The soil WFPS at a depth of 0–15 cm varied intra-seasonally as a result of rainfall fluctuation (Figs. 6.1b, 6.2b) but was not significantly affected by straw incorporation during the study period (P = 0.349 and 0.613 for TZi and TZm, respectively, by Mann-Whitney rank sum test). The WFPS ranged from 1.8 to 38.1% at TZi, and from 5.1 to 63.3% at TZm throughout the study period. At both sites, the maximum WFPS was higher in 2015/16 (38.1% at TZi and 63.3% at TZm) than 2016/17 (28.8% at TZi and 58.9% at TZm). At TZm, a rapid and substantial drop in WFPS coincided with each timing of N application (except the second N application in 2015/16; Fig. 6.2b).

6.3.2 Seasonal variability of N_2O fluxes

N_2O fluxes varied temporally and in response to N applications (Figs. 6.1c, 6.2c). N_2O fluxes from the 0N treatment were generally low (<13 μg N_2O-N m^{-2} h^{-1}), with peaks observed at the beginning of the rainy seasons (at TZi only, up to 7.2 μg N_2O-N m^{-2} h^{-1}) and after the re-wetting of the soils (up to 12.7 and 46.1 μg N_2O-N m^{-2} h^{-1} at TZi and TZm, respectively). In N-fertilized plots, peaks of N_2O fluxes were observed after each N application (Figs. 6.1c, 6.2c) and were generally larger at higher N rates (13.8–36.7 μg N_2O-N m^{-2} h^{-1} in the 50–150N treatments at TZi and 69.2–154.0 μg N_2O-N m^{-2} h^{-1} in the 50–150N treatments at TZm; Table S6.3). The response of N_2O fluxes to fertilizer-N occurred within 1–3 days of the application at TZi, whereas it took >6 days at TZm (except for the second N application in 2015/16; Fig. 6.3). The duration of increased N_2O fluxes was not affected by N rate, and varied substantially at each site (14–38 days for TZi and 5–21 days for TZm; Fig. 6.3). In addition, N_2O uptake was observed in the dry, non-growing seasons, with values down to −1.7 and −7.7 μg N_2O-N m^{-2} h^{-1} at TZi and TZm, respectively (Figs. 6.1c, 6.2c).

Straw incorporation in combination with N application generally increased the N_2O fluxes as compared with N application alone during the crop growing seasons (Figs. 6.1d, 6.2d). Particularly during the periods following N applications, the N_2O peaks varied up to 31.8 and 56.4 μg N_2O-N m^{-2} h^{-1} in the 50N+S and 150N+S treatments, respectively, at TZi; and varied up to 339.7 and 609.5 μg N_2O-N m^{-2} h^{-1} in the 50N+S and 150N+S treatments, respectively, at TZm. Consequently, the arithmetic mean of N_2O fluxes in the 50N+S treatment for each cropping year was higher than that in the 100N treatment, and comparable to that in the 150N treatment at each site (Table S6.3).

Across all treatments and sites, the N_2O flux significantly correlated with WFPS and CO_2 flux but not soil temperature (Table 6.1). The N_2O flux at TZi tended to correlate more closely with the daily rainfall amount on the measurement date rather than with the previous day's rainfall, whereas the opposite trend was observed at TZm. Relatively high N_2O fluxes (>15 μg N_2O-N m^{-2} h^{-1}) were observed across a wide range of WFPS at TZi (8–39%) but were observed only when WFPS was >47% at TZm (Fig. S6.1).

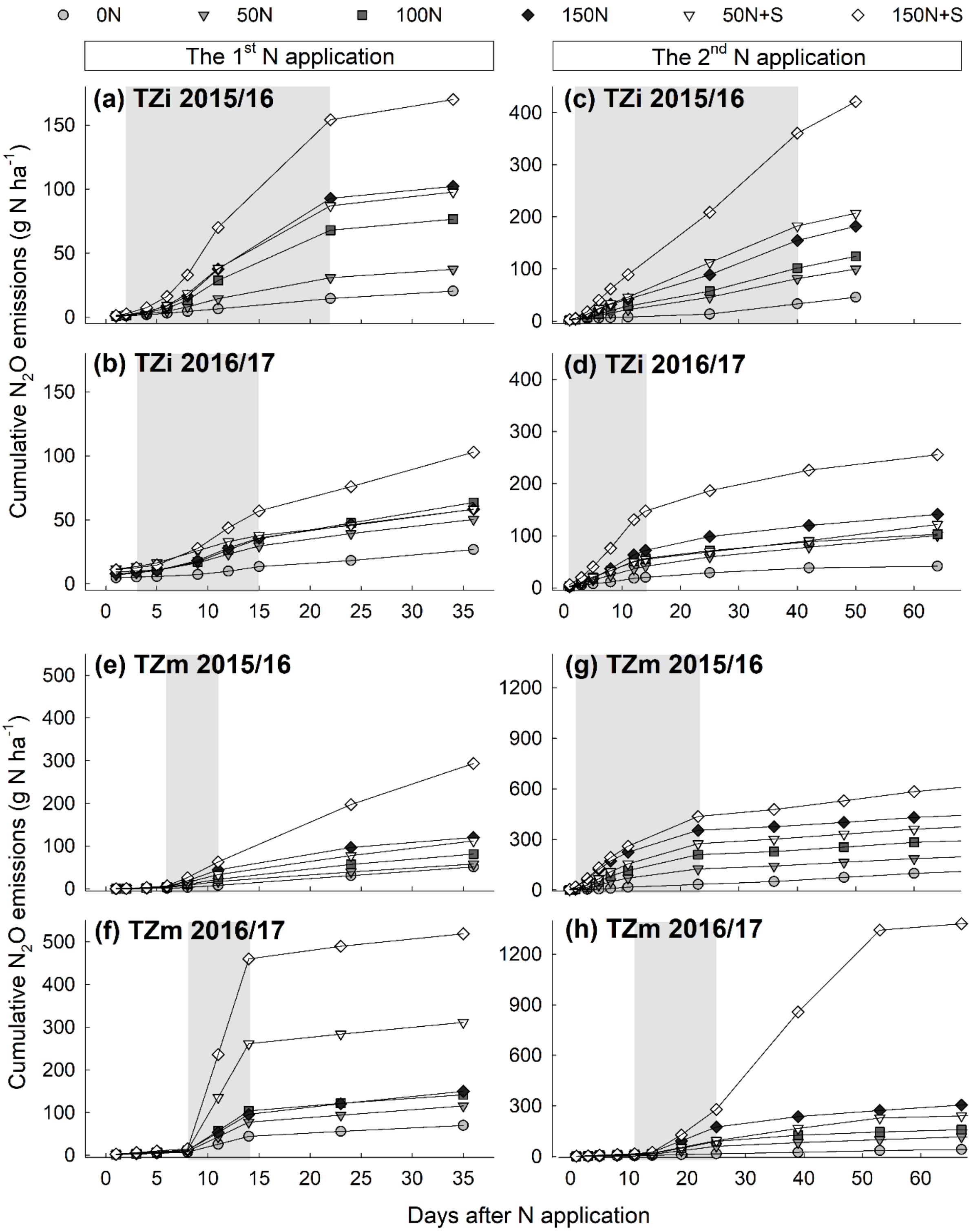

Fig. 6.3 Cumulative N_2O emissions after each N application at TZi (a–d) and TZm (e–h). The shaded portion of the graphs represents the periods (14–38 days for TZi and 5–21 days for TZm) during which N_2O flux was stimulated by N treatments.

Table 6.1 Spearman correlation between N_2O flux and measured soil and environmental variables for each treatment at TZi and TZm, respectively, over the study period (December 2015 to November 2017).

Treatment	WFPS (%)	Soil temperature (5 cm; °C)	Rainfall (mm day^{-1})	Previous day rain (mm day^{-1})	CO_2 flux§ (mg C m^{-2} h^{-1})
TZi					
0N	0.47**	−0.18^{ns}	0.31^{ns}	0.46*	0.39**
50N	0.49**	−0.26^{ns}	0.44*	0.39^{ns}	0.55***
100N	0.54**	−0.06^{ns}	0.53**	0.49*	0.51***
150N	0.53**	−0.06^{ns}	0.56**	0.48*	0.50***
50N+S	0.46**	0.12^{ns}	0.45*	0.30^{ns}	0.44**
150N+S	0.56**	−0.06^{ns}	0.58*	0.48*	0.45***
TZm					
0N	0.30*	0.08^{ns}	0.33*	0.40**	0.372**
50N	0.48***	0.14^{ns}	0.38**	0.44**	0.48***
100N	0.49***	0.20^{ns}	0.30*	0.41**	0.40**
150N	0.57***	0.18^{ns}	0.43**	0.45***	0.61***
50N+S	0.49***	0.18^{ns}	0.37**	0.49***	0.58***
150N+S	0.53***	0.14^{ns}	0.38**	0.52***	0.64***

Values followed by *, **, *** indicate significant at $P < 0.05$, < 0.01, and < 0.001 level, respectively. ns means non-significant

$^{§}CO_2$ flux was measured with the thermal conductivity detector of a gas chromatograph (GC-2014, Shimadzu Inc., Kyoto, Japan) using the same gas sample for N_2O measurement (data not shown)

6.3.3 Average daily fluxes, annual emissions and emission factors

Curve fitting for the average daily flux vs. N rate was performed separately for each cropping year at TZi and TZm (Fig. 6.4). The average daily flux increased significantly at higher N rates, and was well described by either an exponential or a linear model at each site (R^2 = 0.65–0.88, $P \leq 0.0002$). With the same N rate applied, straw incorporation significantly ($P \leq 0.06$) increased the average daily flux (Fig. 6.5). When combined with straw incorporation, the average daily flux from plots with the addition of 50 kg N ha^{-1} was comparable or even higher than that from plots with 150 kg N ha^{-1} alone (Fig. 6.5).

Annual emissions were estimated by summing the emissions from the growing and non-growing seasons. Across sites and cropping years, N_2O emissions were generally higher during the growing than during the non-growing season (except the 0N treatment in 2015/16 at TZi, and the 0N and 50N treatments in 2016/17 at TZm; Fig. 6.6). Across two cropping years, annual emissions from the 0–150N treatments ranged from 0.14 to 0.44 kg N_2O-N ha^{-1} at TZi, and from 0.18 to 0.72 kg N_2O-N ha^{-1} at TZm (Table 6.2). With straw incorporation, annual emissions ranged from 0.37 to 0.79 kg N_2O-N ha^{-1} at TZi, and from 0.62 to 2.24 kg N_2O-N ha^{-1} at TZm (Table 6.2). The EFs for the 50-150N treatments ranged from 0.13 to 0.26% (average, 0.16%) at TZi and from 0.24 to 0.42% (average, 0.32%) at TZm (Table 6.2). Straw incorporation increased the EFs by 0.14–0.33% (average, 0.23%) at TZi and 0.25–1.01% (average, 0.62%) at TZm (Table 6.2).

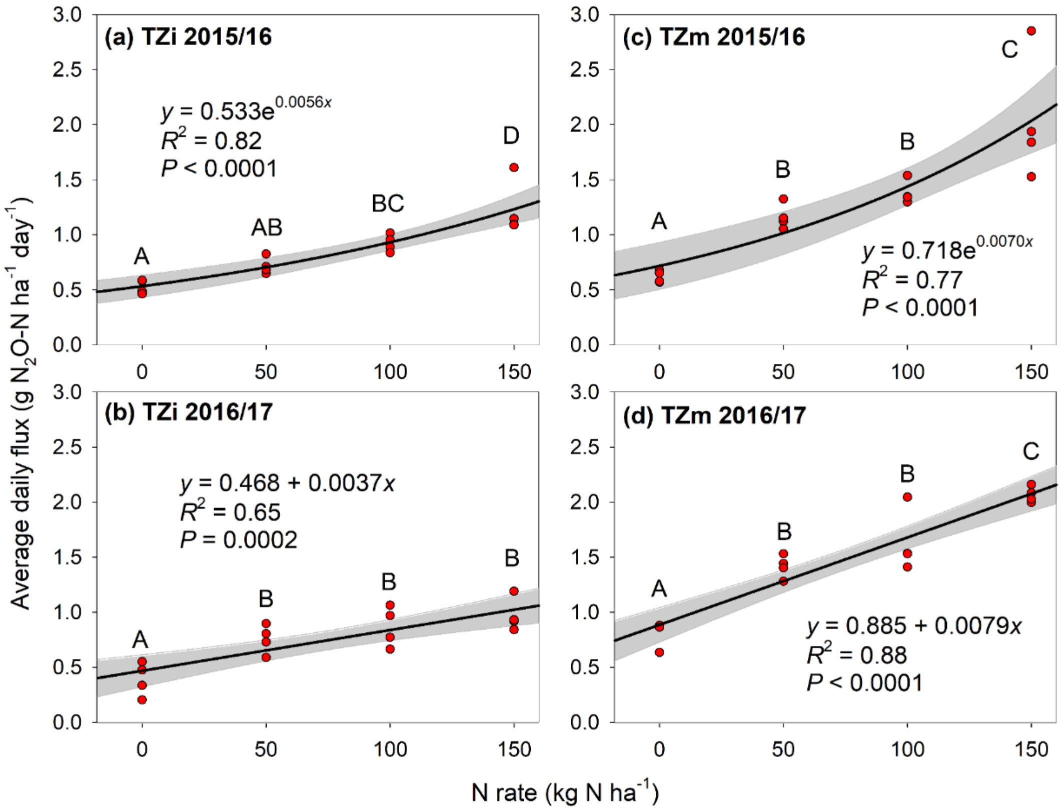

Fig. 6.4 Relationship between N rate and average daily N_2O flux for each cropping year at TZi (a, b) and TZm (c, d). The gray areas indicate the 95% confidence intervals for the individual curve fits. Different capital letters within each graph indicate significant differences at $P < 0.05$ based on the LSD test.

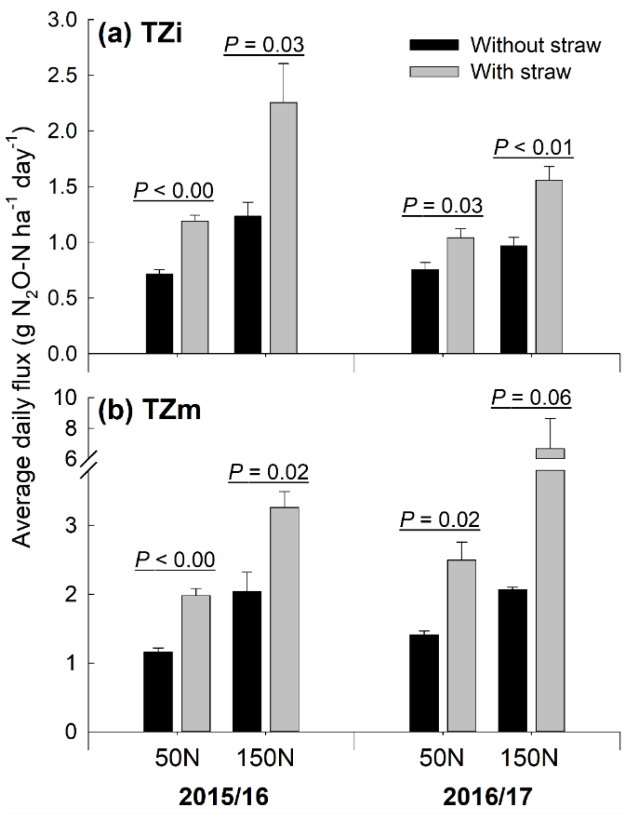

Fig. 6.5 Effect of straw incorporation on the average daily N_2O flux for each cropping year at TZi (a) and TZm (b). Error bars represent standard errors. P values for the resulting t-tests are provided above the bars.

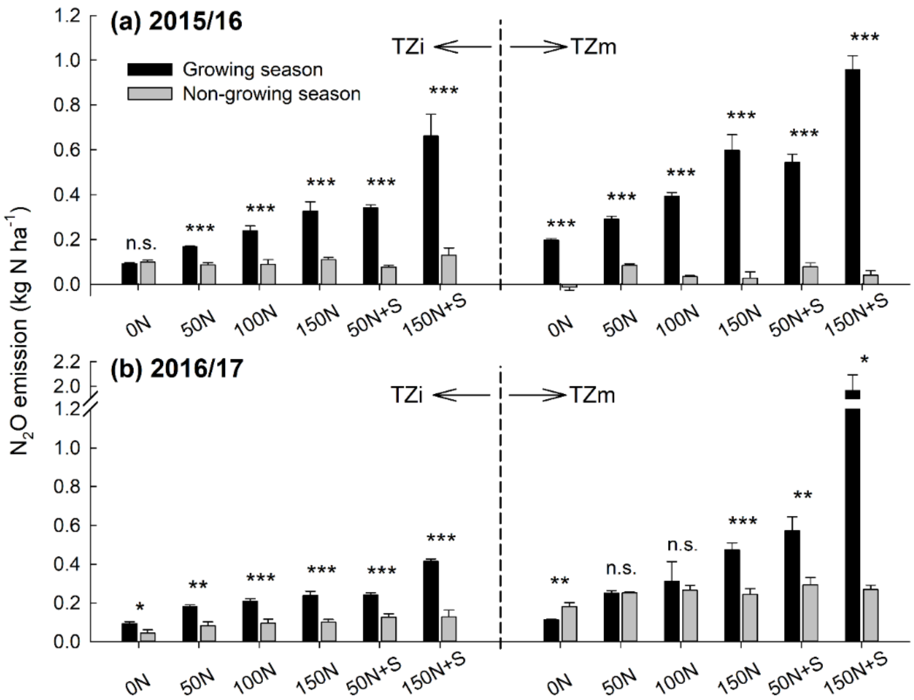

Fig. 6.6 Cumulative N_2O emissions during the growing seasons (~130 days from December to April at TZi and ~140 days from December to May at TZm) and non-growing seasons from each treatment at TZi (left side) and TZm (right side) for 2015/16 (a) and 2016/17 (b). *, **, *** indicate significant differences at $P <$ 0.1, 0.05, 0.01, respectively, based on the *t*-test. n.s. indicates non-significant difference ($P > 0.1$).

Table 6.2 Estimates of annual N_2O emissions and emission factors (EFs).

Treatment	TZi		TZm	
	Annual emission (kg N ha^{-1})	EF (%)	Annual emission (kg N ha^{-1})	EF (%)
		2015/16		
0N	0.191 ± 0.012		0.184 ± 0.011	
50N	0.255 ± 0.014	0.13	0.376 ± 0.019	0.39
100N	0.327 ± 0.014	0.14	0.428 ± 0.016	0.24
150N	0.437 ± 0.044	0.16	0.626 ± 0.093	0.29
50N+S[§]	0.419 ± 0.019	0.46	0.622 ± 0.030	0.88
150N+S[§]	0.792 ± 0.124	0.40	1.000 ± 0.073	0.54
		2016/17		
0N	0.138 ± 0.028		0.297 ± 0.023	
50N	0.266 ± 0.024	0.26	0.505 ± 0.017	0.42
100N	0.305 ± 0.033	0.17	0.579 ± 0.048	0.28
150N	0.341 ± 0.027	0.14	0.719 ± 0.015	0.28
50N+S[§]	0.368 ± 0.029	0.46	0.868 ± 0.089	1.14
150N+S[§]	0.545 ± 0.045	0.27	2.237 ± 0.644	1.29

[§]For the calculation of EFs for the combined fertilizer-N and straw treatments, straw-N was not considered as the source for N_2O emission because of the high C:N ratios (60–206; Table S6.2) of the straw used in this study.

6.3.4 Maize yield and its relationship with annual N_2O emission

At each site, maize yields tended to be affected by an interaction between the N rate and cropping year (Fig. 6.7). Maize yields were significantly enhanced ($P < 0.05$) with increasing N rate, with the yield in 2016/17 (2.0–3.9 Mg ha^{-1} at TZi and 1.8–4.1 Mg ha^{-1} at TZm) being higher than that in 2015/16 (0.8–3.1 Mg ha^{-1} at TZi and 1.1–3.9 Mg ha^{-1} at TZm) under the same N rate. Maize yields were not significantly ($P > 0.05$) affected by straw incorporation across sites and cropping years (Fig. 6.7).

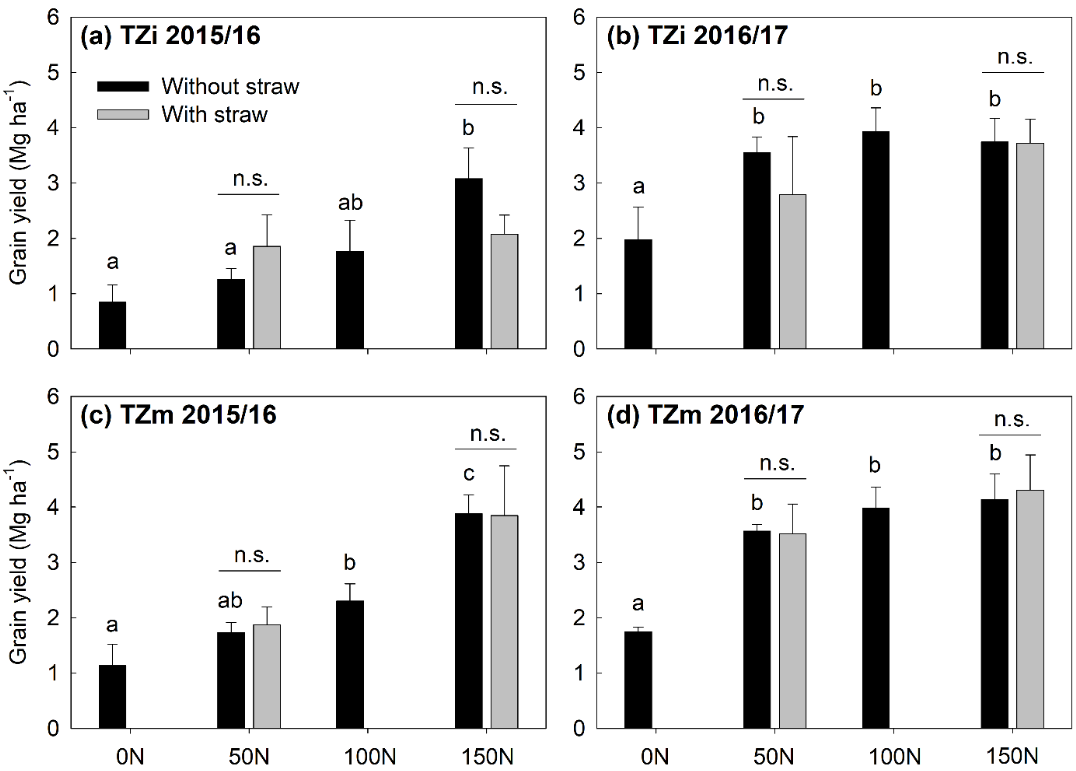

Fig. 6.7 Grain yield at TZi (a, b) and TZm (c, d). Different lowercase letters above the bars indicate a significant difference ($P < 0.05$) in grain yield for different N rates based on the LSD test after a one-way ANOVA. n.s. indicates a non-significant effect ($P > 0.05$) of straw incorporation on grain yield based on the *t*-test. Error bars represent standard errors.

The relationship between maize yield and annual N_2O emission was described by comparing the delta yield with delta annual N_2O emission (Fig. 6.8a, b) and by the yield-scaled N_2O emission (Fig. 6.8c, d). For plots without straw incorporation, an exponential model ($AIC_c = -9.3$ for TZi and $AIC_c = -1.3$ for TZm; Table S6.4) was marginally superior to a linear model ($AIC_c = -8.8$ for TZi and $AIC_c = 0.3$ for TZm; Table S6.4) for describing the relationship between delta annual emission and delta yield at each site (Fig. 6.8a, b). Data points for the plots with straw incorporation are all located above the fitted curve in Fig. 6.8a and b, showing that straw incorporation resulted in additional emission of N_2O

for the same level of yield increment at both sites. Across cropping years and soil types, yield-scaled N_2O emissions were consistently higher for plots that incorporated straw than those that did not (Fig. 6.8c, d). Despite the inter-annual variation observed for the effect of N rate on the yield-scaled N_2O emission at each site, data combining results from 2 years showed negligible differences in yield-scaled N_2O emissions among the plots receiving fertilizer-N only (0.11–0.12 and 0.16–0.17 kg N_2O-N Mg^{-1} grain at TZi and TZm, respectively). These levels were markedly lower than those with combined input (N+S treatment; 0.17–0.23 and 0.28–0.40 kg N_2O-N Mg^{-1} grain at TZi and TZm, respectively) (Fig. 6.8c, d).

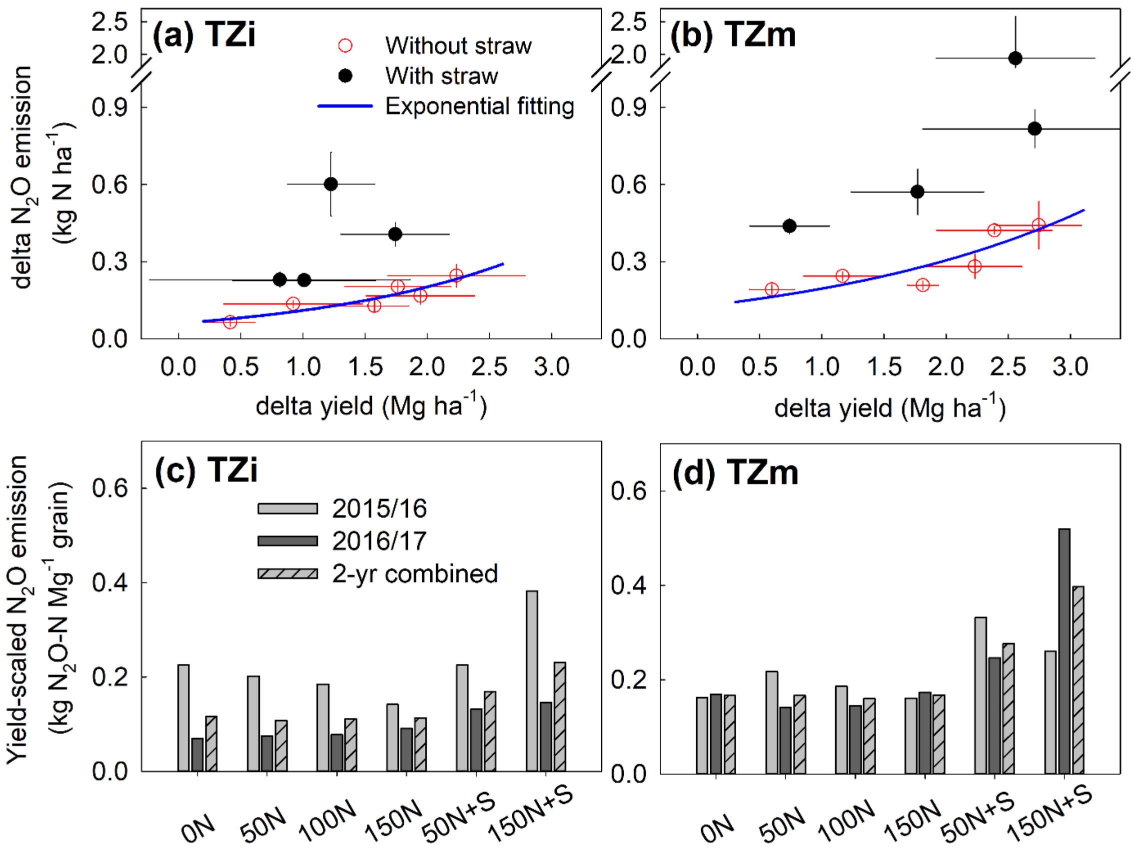

Fig. 6.8 The relation between yield and annual N_2O emission described by comparing the delta yield with delta annual N_2O emission (a, b) and the yield-scaled N_2O emission (c, d). Error bars represent standard errors.

6.4 Discussion

6.4.1 N_2O emissions from SSA croplands

Few studies have examined the soil-atmospheric flux of N_2O from SSA croplands (Rosenstock et al. 2016), despite their areal extent and the inevitable trend of future intensification. The few previous measurements have primarily been confined to natural ecosystems, such as forests and savannahs (e.g., Rees et al. 2006; Werner et al. 2007; also see a recent synthesis by Kim et al. 2016). From 2004 to 2018, I found only 18 studies with in situ measurements for various crops in this region (Table S6.5). By contrast, in China a total of 6089 site-years of field trials were conducted for maize alone during 2005–2015 (Cui et al. 2018). Furthermore, among these 18 studies, few included measurements across an entire year (e.g., Ortiz-Gonzalo et al. 2018) or adopted a proper sampling design to capture the critical temporal variations induced by land management (e.g., fertilizer-N input; Hickman et al. 2015). Non-growing or dry seasons were mostly neglected in the measurements (e.g., Mapanda et al. 2011), yet their contributions to annual emissions may vary up to 61% (Fig. 6.6). Following the fertilizer-N application, the N_2O fluxes can be highly variable (Figs. 6.1, 6.2), and therefore a low temporal resolution of measurements would translate to high uncertainty in the estimate of annual emissions. The current study provides some of the first reliable in situ N_2O measurements in SSA croplands with multiple N rates and the combined application of fertilizer-N and straw.

The annual emissions from unfertilized plots (or the background emissions; Kim et al. 2013a) in the current maize fields (0.14–0.30 kg N_2O-N ha^{-1} yr^{-1}) were comparable to those (0.10–0.22 kg N_2O-N ha^{-1} yr^{-1}) in Western and Central Kenya (Hickman et al. 2015; Ortiz-Gonzalo et al. 2018). However, Hickman et al. (2014) and Rosenstock et al. (2016) reported higher background emissions from maize fields in Kenya (0.71 kg N_2O-N ha^{-1} for 99 days) and Eastern Tanzania (0.90 kg N_2O-N ha^{-1} yr^{-1}), respectively. The higher background emissions in Kenya could be explained by the presence of more fertile soil with a history of manure deposition (Hickman et al. 2014), whereas that in Eastern Tanzania was likely due to higher nutrient availability (particularly C and N) under slash-and-burn management (Rosenstock et al. 2016). These variations suggest that heterogeneity in soil fertility and diversity in farm management practices should be considered when estimating N_2O emissions from SSA croplands. Based on Table S6.5 (only those studies that reported annual emissions) and current results, the calculated mean background emissions from SSA croplands (0.48 kg N_2O-N ha^{-1} yr^{-1}; SD = 0.35; n = 28) was lower than the global average of 1.08–1.40 kg N_2O-N ha^{-1} yr^{-1} (cultivated mineral soils; Gu et al. 2007; Gu et al. 2009; Kim et al. 2013a) (Fig. 6.9). The general depletion of N (Vitousek et al. 2009) and lower organic C content (Zomer et al. 2017) in the soil could be the main reasons for lower background N_2O emissions from SSA croplands.

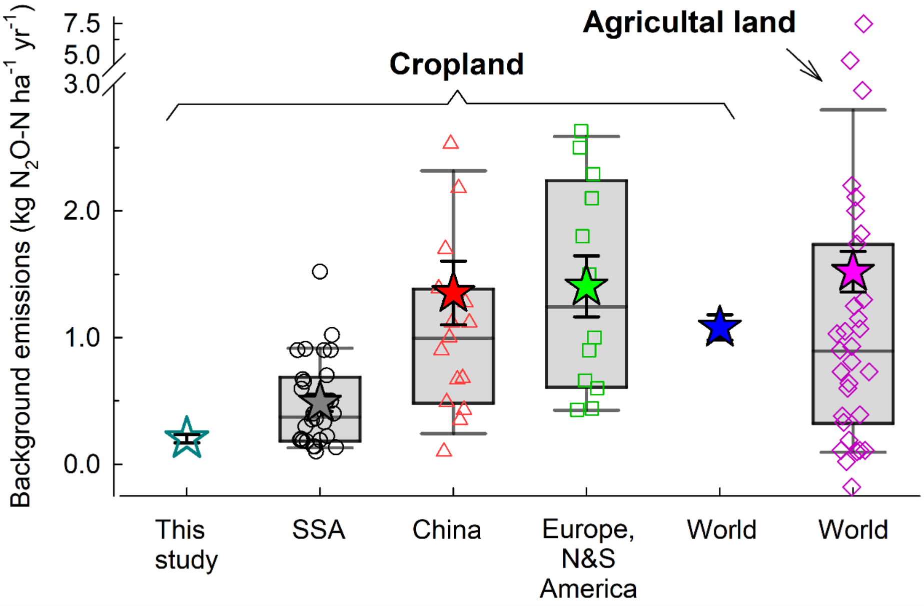

Fig. 6.9 Background emissions of N_2O in this study and in SSA croplands from other studies as compared with croplands in other parts of the world. Data for SSA croplands were from the studies in Table S5; data for Chinese croplands were synthesized by Gu et al. (2007); data for croplands in Europe and North and South (N&S) America were synthesized by Gu et al. (2009); data for the world's cropland and agricultural land was synthesized by Kim, Giltrap, et al. (2013). Large star with error bar indicate the mean value with standard error. Individual data points, where possible, are presented along with the box-whisker plots

Precipitation and accordingly the soil moisture could be an important driver of N_2O emissions from SSA croplands. Compared with temperate zones, less variation in air and soil temperature in tropical highlands (e.g., Figs. 6.1, 6.2) would accentuate the influence of soil moisture on the activity of microbes (Sugihara et al. 2012b), including nitrifiers and denitrifiers (Bateman and Baggs 2005). Unlike similar studies in temperate regions (Adviento-Borbe et al. 2007; Liu et al. 2014; Ma et al. 2010), this study found no correlation between N_2O flux and soil temperature (Table 6.1). Also, the pulses of N_2O fluxes from the 0N treatment always occurred at the onset of rains or after the rewetting of the soils (Figs. 6.1, 6.2). These N_2O pulses from unfertilized plots were sometimes of a similar magnitude to those from fertilized treatments (e.g., the N_2O peak on Apr-6-2016 at TZi following a prolonged dry period), which is consistent with observations from other studies (Barton et al. 2007; Hickman et al. 2014). Such N_2O pulses could be contributed by the release of readily available C and N during the rewetting process (Davidson 1992).

Rainfall events and, accordingly, WFPS also influenced the response of N_2O fluxes to N applications. At TZi, the N_2O peaks following the second application (higher N rates) were lower than those following the first application (lower N rates) in 2015/16 (Fig. 6.1c), which coincided with the lower WFPS after the second application (Fig. 6.1b). At TZm, with a high WFPS, the N_2O fluxes responded immediately to the N application (the second application in 2015/16; Figs. 6.2b, 6.3g), whereas with a dropping WFPS, no response was observed until the soils were rewetted by rainfall (Figs. 6.2b, 6.3e, f, h). These results confirmed that there was an interaction between the timing of N addition and rainfall events with respect to effects on the N_2O emission (Hayakawa et al. 2009) and that there may be no response to N addition under dry conditions (Ma et al. 2010).

6.4.2 Effect of N application on N_2O emissions

It is within expectation that the application of fertilizer-N stimulated N_2O fluxes (Figs. 6.1c, 6.2c; Table S6.3), as available N from fertilizer provided the substrate for microbial nitrification and denitrification (Firestone and Davidson 1989). The weaker stimulating effect of fertilizer-N at TZi as compared with TZm (with fluxes up to 37 vs. 154 μg N_2O-N m^{-2} h^{-1}; Table S6.3) was likely due to the dominance of nitrification in producing N_2O at TZi, as suggested by the soil aerobiosis (WFPS < 40%; Figs. 6.1b, S6.1a) largely resulting from the coarse texture (88% sand, Table S6.1). Further evidence includes the relatively high N_2O flux (>15 μg N_2O-N m^{-2} h^{-1}) observed at low WFPS (<20%) at TZi (Fig. S6.1a). N_2O production in soils during nitrification is generally considered to be minor compared with denitrification (Bateman and Baggs 2005; Khalil et al. 2004), the latter of which likely contributed to the higher N_2O fluxes from fertilized plots at TZm (Table S6.3). Denitrification may have been stimulated at the TZm plots because of the anaerobic conditions when WFPS was > 47% (Fig. S6.1b), though this threshold value may vary (Bateman and Baggs 2005; Gagnon et al. 2011; Ma et al. 2010).

Similar to background emissions, N_2O fluxes from the fertilized plots in the current study (up to 37 and 154 μg N_2O-N m^{-2} h^{-1} at TZi and TZm, respectively; Table S6.3) were generally of similar magnitudes relative to other N-fertilized maize fields in SSA (up to 32–123 μg N_2O-N m^{-2} h^{-1}; Chapuis-Lardy et al. 2009; Hickman et al. 2014; Hickman et al. 2015; Mapanda et al. 2011; Ortiz-Gonzalo et al. 2018), but much lower than those comparably fertilized maize fields in other parts of the world with similar water input—precipitation or plus irrigation (maximum peaks generally >300 μg N_2O-N m^{-2} h^{-1}; up to >1000 μg N_2O-N m^{-2} h^{-1}; Gagnon et al. 2011; Hoben et al. 2011; Liu et al. 2012; Ma et al. 2010; McSwiney and Robertson 2005). One exception reported high fluxes (up to 733 μg N_2O-N m^{-2} h^{-1}) in Kenya (Millar et al. 2004) was possibly due to high N input (>200 kg N ha^{-1}) using high-quality crop residue (C:N ratio < 20).

There are simply too few field studies across SSA that have measured EFs based on year-round measurements. I here report the EFs to be 0.13–0.26% and 0.24–0.42% at TZi and TZm, respectively, for the application rates of 50–150 kg N ha^{-1}. These values are well below the 1% of the Tier 1 method by IPCC (2006), which is used widely for national inventories across SSA. Current results are consistent with previous estimates of EFs based on seasonal measurements in SSA croplands, most of which are <0.7% (Fig. S6.2). The exceptionally high estimate of EF (4.1%; Fig. S6.2) by Dick et al. (2008) was likely due to field heterogeneity or to interference from management during the preceding season. A close inspection of the data from that study revealed that higher N_2O flux in the fertilized plots relative to unfertilized plots mostly occurred before fertilizer-N application. Therefore, this high EF does not represent fertilizer-induced emission.

With increasing N rates, the average daily N_2O flux increased either linearly or exponentially, depending on the cropping year (Fig. 6.4). It is of interest that in 2016/17, linear patterns were observed at both sites (Fig. 6.4b, d), coinciding with the quadratic-plateau pattern of the yields (Fig. 6.7b, d). This seems to contradict the widespread notion that with increasing N rates, a nonlinear exponential increase in N_2O emissions occurs when the N rate exceeded that required for maximum yields (Kim et al. 2013b; Ma et al. 2010; McSwiney and Robertson 2005). However, previous studies have noted poor correlations between soil mineral N concentration and N_2O flux (e.g., Adviento-Borbe et al. 2007; Chapuis-Lardy et al. 2009), indicating the importance of considering the interaction between N availability and environmental factors (Gagnon et al. 2011), such as rainfall. The linear patterns (Fig. 6.4b, d) were mainly attributed to the lower precipitation in 2016/17 as compared with 2015/16 (e.g., nearly half the amount of rainfall occurred at TZm). With lower precipitation, urea-N loss through NH_3 volatilization in the current fields might increase (Zheng et al. 2018a), which could have offset the increased N available for N_2O production at a higher rate. A similar 2-year study in Kenya (Hickman et al. 2015) also showed that a linear pattern might describe the response of N_2O emissions to N input in a drier year, provided that N rates and yields be the same across years. These results confirm that N_2O emission may increase linearly with the N rate (Hoben et al. 2011; Kim et al. 2013b), even when the N addition exceeded the demand for the optimal agronomic yield (e.g., Gagnon et al. 2011; Liu et al. 2012).

6.4.3 Effect of straw incorporation on N_2O emissions

To date, this is the first in situ study examining the effect of combined application of fertilizer-N and straw on N_2O emissions in SSA croplands. The other two related studies in this region (Baggs et al. 2006; Millar et al. 2004) tested the effects of only a single input of plant residue on N_2O emissions, leaving the potential interaction between inorganic fertilizer and plant residue unevaluated.

Combined input of fertilizer-N and straw further increased the N_2O emissions with a synergistic effect as compared with fertilizer-N input alone (Fig. 6.5). The synergistic effect was evidenced by the similar or even higher average daily flux from the 50N+S treatment as compared with the 150N treatment (Fig. 6.5). Straw is therefore playing roles beyond N supply for N_2O production (Chen et al. 2013). The result thus questions the simple additive estimation of N_2O emission by the Tier 1 method of the IPCC (2006) when these two resources are used. This result also suggests that the potential benefit of using straw to sequester C and improve soil quality (Kumar and Goh 1999; Sugihara et al. 2012b) may be compromised by enhanced N_2O emissions.

Mechanisms underlying the synergistic effect of combined inputs on N_2O emissions may vary with soil type. Such a synergistic effect has generally been attributed to the supply of C with high N availability as well as the anaerobic microsites formed in bulk soils that favor denitrification; the anaerobic microsites are due to enhanced O_2 consumption that exceeds diffusion, as a result of residue decomposition (Chen et al. 2013; Loecke and Robertson 2009; Millar et al. 2004). This likely occurred at TZm with a high WFPS (>47%), but not at TZi, where the clay content (<7%) and WFPS (<40%) may have been too low to form anaerobic microsites in such a way. Instead, at TZi, by absorbing the water from surrounding soil, the wet straw fragments themselves may have served as local anaerobic hotspots for denitrification (Kravchenko et al. 2017). The increased N_2O emission at TZi was further supported by a laboratory ^{15}N-tracer study (Li et al. 2016) with a similar sandy soil (79.4% sand), in which denitrification became the dominant source (>50%) of N_2O emission after soil treatment with crop residue, even at low WFPS (40%).

The stimulating effects of the combined application of low-quality straw (particularly those with C:N ratio > 190 in 2015/16; Table S6.2) and fertilizer-N on N_2O emissions in the current study contradicted to the findings of some previous researches in other continents (e.g., Chen et al., 2013; Congreves et al. 2017; Wu et al. 2012). The general bases for the negative effect of residue incorporation on N_2O emission are (i) N immobilization that lowers the N availability for N_2O production (Chen et al. 2013; Wu et al. 2012); and (ii) a more complete stepwise denitrification to N_2, which consumes produced N_2O (Congreves et al. 2017; Wang et al. 2011; Zhou et al. 2017). However, the large pieces of straw (~0.15 m) used in the current study were inefficient to immobilize soil N (1.2–2.7 kg N Mg^{-1} added C; Chapter 5) due to the limited surface area exposed to microbes for decomposition (Kumar and Goh 1999). In addition, the recorded WFPS at each site (up to 63.3%) was far from forming an environment conducive to complete denitrification (Bateman and Baggs 2005). Instead, higher dissolved organic C flux was observed from straw incorporated plots (Zheng et al., *unpublished*), which could provide a C source for denitrification. Other studies also indicate that straw with C:N ratio > 100 can have a positive effect on N_2O emissions (Abalos et al. 2012; Li et al. 2013).

6.4.4 Annual N_2O emission as related to maize yield

With the single N input, the non-significant difference between exponential and linear fitting for delta yield vs. delta N_2O emission (Fig. 6.8a, b) indicated the absence of an evident tipping point, which is consistent with the similar yield-scaled emissions among N rates of 0–150 kg N ha^{-1} for the 2-yr study period (Fig. 6.8c, d). The yield-scaled emissions (<0.18 kg N_2O-N Mg^{-1} grain) for maize plots receiving only fertilizer-N were within the lower ranges of some reported values (Kim et al. 2017; Zhao et al. 2017). All of the above may suggest that N application rates up to 150 kg N ha^{-1} are acceptable for increasing yield relative to N_2O emissions in the studied regions. This is in line with a meta-analysis of Van Groenigen et al. (2010) that no significant difference in yield-scaled emissions was found for N inputs below 200 kg N ha^{-1}. Considering the yield potential, efforts to further increase the yield (e.g., management of water and other nutrients, etc.) within this range of N rates will make this region a climate-friendly area for crop production.

Straw incorporation markedly increased the yield-scaled N_2O emissions (Fig. 6.8). The potential benefit of combining low-quality straw and fertilizer-N to mitigate N leaching loss and to improve N synchrony proposed for SSA croplands (Gentile et al. 2009; Sugihara et al. 2012a) should therefore be reconsidered in the context of N_2O emissions.

6.5 Conclusions

The current study provides some of the first reliable in situ measurements in SSA croplands (TZi, sandy Alfisols; TZm, Andosols) to quantify N_2O emissions in response to increasing N rates and in combination with maize straw incorporation. I found that in SSA croplands both exponential and linear patterns are present for describing the response of N_2O emissions to increasing N rates, regardless of soil type. Mechanisms underlying the stimulating effects of treatments (N applied alone or N plus straw) on N_2O fluxes seemed to vary with soil type, and were associated with soil mositure. When N was applied alone (50–150 kg N ha^{-1}), the direct N_2O EFs were well below the 1% of the IPCC Tier 1 method, ranging from 0.13 to 0.26% at TZi and from 0.24 to 0.42% at TZm across 2 years. However, combining N with straw markedly increased the EFs (up to 0.46% at TZi and 1.29% at TZm) because of a synergistic effect on N_2O emissions. The combined application also increased the yield-scaled N_2O emissions. These results contribute to the rigorous documentation of soil- and country-specific EFs of N_2O in understudied SSA croplands, and suggest that IPCC should consider the synergistic effect to refine the N_2O EFs when two resources (fertilizer-N and straw) are combined. Further, current results challenge the promotion of combining straw with fertilizer-N for the potential benefit of a better N synchrony in this region. More in situ N_2O emission data with good quality are needed to cover a broader range of agro-ecological zones, soil types, and land management practices in SSA if we are to better define the regional N_2O flux and mitigation opportunities.

Supplementary materials

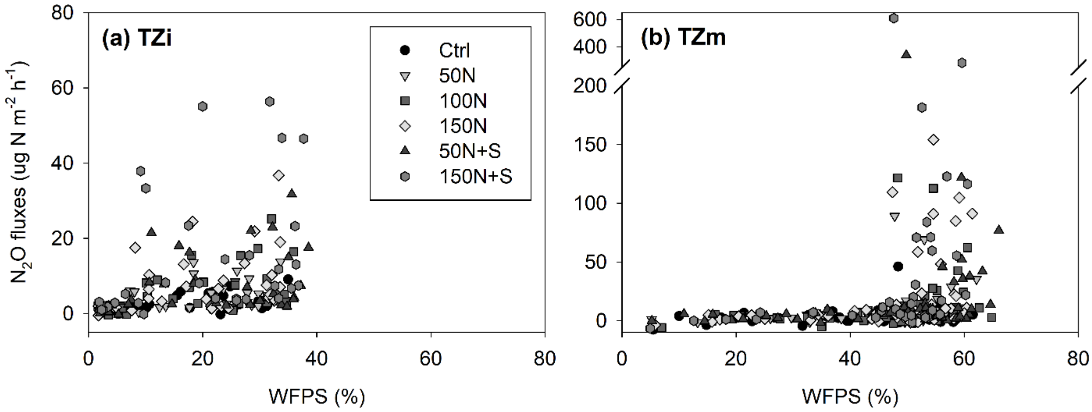

Fig. S6.1 Relationship between N_2O flux and water-filled pore space (WFPS) across the experimental period (from December 2015 to November 2017).

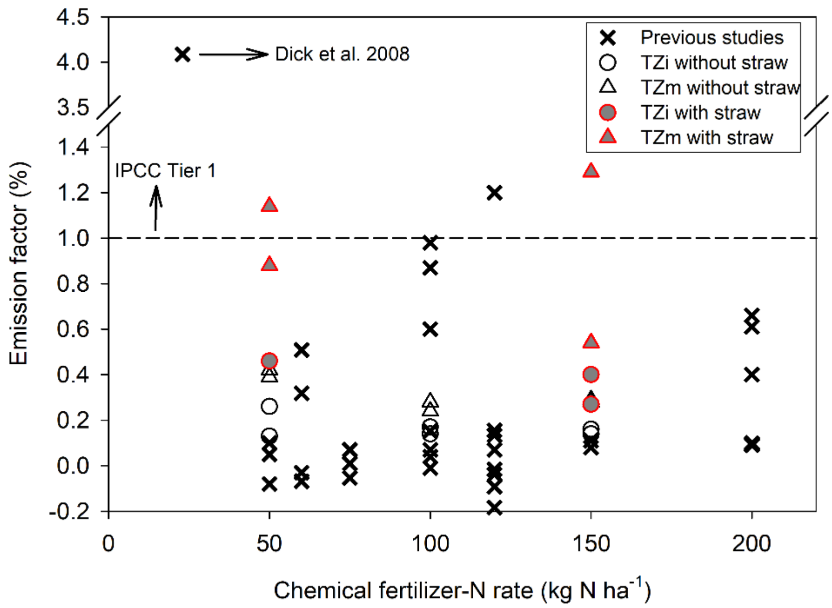

Fig. S6.2 Emission factors from this study and published field measurements of direct N_2O emission from SSA croplands. Emission factors were calculated based on the total N_2O emissions from fertilized and unfertilized plots during the measurement periods. All of the previous studies, except Dick et al. (2008), did not include measurement throughout a year. Therefore, emission factors were mostly calculated based on seasons that covered by the measurements. The study by Hickman et al. (2015) extrapolated data for non-growing seasons (not measured) and calculated the emission factor based on annual emissions. Only studies for croplands and applied with chemical fertilizer were included; studies using crop residues as N source (Baggs et al. 2006; Millar et al. 2004) and urban vegetable gardens (Lompo et al. 2012; Predotova et al. 2010) are excluded; studies without background correction (unfertilized treatment) are excluded (e.g., Chapuis-Lardy et al. 2009).

List of the studies: Baggs et al. (2006); Dick et al. (2008); Hickman et al. (2014); Hickman et al. (2015); Mapanda et al. (2011); Mapanda et al. (2012b); Masaka et al. (2014).

Table S6.1 Selected soil physico-chemical properties of profiles for TZi and TZm.

Site	Depth	pH	TC†	TN†	CEC‡	BD§	PDǂ	Soil texture⁋ (%)		
	cm	(H_2O)	g kg^{-1}		cmol$_c$ kg^{-1}	g cm^{-3}		Clay	Silt	Sand
TZi	0–15	6.45	3.5	0.3	1.1	1.55	2.56	4.7	6.9	88.4
	15–30	5.96	1.9	0.2	0.9	1.54	ND[δ]	6.4	7.9	85.7
TZm	0-25	6.85	17.5	1.3	17.5	0.90§	2.42ǂ	28.4	42.0	29.5
	25-50	7.09	9.6	0.8	22.7	0.94§	ND	34.6	32.9	32.5

†Total carbon (TC) and N (TN) determined by dry combustion of finely ground soils using Vario Max CHN elemental analyzer.

‡Cation exchange capacity (CEC) determined by the ammonium acetate saturation method.

§Bulk density (BD) determined by the core method. For TZm, BD determined for 0–15 cm and 15–30 cm layers.

ǂSoil particle density (PD) = soil mass/volume of soil particles. Volume of soil particles determined by filling deionized water to a 100 ml glass flask containing 25 g oven-dried soil after removing the air between particles by boiling the soil/water mixture (volume of soil particle [ml] = 100 – volume of filled water [ml]; given that the density of water is 1 g cm^{-3}). For TZm, PD determined for 0–15 cm.

δND = not determined.

⁋Soil texture determined by wet sieving (sand fraction) and sedimentation (silt and clay fractions).

Table S6.2 Application date, DAS (days after sowing), averaged content (n = 2) of total carbon (TC), total N (TN), and C:N ratio of applied crop residues and the equivalent amount of added C and N to the corresponding PVC chambers.

	Season	Date	DAS	TC† %	TN† %	C:N ratio	Added C Mg C ha^{-1}	Added N kg N ha^{-1}
TZi	2015/16	Nov-24-2015	–38§	45	0.36	191	2.3	18.9
	2016/17	Nov-24-2016	–15	43	0.73	60	2.2	38.2
TZm	2015/16	Nov-28-2015	–12	46	0.22	206	2.7	13.1
	2016/17	Dec-3-2016	–11	43	0.46	93	2.2	23.3

§Due to heavy rainfall, seeding on Dec-14-2015 failed to germinate at TZi and re-sowing was conducted on Jan-1-2016, leading to much earlier date of straw incorporation.

†TC and TN determined by dry combustion of finely ground soils using Vario Max CHN elemental analyzer.

Table S6.3 Minimum (Min), maximum (Max), arithmetic mean (Mean), and coefficient of variation (CV) of chamber measurements of N_2O fluxes (μg N_2O-N m^{-2} hr^{-1}) for each cropping year at TZi and TZm, respectively.

Treatment	TZi				TZm			
	Min	Max	Mean	CV	Min	Max	Mean	CV
	—μg N_2O-N m^{-2} h^{-1}—			(%)	—μg N_2O-N m^{-2} h^{-1}—			(%)
				2015/16				
0N	1.0	9.1	2.5	67.6	-7.7	11.7	3.7	123.0
50N	0.2	13.8	4.5	80.0	-1.4	69.2	8.8	161.7
100N	-0.3	25.2	6.4	96.4	-5.7	112.7	12.7	186.8
150N	-0.5	36.7	8.8	101.8	-3.6	154.0	23.3	169.2
50N+S	-0.2	31.8	9.0	102.0	-0.5	121.8	17.6	155.9
150N+S	-0.1	56.4	16.9	110.4	-6.5	181.5	30.7	151.2
				2016/17				
0N	-0.5	12.7	3.0	108.4	-4.5	46.1	4.3	203.0
50N	-1.7	16.4	6.2	72.3	-1.3	89.1	8.7	195.6
100N	-0.8	24.5	7.5	92.3	-4.9	121.4	10.9	216.3
150N	0.2	30.4	8.4	99.9	-0.7	109.5	14.2	180.5
50N+S	-0.9	27.9	8.1	85.5	-1.6	339.7	20.5	314.7
150N+S	-1.3	58.9	15.6	108.8	2.7	609.5	47.7	266.0

Table S6.4 Model parameters, corrected Akaike's information criterion (AIC_c), and R^2 for models describing the delta N_2O emission (ΔN_2O) in response to delta yield (Δyield) in plots without straw incorporation.

Model	TZi			TZm		
	parameters	AIC_c	R^2	parameters	AIC_c	R^2
Exponential	a = 0.0608	-9.3	0.82	a = 0.125	-1.3	0.76
$\Delta N_2O = a \times \exp(b \times \Delta yield)$	b = 0.601			b = 0.446		
Linear	a = 0.0350	-8.8	0.80	a = 0.0968	0.3	0.69
$\Delta N_2O = a + (b \times \Delta yield)$	b = 0.0830			b = 0.111		
Quadratic	a = 0.0605	20.9	0.81	a = 0.280	26.8	0.83
$\Delta N_2O = a + (b \times \Delta yield) + (c \times \Delta yield^2)$	b = 0.0313			b = -0.169		
	c = 0.0198			c = 0.0843		

Table S6.5. List of in situ empirical studies of N_2O fluxes from croplands (annual and seasonal fluxes) in sub-Saharan Africa. Short duration studies (i.e., <2 months) were not included.

Ref.	Country	Crop type	Soil type	Rainfall (mm yr^{-1})	N type[§]	N rate (kg N ha^{-1})	Measurement period	Sampling frequency	Flux rate
Annual flux (kg N_2O-N ha^{-1} yr^{-1})									
1[b]	Burkina Faso	Sorghum; Cotton; Peanut	Loamy sand, Loam	926	No input	0	Jun–Sept 2005; Apr–Sept 2006	1–3 times per week	0.19–0.20
2[a]	Kenya	Coffee; Maize & beans; Niaper	Clay	1200–2000	NPK; Manure; DAP; CAN	0–542	Feb 2015–Feb 2016	Twice weekly to weekly	0.18–1.89
3[a]	Kenya	Tea	Clay	1988	NPK	0–250	Aug 2015–Jul 2016	Every two days to weekly	0.67–2.34
4[b]	Kenya	Annual crops; Grazing land; Woodlots; Fodder grass	Various	1127–1417	DAP; Urea	<25	Aug 2013–Aug 2014	Weekly	−0.13–1.83
5[b]	Kenya	Maize	Sandy clay	1750	DAP; Urea	0–200	Mar–Jul 2011; Apr 2012–Jan 2013	Daily to weekly or monthly	0.13–0.33
6[c]	Mali	Pearl millet with/without legume	*Sandy*	1100	Urea; Manure	0–113	Jan 2004–Jan 2005	Monthly	0.60–1.54
7[a]	Tanzania; Kenya	Forages; Tea; Maize Vegetable; Cassava	Sandy clay loam; Sandy loam; Loamy sand	2708; 1115	DAP; Manure; NPK	0–114	Jan–Dec 2013	Twice per week to weekly	0.4–0.9
8[c]	Tanzania	Maize	Sandy clay loam	N.A.	Urea;	100	Oct 2012–Jun 2014	N.A.	0.4–0.7
9[a]	Tanzania	Coffee; Homegarden	Loam; Silt clay	1485; 2616	N.A.	N.A.	Feb 2011–Jul 2013	Weekly to monthly	0.35–0.36 (mean annual)
10[c]	Zimbabwe	Tomato; Rape	Loamy sand	808	Manure; AN	0–1208	Sept 2007–Oct 2008	Biweekly	1.52–5.03
11[c]	Zimbabwe	Tomato;Rape	Loamy sand	808	Manure	0–408	Sept 2007–Oct 2008	Biweekly	0.91–2.30

Table S6.5 to be continued

Table S6.5 continued

Seasonal flux (kg N_2O-N ha^{-1} season^{-1})									
12[b]	Kenya	Maize	Silty clay loam	1800	Urea; Residues	0–266	Mar–Jun 2002 (99 days)	Weekly to monthly	0.13–0.57
13[b]	Kenya	Maize	Clay	1750	DAP; Urea	0–200	Mar–Jun 2010	Daily to weekly	0.62–0.81
14[b]	Kenya	Maize	Silty clay loam	1800	Residues	115–360	Sept–Nov 1999; Apr-Jun 2000	Daily to Monthly	0.20–4.13
15[b]	Madagascar	Maize with soybean	*Clayey*	1500	NPK; Urea; Manure; Rice straw	55–57	Nov 2006–Apr 2007	Weekly	0.259–0.263
16[c]	Zimbabwe	Maize	Sandy loam; Clay	596–1154	AN; Manure	0–120	Nov 2007–Apr 2008; Nov 2008–Apr 2009	~Monthly	0.06–0.52
17[c]	Zimbabwe	Maize; Woodland	Clay; Loamy sand	564–997	AN	0–120	Nov 2007–Apr 2008; Nov 2008–Apr 2009	~Monthly	0.11–2.50
18[c]	Zimbabwe	Maize	Sandy loam	1218	Fallow manage.	0	Dec 2000–Jan 2001 (56 days)	Weekly	0.06–0.29

[a] = good quality data (measurements covered at least a year with proper temporal resolution); [b] = medium quality data (measurements included a good temporal resolution but did not cover an entire year, or measurements covered at least a year with acceptable temporal resolution); [c] = poor quality data (data with very low temporal resolution or measurements only covered a short period, or both)

[§]NPK = NPK fertilizer; DAP = Diammonium phosphate; CAN = Calcium ammonium nitrate; AN = Ammonium nitrate; N.A. = not available

Ref.: [1]Brummer et al. (2008); [2]Ortiz-Gonzalo et al. (2018); [3]Wanyama et al. (2018); [4]Pelster et al. (2017); [5]Hickman et al. (2015); [6]Dick et al. (2008); [7]Rosenstock et al. (2016); [8]Kimaro et al. (2016); [9]Gutlein et al. (2018); [10]Masaka et al. (2014); [11]Masaka et al. (2016); [12]Baggs et al. (2006); [13]Hickman et al. (2014); [14]Millar et al. (2004); [15]Chapuis-Lardy et al. (2009); [16]Mapanda et al. (2011); [17]Mapanda et al. (2012b); [18]Chikowo et al. (2004)

CHAPTER 7

General Discussion

7.1 Integrated assessment on the response of maize yield and N losses to external N supply

The integration of data shows a holistic view to examine the relationships between crop yield and N losses under an N input gradient (Fig. 7.1). Also, the data from multiple years provides a better insight into the general pattern of these relationships, which could be masked or biased if the research were conducted in a short-term interval (e.g., one year, as subject to large inter-annual variations).

Two categories of fitting are presented in Fig. 7.1. The solid lines were fitted for the plots receiving only fertilizer-N input (four N rates); the response of mean annual maize yield, NO_3^- leaching loss, and N_2O emission to fertilizer-N rate were generally well described by quadratic, exponential, and linear patterns, respectively (Fig. 7.1; R^2 = 0.999–0.998 with P = 0.006–0.046 at TZi and R^2 = 0.963–0.990 with P = 0.017–0.098 at TZm; Table 7.1a). The dash lines were fitted for the plots receiving fertilizer-N or fertilizer-N plus straw input (six N rates); well fittings were also obtained (Fig. 7.1; R^2 = 0.828–0.973 with P = 0.000–0.012 at TZi and R^2 = 0.684–0.972 with P = 0.000–0.042 at TZm; Table 7.1b). At TZi, maize yield and NO_3^- leaching loss showed large inter-annual variations (large standard errors, Fig. 7.1a), despite the general well fittings; the inter-annual variations of corresponding variables at TZm were much smaller (Fig. 7.1b).

Simply based on the relationships between yield and N losses under only fertilizer-N input (solid lines in Fig. 7.1), the optimum N range balancing the crop yield and environmental consequences likely occurred at around 90 kg N ha^{-1} of fertilizer-N input at TZi, whereas it seemed to occur at lower rates of fertilizer-N at TZm (e.g., around 70 kg N ha^{-1}). Such determined optimum N ranges at two sites are further supported by the analysis of N use efficiency (see detailed discussion below in Section 7.2). However, it is noteworthy that the optimum N range at TZi (~90 kg N ha^{-1}) provide the averaged maize yield of no more than 2 Mg ha^{-1}; this may indicate that the simple N application with such optimum rate (~90 kg N ha^{-1}) could not be a practical recommendation for TZi soils.

When straw was also considered as the N source (dash lines in Fig. 7.1), maize yields seemed to be slightly reduced, NO_3^- loss was negligibly affected, and N_2O emission was markedly increased (Fig. 7.1). Particularly at TZm, the combined input of straw and fertilizer-N at a lower rate (50 kg N ha^{-1}) lowered the maize yield and increased the N losses through NO_3^- leaching and N_2O emission compared to fertilizer-N only treatment; as a result, a slower increase of the yield for the quadratic fitting was observed (Fig. 7.1b) as well as a lower proportion of applied-N uptake by crop (Fig. 7.2).

The pathway of NH_3-N loss was not included in the analysis of Fig. 7.1, because the results in Chapter 4 of this dissertation provided the upper bound estimate under the field condition. The semi-open static chambers prevent the influence of rainfall and therefore may not represent the "true" field NH_3-N loss, unless no rainfall events occurred following the urea application (Chapter 4). Therefore, the actual field N loss through NH_3 volatilization could be highly variable (Fig. 7.2) and strongly depended on the timing of the rainfall events relative to N applications (Kissel et al. 2004). Unfortunately, capturing such actual NH_3-N loss in the field requires micrometeorological approach and technique, such as eddy correlation (Sommer et al. 2004), which does not allow the simultaneous assessment of multiple treatments and has higher costs compared to the semi-open static chamber method.

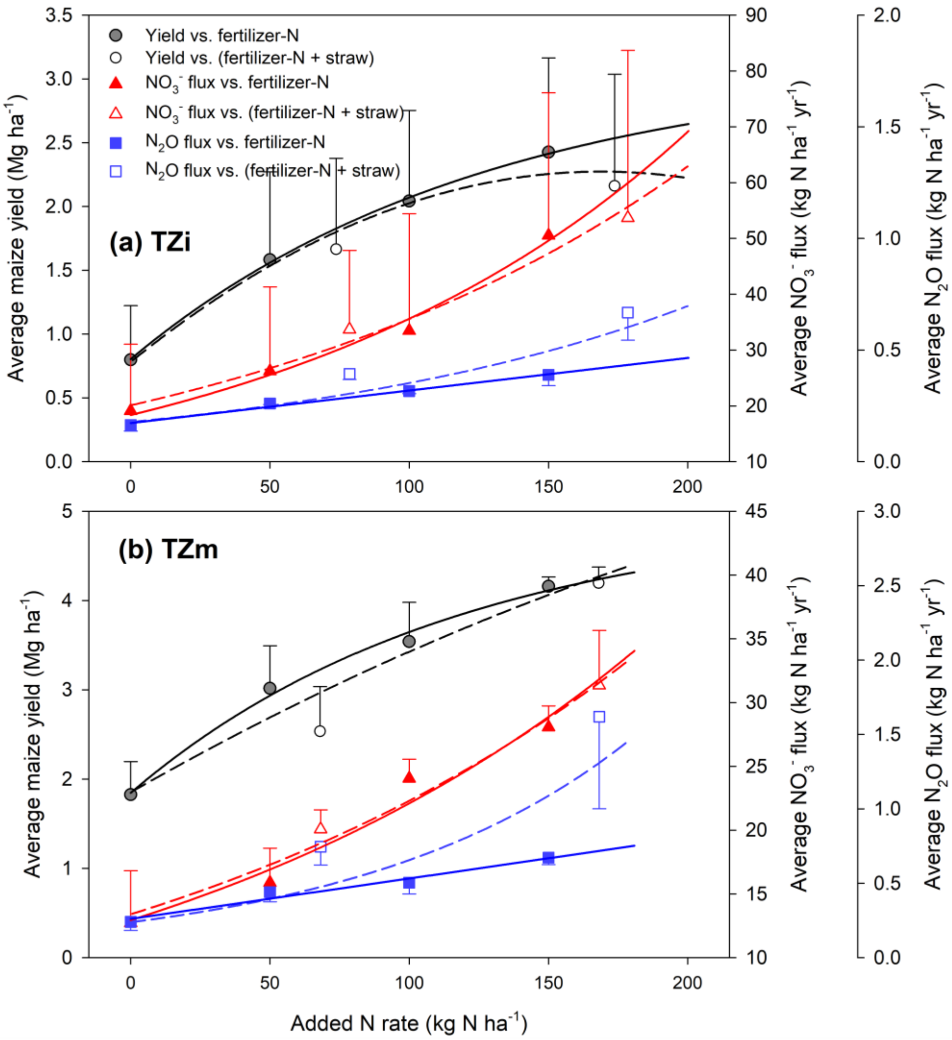

Fig. 7.1 Average maize yield (Mg ha^{-1}), NO_3^- flux (kg N ha^{-1} yr^{-1}), and N_2O flux (kg N ha^{-1} yr^{-1}) in response to external N input (i.e., fertilizer-N or fertilizer-N plus straw) at TZi (a) and TZm (b). Data were synthesized from the four-year study where available (e.g., the trial of combined input of fertilizer-N plus N was not conducted in the first year of this study and therefore had only three-year data for the yield). Solid lines represent the fittings for the plots receiving only fertilizer-N input (four N rates), whereas dash lines represent the fittings for all external N input (six N rates). Error bars represent standard errors of means.

Table 7.1a Fitted model parameters, R^2, and P value for models describing the response of mean annual yield (Mg ha^{-1}), NO_3^- flux (kg N ha^{-1} yr^{-1}), and N_2O flux (kg N ha^{-1} yr^{-1}) in response to only fertilizer-N input at TZi and TZm in Figure 7.1 (solid line fitting).

Variable	Model	TZi			TZm		
		Fitted parameter	R^2	P	Fitted parameter	R^2	P
Yield	Quadratic $a + b \times N + c \times N^2$	a = 0.811 b = 0.0167 c = –4.00 × 10^{-5}	0.998	0.046	a = 1.86 b = 0.0236 c = –5.70 × 10^{-5}	0.990	0.098
NO_3^-	Exponential $a \times \exp(b \times N)$	a = 18.4 b = 0.0066	0.988	0.006	a = 12.9 b = 0.0054	0.963	0.019
N_2O	Linear $a + b \times N$	a = 0.173 b = 0.0015	0.989	0.006	a = 0.260 b = 0.0027	0.966	0.017

Table 7.2b Fitted model parameters, R^2, and P value for models describing the response of mean annual yield (Mg ha^{-1}), NO_3^- flux (kg N ha^{-1} yr^{-1}), and N_2O flux (kg N ha^{-1} yr^{-1}) in response to external N input (fertilizer-N and fertilizer-N plus straw) at TZi and TZm in Figure 7.1 (dash line fitting).

Variable	Model	TZi			TZm		
		Fitted parameter	R^2	P	Fitted parameter	R^2	P
Yield	Quadratic $a + b \times N + c \times N^2$	a = 0.783 b = 0.0177 c = –5.23 × 10^{-5}	0.962	0.007	a = 1.85 b = 0.0178 c = –2.01 × 10^{-5}	0.927	0.020
NO_3^-	Exponential $a \times \exp(b \times N)$	a = 20.1 b = 0.0057	0.973	0.000	a = 13.4 b = 0.0051	0.972	0.000
N_2O	Exponential $a \times \exp(b \times N)$	a = 0.179 b = 0.0068	0.828	0.012	a = 0.238 b = 0.0101	0.684	0.042

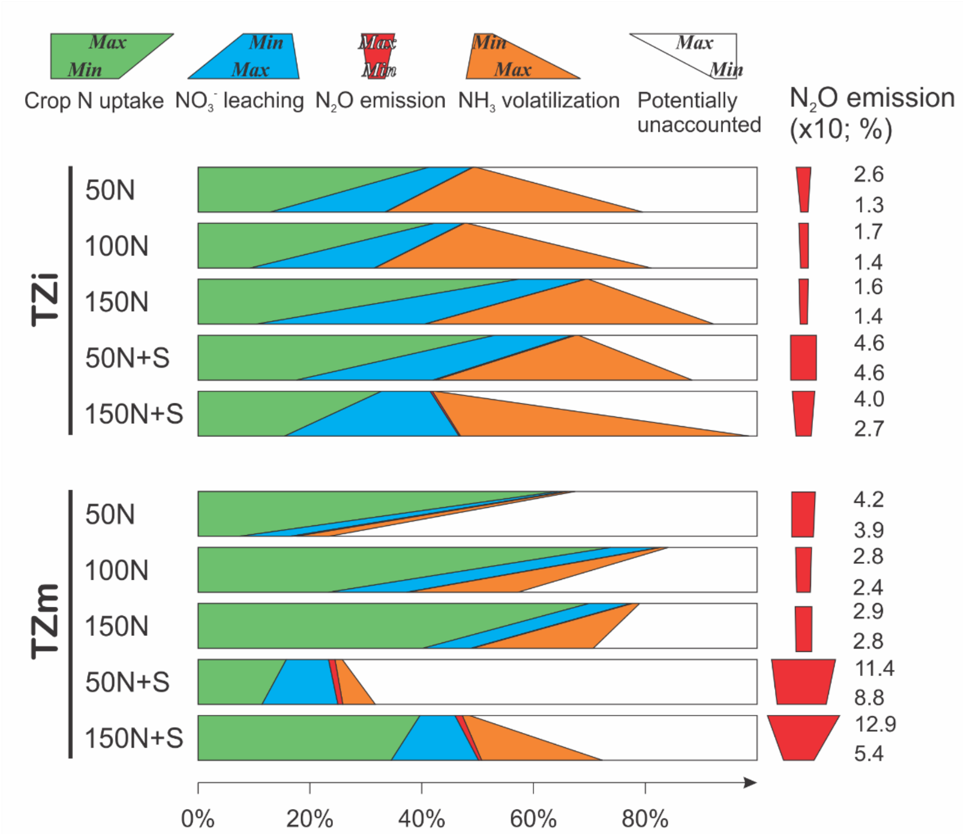

Fig. 7.2 Apportionment of the added-N pathways, including crop N uptake, NO_3^- leaching, N_2O emission, NH_3 volatilization, and potentially unaccounted-for N (e.g., denitrification to N_2, priming effects of added fertilizer-N and straw, etc.). The apportionment of each added-N pathways was calculated based on the comparison between the treatment and control plots; for example, crop N uptake (%) = (N_{uptake} at treatment plot − N_{uptake} at control plot) (kg N ha^{-1}) / amount of added N (kg N ha^{-1}) × 100%. Data were synthesized from the four-year study where available (e.g., the trial of combined input of fertilizer-N plus N was not conducted in the first year of this study and therefore had only three-year data for the crop N uptake). The N flux of each pathway was in an annual basis; the maximum and minimum value were obtained from the multiple year experiment and were used to represent the inter-annual variation. For the pathway of N loss through NH_3 volatilization, the minimum value was assumed with the condition of sufficient rainfall immediately following the N (urea) application (effective reduction of NH_3 volatilization; see Fig. 4.4), whereas the maximum value was assumed with the condition of no rainfall following the N application until the NH_3 volatilization dropped back to the background level (the potential of applied-N loss as NH_3; see Fig. 4.3c, d). It should be noted that the maximum crop N uptake does not necessarily correspond to the minimum NO_3^- leaching loss.

7.2 Use efficiency of added N

Recovery N efficiency (RNE)—the fraction of added N taken up by crops, is one of the most commonly used indices to evaluate N use efficiency, which holds the key to approaching the higher grain yield with lower environmental costs (Zhang et al. 2015). The RNE showed high variability across years (Fig. 7.2), ranging from 9.3% to 57.4% at TZi, and from 7.4% to 73.8% at TZm, across the treatments. No specific pattern was observed for the RNE across treatments at each site. These variations were likely induced by the inter-annual variations of climate and soil conditions, including drought, residual N from preceding seasons (Chapter 3), and a wetter year (Chapter 5) that directly or indirectly affected the crop N uptake. Such high annual variability may necessitate the long-term research to better define the effect of treatments on the RNE.

In addition to RNE, agronomic N efficiency (ANE) and N partial factor productivity (PFP_N) are the other two most commonly used indices (Chen et al. 2014; Cui et al. 2018), which are of more economic significance to farmers (Wang et al. 2017). ANE is the yield increase per unit of N applied (kg grain kg^{-1} N applied), and PFP_N is calculated by dividing the yield by the amount of N applied (kg grain kg^{-1} N applied). The difference between the two indices is that the latter one integrates the use efficiency of both indigenous and applied N resource.

Both ANE and PFP_N decreased with increasing N rate (Fig. 7.3), as expected (Cassman et al. 2007); the 100N treatment (100 kg N ha^{-1}) provided the second highest ANE and PFP_N values at TZi, and there was a substantial drop of ANE and PFP_N from the 50N to 100N treatment at TZm (Fig. 7.3). These agree with the result from Fig. 7.1 that fertilizer-N rates of around 90 and 70 kg N ha^{-1}, for TZi and TZm, respectively, could be defined as the optimum N ranges. Straw incorporation tended to decrease both the ANE and PFP_N values, particularly at TZi; values of both indices for the 50N+S treatment was dropped to the similar level to that of the 100N treatment (Fig. 7.3). This may be explained by the non-significant effect of straw application on the yield, yet straw itself also provided N input to the soils (e.g., 14–38 and 13–23 kg N ha^{-1} at TZi and TZm, respectively). These straw-N might largely be unavailable to maize if the mineralization (and the re-mineralization of microbial assimilated N) did not occur at the vicinity of the maize roots (Chapter 5). Nevertheless, the straw incorporation, at least when combined with fertilizer-N at a lower rate (i.e., 50 kg N ha^{-1}), did not seem to be a preferable practice from a short-term perspective (Figs. 7.1, 7.3). Yet the trade-offs between short-term profit (maize yield) and long-term benefit (soil fertility, such as soil organic matter stabilization) (Gentile et al. 2011; Sugihara et al. 2012b) should be considered with further evaluations. Both the ANE and PFP_N values were higher at TZm (15.5–23.8 and 25.0–60.3 kg grain kg^{-1} N for ANE and PFP_N, respectively) than those at TZi (6.7–15.7 and 12.4–31.6 kg grain kg^{-1} N for ANE and PFP_N, respectively). This suggests that soil type with higher fertility like TZm should be given with a priority in the agricultural intensification.

The ANE at both TZi and TZm (up to 15.7 and 23.8 kg grain kg^{-1} N, respectively) were much lower than those in the maize fields of China under farmers' practice (FP; 40 kg grain kg^{-1} N) and the Integrated Soil-Crop System Management (ISSM) practice (53.4 kg grain kg^{-1} N). The 50N treatment at TZm seemed to have a high PFP_N value of a similar magnitude to that of ISSM. This high PFP_N was likely contributed in part by substantial residual N from the preceding season in an abnormal year at

TZm (Chapter 3). Also, it should be noted that the N application averages to 305 kg N ha^{-1} in Chinese agricultural systems (Zhang et al. 2015). By contrast, the PFP_N in the150N treatment at TZm was only approximately half of that of ISSM.

Increasing N use efficiency in developing region like SSA, including Tanzania, is particularly challenging. It took 20 years for the USA to increase ANE from 42 to 57 kg grain kg^{-1} N applied (Cassman et al. 2002). Also, China spent more than 10 years to develop the ISSM (Cui et al. 2018), which achieved to increase PFP_N from 43 to 56 kg grain kg^{-1} N. The understudied tropical regions of SSA would likely require much more time to understand the biophysical and socioeconomic characteristics of the agroecosystems (Cassman et al. 2003) before appropriate N management and other associated management factors (e.g., water, crop) can be developed in a large scale in this region.

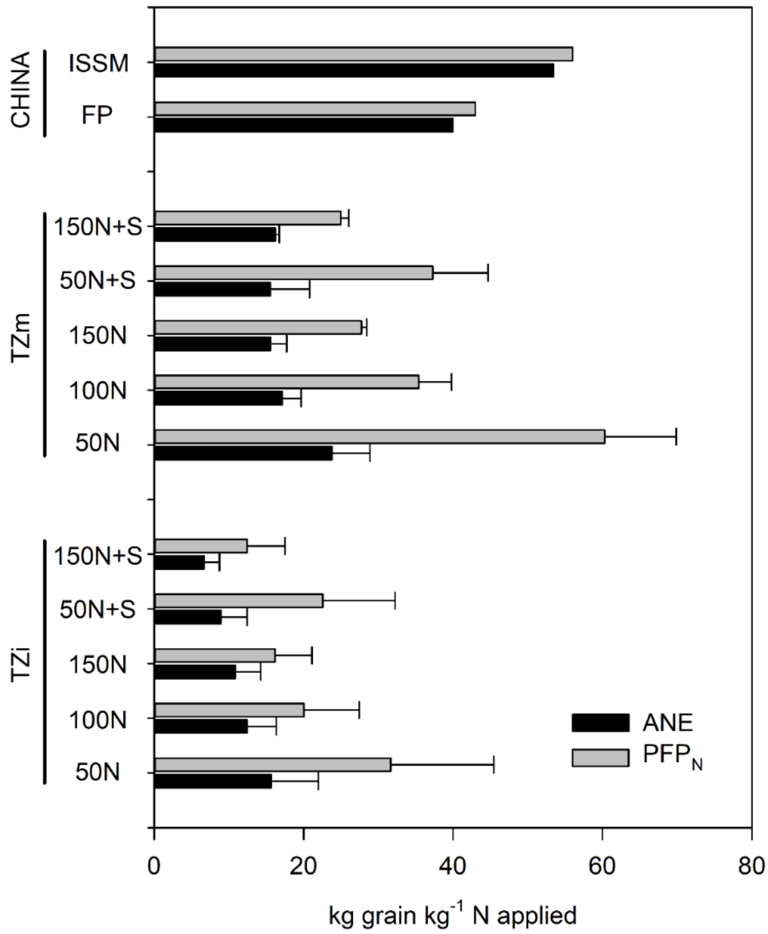

Fig. 7.3 Agronomic N efficiency (ANE) and N partial factor productivity (PFP_N) for each treatment at TZi and TZm as compared to the farmers' practice (FP) and the Integrated Soil-Crop System Management (ISSM) practice in maize fields of China; note that the N application averages to 305 kg N ha^{-1} in Chinese agricultural systems (Chen et al. 2014; Cui et al. 2018). Data were synthesized from the four-year study where available (e.g., the trial of combined input of fertilizer-N plus N was not conducted in the first year of this study and therefore had only three-year data for the crop N uptake). Error bars represent standard errors of means.

7.3 Towards a higher yield with lower environmental costs in SSA croplands

To achieve a higher yield with lower environmental costs in SSA croplands and finally move toward sustainable intensification, a growth understanding of the biophysical characteristics of the agroecosystems as well as a series of additive interventions including N management are needed (Fig. 7.4). The scenario discussed in Fig. 7.4 is particularly for the maize-based agriculture and mainly from the perspective of the management interventions. The detailed interpretation of Fig. 7.4 is provided below.

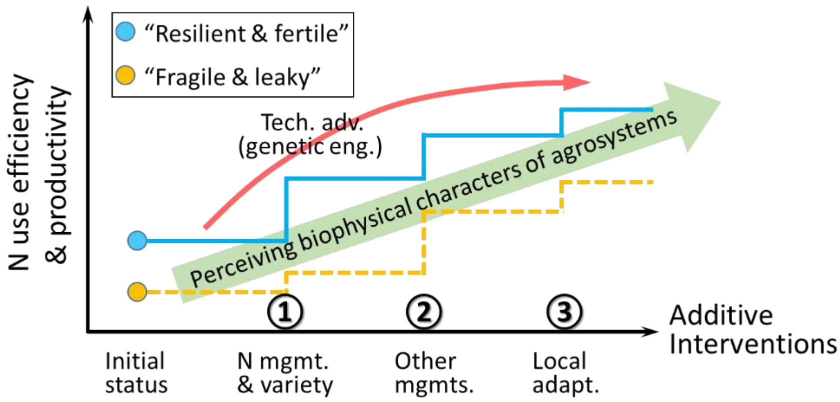

Fig. 7.4 A conceptual pathway to reaching higher N use efficiency and productivity with additive stages of interventions in SSA croplands (adapted from Vanlauwe et al.2014a). Two general classes of the maize systems were considered: "resilient & fertile" and "fragile & leaky." The additive stages of interventions include: ① N management and use of suitable seed variety; ② other management (e.g., crop, water, etc.); and ③ local adaptation. The increase in knowledge and a better understanding of biophysical characteristics of the agroecosystems are critical in moving these stages forward. Technological advances like genetic engineering to improve plant N uptake may boost up the N use efficiency and productivity.

Two general initial status were distinguished for the maize systems (Fig. 7.4), which largely depended on the biophysical characteristics of the agroecosystems (e.g., soil properties, climate, etc.). Soils in SSA commonly exhibit high spatial heterogeneity (e.g., Funakawa et al. 2012; Tittonell et al. 2013), partly due to the inherent soil-landscape variability. As exemplified in this dissertation, soil at TZi was much more susceptible to NH_3 volatilization (Chapter 4), and showed high inter-annual variation in NO_3^- leaching loss in response to the varying soil and climatic conditions (Chapter 5) compared to that at TZm. These largely contributed the different responses of the yield to the same N management at two sites (Fig. 7.1). Accordingly, the maize system at TZi may be described as "fragile & leaky" relative to the more "resilient & fertile" one at TZm.

The first stage of the intervention (N management and the use of suitable seed variety; Fig. 7.4) exhibited much better yield response in the "resilient & fertile" (TZm) than the "fragile & leaky" (TZi) maize system (Fig. 7.1). As supported by the analysis in Section 7.2, targeting intensification to "resilient & fertile" areas will reduce N loss and achieve higher yields (also see Palm et al. 2017), particularly when the available nutrient resource is limited. The "fragile & leaky" systems like TZi would require much more efforts to improve and maintain the productivity; restoring the soil health could be the pre-requisite to obtaining a better yield response to the N management (Zingore et al. 2007), which is likely to be a long-term investment with a large amount of organic resource inputs (e.g., manure).

In the second stage of the intervention, other management factors (e.g., crop, water, etc.) should be involved (Fig. 7.4), which contribute to the secondary constraint on the cropland productivity. The maize yield levels with only N management (Fig. 7.1) did not seem to be satisfactory when compared to the world average level (5.6 Mg ha^{-1} for the year 2016; FAO 2018). Indeed, main results from this dissertation revealed the potential to further improve the yield level when coupled with other management factors. For example, plateaued yield at TZm in Chapter 3 (Fig. 3.5) indicated some secondary or micronutrients could be needed for a balanced supply. Also, water management like dripping irrigation could be multifunctional, such as depressing NH_3 volatilization (Chapter 4) and supplying water for mitigating unexpected drought periods (Chapter 3). Though the cost of initial investment for a complicated dripping irrigation system may be high, an affordable and easy-to-construct design could be adapted for smallholder farmers in SSA (Figs. S3.3, S3.4). Further, plant density may be increased to expand the root covering area and improve the capability of crops to capture more N in the soil. As showed in Chapter 5, combined fertilizer-N and straw input failed to improve the N synchrony; the higher NO_3^- loss in the latter period of the cropping season was mainly attributed to the inaccessibility of roots to the re-mineralized N.

In the third stage, local adaptation of the management interventions is proposed to further improve the farm productivity (Fig. 7.4). Despite that the experiments in this dissertation were conducted in the plot (5 m × 5 m) scale, soil fertility gradients at the scale of farm or larger field have been well recognized (e.g., Tittonell et al. 2007; 2013). Targeted management practices as well as the allocation of nutrient resources were reported to result in higher productivity and better fertilizer-N use efficiency compared with the blanket recommendations (Vanlauwe et al. 2015), particularly for farms and fields where soil fertility gradients are strong. In addition, resource diversity and the level of resource endowment are also involved in the perspectives of local adaption. Although maize straw as an organic residue is easily accessible, its direct return to the soil did not seem to have an evident benefit on the yield (Fig. 7.1). If the low-quality maize straw can be transformed to high-quality animal manure by involving livestock keeping in the nutrient cycling of the maize systems, the return of the latter (i.e., manure) to the soil may have a higher potential to benefiting the yield, even within a short-term perspective. The level of resource endowment may largely be decided based on the farmer's capacity as well as the physical conditions of farms (e.g., the distance for the transportation of resources), which could be highly variable across households and farms.

As discussed above, the increase in knowledge and a better understanding of the biophysical characteristics of the agroecosystems are critical in moving these stages forward; the stage of the intervention is developed based on the identification of constraints on the fertilizer-N use efficiency and cropland productivity. These management interventions are developed mainly from the perspective of soil nutrient management to better meet the crop demand, yet the technological advances such as genetic engineering in the crop breeding may boost up the process (Fig. 7.4). Manipulation of the key genes involved in the N transport, assimilation, and signaling was reported to be feasible to improving the fertilizer-N use efficiency (Xu et al. 2012; Wang et al. 2018).

Developing such an integrated soil-crop management system requires long-term research investment, but is essential to approach sustainable intensifications.

CHAPTER 8

Concluding Remarks

8.1 Summary and conclusions

With a multiple site-year experiment, this study examined the effects of N management practices on the fertilizer-N partitioning within the soil-crop system, and accordingly the crop yield response, as well as on the N losses through different pathways from maize-based systems of the Tanzania highlands. The study included two different sites (TZi, sandy Alfisols; TZm, clayey Andisols) to represent the diversity in soil type.

High temporal resolution of soil inorganic N fluctuation revealed the leaching risk of excessive soil mineralized N in the early growing season due to small crop N demand. Soil type was identified as a key factor controlling the efficiency of applied urea-N in increasing soil inorganic availability, which largely contributed to the different yield levels across sites. The best-fitted linear-plateau model indicated that the soil inorganic N availability (0–0.3 m) at the tasseling stage significantly accounted for the yield. Furthermore, yield at TZi was still limited by N availability at the tasseling stage due to fast depletion of applied-N, whereas it no longer limited the yield at TZm once above 67 kg N ha^{-1}. These results contribute to a better understanding of the temporal patterns of soil N pools across soil types and how they affect the yield response in SSA croplands.

The TZi soil was found to be much more susceptible to NH_3-N loss from surface-applied urea-N (36%–52%) compared to that at TZm (5%–25%). Sigmoid models could be useful in identifying the soil's inherent capacity to buffer NH_3 loss; simple surface urea application is not recommended at TZi, whereas TZm is inherently capable of buffering NH_3-N loss for a single application of up to 60 kg N ha^{-1}. Mitigation of NH_3 loss through irrigation and urea deep placement all performed well, mainly owing to their effective inhibition of soil pH rise following urea hydrolysis. These results suggest that in acidic soils common to SSA croplands, the proportional NH_3-N loss can be substantial even at a low urea-N rate; and that the design of mitigation treatments should consider the soil's inherent capacity to buffer NH_3 loss.

The soil rewetting process, particularly at the onset of the rainy season and following N applications, was an important driver of NO_3^- loss. Nitrate loss increased exponentially with N rates, and varied inter-annually. Relating cumulative NO_3^- loss to maize yield under increasing N rates revealed a tipping point—occurrence depending on season—above which yield increment was accompanied by substantial NO_3^- loss. Straw incorporation induced net N immobilization in the early growing season, and reduced NO_3^- losses by 3.3–6.3 kg N ha^{-1}, but no effect was observed on the cumulative NO_3^- losses or maize yields. The NO_3^- loss reductions (equivalent to 1.2–2.7 kg N Mg^{-1} added C) were far below the potential of net N immobilization by the decomposition of the straw (18.0–

38.1 kg N Mg^{-1} added C), which was likely due to the large pieces of straw (~0.15 m) used in the field, which could have induced N limitation and biomass-N recycling in the decomposition microsites. These results highlight that temporary immobilization of leachable N by using large pieces of straw (~0.15 m) in the field was inefficient in improving N synchrony and benefiting yield.

Both exponential and linear pattern are present in SSA croplands for describing the response of N_2O emissions to increasing N rates, regardless of soil type. Mechanisms underlying the stimulating effects of treatments (N applied alone or N plus straw) on N_2O fluxes seemed to vary with soil type, and were associated with soil moiture. When N was applied alone, the direct N_2O EFs were well below the 1% of the IPCC Tier 1 method, ranging from 0.13 to 0.26% at TZi and from 0.24 to 0.42% at TZm across 2 years. However, combining N with straw markedly increased the EFs (up to 0.46% at TZi and 1.29% at TZm) because of a synergistic effect on N_2O emission, which also contributed to the higher yield-scaled N_2O emissions. These results contribute to rigorous documentation of soil- and country-specific EFs of N_2O in understudied SSA croplands, and suggest that IPCC should consider the synergistic effect to refine the N_2O EFs when two resources (fertilizer-N and straw) are combined. In addition, these results challenge the promotion of combining straw with fertilizer-N for the potential benefit of a bettern N synchrony in this region.

Increasing crop production remains a first-order priority in SSA, and an improved understanding of the potential environmental impacts of increased fertilizer-N use accompanying the agricultural intensification will be of great help to inform efforts toward the sustainable development in this region. This dissertation provides some of the first in situ evaluations, including the NH_3, NO_3^-, and N_2O losses in response to N practices, and the applicability of straw to mitigate NO_3^- loss in two maize systems of the Tanzanian highlands. The results are valuable references for designing the N strategies targeting higher yields with lower environmental costs for the cropland intensification across SSA.

8.2 Unanswered questions and future research perspective

Sandy soils that are poor in fertility like TZi contributed to a more “fragile & leaky” agroecosystem (e.g., high variability of yield and N losses; Fig. 7.1); the long-term investment for soil rehabilitation could be challenging as the immediate return (e.g., yield increment and thus profit) is expected by the farmers—sustainability may not necessarily be their prior concern (Vanlauwe et al. 2014a). For relatively fertile soils like TZm, yield plateaued at around 4 Mg ha^{-1} and no longer respond to the further increased N input, indicating the existence of other yield-limiting factors, which should be identified in the near future.

Field trials using low-quality straw likely failed to mitigate NO_3^- leaching loss and improve N synchrony in this study, though laboratory incubations have proved the potential of using low-quality residues to alter the N immobilization-mineralization turnover. Mechanistic insight into the different performance of residues under field and laboratory conditions is needed.

The mechanisms underlying the synergistic effect of the combined fertilizer-N and straw on the soil emissions of N_2O should be better understood to define the targeted mitigation strategy. Organic amendments may be utilized in combination with other management (e.g., water) to stimulate a more complete microbial reduction of N_2O to environmental benign N_2 (Kramer et al. 2006; Sanchez-Martín et al. 2010). The finely ground straw with uniform distribution in the soil may also help to reduce N_2O (Loecke and Robertson, 2009). Nevertheless, field verifications are needed before they can be applicable. Also, an integrated evaluation on the greenhouse gas emissions (N_2O, CO_2, and CH_4) and dynamics of soil C pool following N management practices (particularly those involved organic resource input) is recommended to better understand the global warming potential in maize systems experiencing intensification.

Further, more agro-ecological zones across SSA associated with different soil resources and climate conditions should be involved to develop field-specific N managements. Also, long-term monitoring is required to better characterize and understand the cycle of N in the cropping systems, which is the prerequisite to further improve the N use efficiency.

REFERENCES

Abalos D, Sanz-Cobena A, Garcia-Torres L, van Groenigen JW, Vallejo A (2012) Role of maize stover incorporation on nitrogen oxide emissions in a non-irrigated Mediterranean barley field. Plant Soil 364:357-371

Adviento-Borbe MAA, Haddix ML, Binder DL, Walters DT, Dobermann A (2007) Soil greenhouse gas fluxes and global warming potential in four high-yielding maize systems. Global Change Biol 13:1972-1988

AGRA (2009) Building on the New Momentum in African Agriculture: AGRA in 2008, Alliance for a Green Revolution in Africa, Nairobi

Amougou N, Bertrand I, Machet JM, Recous S (2010) Quality and decomposition in soil of rhizome, root and senescent leaf from Miscanthus x giganteus, as affected by harvest date and N fertilization. Plant Soil 338:83-97

Angers DA, Recous S (1997) Decomposition of wheat straw and rye residues as affected by particle size. Plant Soil 189:197-203

Avrahami S, Liesack W, Conrad R (2003) Effects of temperature and fertilizer on activity and community structure of soil ammonia oxidizers. Environ Microbiol 5:691-705

Baggs EM, Chebii J, Ndufa JK (2006) A short-term investigation of trace gas emissions following tillage and no-tillage of agroforestry residues in western Kenya. Soil Tillage Res 90:69-76

Barrows HL, Kilmer VJ (1963) Plant nutrient losses from soils by water erosion. In: Norman AG (ed) Advances in Agronomy, vol 15. Academic Press, pp 303-316

Barton L, Kiese R, Gatter D, Butterbach-Bahl K, Buck R, Hinz C, Murphy DV (2007) Nitrous oxide emissions from a cropped soil in a semi-arid climate. Global Change Biol 14:177-192

Bartiono A, Waswa B, Kihara J, Kimetu J (2007) Advances in integrated soil fertility management in sub Saharan Africa: challenge and opportunities. Nutr Cycl Agroecosys. https://doi.org/10.1007/s10705-007-9096-4

Bateman EJ, Baggs EM (2005) Contributions of nitrification and denitrification to N_2O emissions from soils at different water-filled pore space. Biol Fert Soils 41:379-388

Bergstrom A-K, Jansson M (2006) Atmospheric nitrogen deposition has caused nitrogen enrichment and eutrophication of lakes in the northern hemisphere. Global Change Biol 12:635-643

Birch HF (1964) Mineralization of plant nitrogen following alternate wet and dry conditions. Plant Soil 20:43-49

Bisanda S, Mwangi W, Verkuijl H, Moshi AJ, Anandajayasekeram P (1998) Adoption of Maize Production Technologies in the Southern Highlands of Tanzania. International Maize and Wheat Improvement Center (CIMMYT), the United Republic of Tanzania, and the Southern Africa Centre for Cooperation in Agricultural Research (SACCAR), Mexico, DF

Black AS, Sherlock RR, Smith NP (1987a) Effect of timing of simulated rainfall on ammonia volatilization from urea, applied to soil of varying moisture content. J Soil Sci 38:679-687

Black AS, Sherlock RR, Smith NP (1987b) Effect of urea granule size on ammonia volatilization from surface-applied urea. Fert Res 11:87-96

Bobbink R, Hicks K, Galloway J, Spranger T, Alkemade R, Ashmore M, Bustamante M, Cinderby S, Davidson E, Dentener F, Emmett B, Erisman JW, Fenn M, Gilliam F, Nordin A, Pardo L, De Vries W (2010) Global assessment of nitrogen deposition effects on terrestrial plant diversity: a synthesis. Ecol Appl 20:30-59

Bouwman AF, Boumans LJM, Batjes NH (2002a) Estimation of global NH_3 volatilization loss from synthetic fertilizers and animal manure applied to arable lands and grasslands. Global Biogeochem Cy 16:8-1-8-14

Bouwman AF, Boumans LJM, Batjes NH (2002b) Emissions of N_2O and NO from fertilized fields: Summary of available measurement data. Global Biogeochem Cy 16:6-1-6-13

Braker G, Conrad R (2011) Diversity, structure, and size of N_2O-producing microbial communities in soils—what matters for their functioning? In: Laskin AI, Sariaslani S, Gadd GM (eds) Advances in Applied Microbiology, vol 75. Academic Press, California, pp 33-70

Brink AB, Eva HD (2009) Monitoring 25 years of land cover change dynamics in Africa: a sample based remote sensing approach. Appl Geogr 29:501-512

Brummer C, Bruggemann N, Butterbach-Bahl K, Falk U, Szarzynski J, Vielhauer K, Wassmann R, Papen H (2008) Soil-atmosphere exchange of N_2O and NO in near-natural savanna and agricultural land in Burkina Faso (W. Africa). Ecosystems 11:582-600

Burney JA, Davis SJ, Lobell DB (2010) Greenhouse gas mitigation by agricultural intensification. Proc Natl Acad Sci USA 107:12052-12058

Butterbach-Bahl K, Baggs EM, Dannenmann M, Kiese R, Zechmeister-Boltenstern S (2013) Nitrous oxide emissions from soils: how well do we understand the processes and their controls? Philos T R Soc B. http://dx.doi.org/10.1098/rstb.2013.0122

Cantu RR, Aita C, Doneda A, Giacomini DA, Dessbesell A, Arenhardt M, De Bastiani GG, Pujol SB, Rochette P, Chantigny MH, Giacomini SJ (2017) Alternatives to regular urea for abating N losses in lettuce production under sub-tropical climate. Biol Fert Soils 53:589-599

Cassman KG, Dobermann A, Walters DT (2002) Agroecosystems, nitrogen-use efficiency, and nitrogen management. Ambio 31:132-40

Cassman KG, Dobermann A, Walters DT, Yang H (2003) Meeting cereal demand while protecting natural resources and improving environmental quality. Annu Rev Env Resour 28:315-358

Chaplin-Kramer R, Sharp RP, Mandle L, Sim S, Johnson J, Butnar I, Mila ICL, Eichelberger BA, Ramler I, Mueller C, McLachlan N, Yousefi A, King H, Kareiva PM (2015) Spatial patterns of agricultural expansion determine impacts on biodiversity and carbon storage. Proc Natl Acad Sci USA 112:7402-7407

Chapuis-Lardy L, Metay A, Martinet M, Rabenarivo M, Toucet J, Douzet JM, Razafimbelo T, Rabeharisoa L, Rakotoarisoa J (2009) Nitrous oxide fluxes from Malagasy agricultural soils. Geoderma 148:421-427

Chen H, Li X, Hu F, Shi W (2013) Soil nitrous oxide emissions following crop residue addition: a meta-analysis. Glob Chang Biol 19:2956-2964

Chen X, Cui Z, Fan M, Vitousek P, Zhao M, Ma W et al. (2014) Producing more grain with lower environmental costs. Nature 514:486-489

Chikowo R, Mapfumo P, Nyamugafata P, Giller KE (2004) Mineral N dynamics, leaching and nitrous oxide losses under maize following two-year improved fallows on a sandy loam soil in Zimbabwe. Plant Soil 259:315-330

Chikowo R, Mapfumo P, Nyamugafata P, Nyamadzawo G, Giller KE (2003) Nitrate-N dynamics following improved fallows and maize root development in a Zimbabwean sandy clay loam. Agroforest Syst 59: 187-195

Chivenge P, Vanlauwe B, Six J (2010) Does the combined application of organic and mineral nutrient sources influence maize productivity? A meta-analysis. Plant Soil 342:1-30

Congreves KA, Brown SE, Németh DD, Dunfield KE, Wagner-Riddle C (2017) Differences in field-scale N_2O flux linked to crop residue removal under two tillage systems in cold climates. GCB Bioenergy 9:666-680

Corbeels M, Hofman G, Cleemput OV (2000) Nitrogen cycling associated with the decomposition of sunflower stalks and wheat straw in a Vertisol. Plant Soil 218:71-82

Corstanje R, Kirk GJD, Pawlett M, Read R, Lark RM (2008) Spatial variation of ammonia volatilization from soil and its scale-dependent correlation with soil properties. Eur J Soil Sci 59: 1260-1270

Cui Z, Zhang H, Chen X, Zhang C, Ma W, Huang C, Zhang W, Mi G, Miao Y, Li X, Gao Q, Yang J, Wang Z, Ye Y, Guo S, Lu J, Huang J, Lv S, Sun Y, Liu Y, Peng X, Ren J, Li S, Deng X, Shi X, Zhang Q, Yang Z, Tang L, Wei C, Jia L, Zhang J, He M, Tong Y, Tang Q, Zhong X, Liu Z, Cao N, Kou C, Ying H, Yin Y, Jiao X, Zhang Q, Fan M, Jiang R, Zhang F, Dou Z (2018) Pursuing sustainable productivity with millions of smallholder farmers. Nature 555:363-366

Dalal RC (1975) Urease activity in some Trinidad soils. Soil Biol Biochem 7:5-8

Davidson EA (1992) Pulses of nitric oxide and nitrous oxide flux following wetting of dry soil: an assessment of probable sources and importance relative to annual fluxes. Ecol Bull 42:149-155

Davidson EA (2009) The contribution of manure and fertilizer nitrogen to atmospheric nitrous oxide since 1860. Nat Geosci 2:659-662

Dewitte O, Jones A, Spaargaren O, Breuning-Madsen H, Brossard M, Dampha A, Deckers J, Gallali T, Hallett S, Jones R, Kilasara M, Le Roux P, Michéli E, Montanarella L, Thiombiano L, Van Ranst E, Yemefack M, Zougmore R (2013) Harmonisation of the soil map of Africa at the continental scale. Geoderma 211-212:138-153

Diaz RJ, Rosenberg R (2008) Spreading dead zones and consequences for marine ecosystems. Science 321:926-929

Dick J, Kaya B, Soutoura M, Skiba U, Smith R, Niang A, Tabo R (2008) The contribution of agricultural practices to nitrous oxide emissions in semi-arid Mali. Soil Use Manage 24:292-301

Dijk MV, Meijerink GW, Rau ML, Shutes K (2012) Mapping maize yield gaps in Africa; Can a leopard change its spots? LEI, part of Wageningen UR, The Hague

Ekpa O, Palacios-Rojas N, Kruseman G, Fogliano V, Linnemann AR (2018) Sub-Saharan African maize-based foods: Technological perspectives to increase the food and nutrition security impacts of maize breeding programmes. Glob Food Secur 17:48-56

Elliot JR, Fox TR (2014) Ammonia volatilization following fertilization with urea or ureaform in a thinned loblolly pine plantation. Soil Sci Soc Am J 78:1469-1473

Fan J, Xiao J, Liu D, Ye G, Luo J, Houlbrooke D et al. (2017) Effect of application of dairy manure, effluent and inorganic fertilizer on nitrogen leaching in clayey fluvo-aquic soil: A lysimeter study. Sci Total Environ 592:206-214

FAO (2001) Major Farming Sytems: Sub-Saharan Africa. Food and Agriculture Organization of the United Nations. http://www.fao.org/FarmingSystems/FarmingMaps/SSA/01/FS/index.html. Accessed 10 September 2018

FAO (2018) FAOSTAT. http://www.fao.org/faostat/en/#data/QC. Accessed 10 September 2018

Fares A, Deb SK, Fares S (2009) Review of vadose zone soil solution sampling techniques. Environ Rev 17:215-234

Ferguson RB, Kissel DE, Koelliker JK, Basel W (1984) Ammonia volatilization from surface-applied urea—effect of hydrogen-ion buffering capacity. Soil Sci Soc Am J 48:578-582

Firestone MK, Davidson EA (1989) Microbiological basis of NO and N_2O production and consumption in soil. In Andreae MO, Schimel DS (eds) Exchange of Trace Gases Between Terrestrial Ecosystems and the Atmosphere, vol 47. Wiley, New York, pp 7-21

Fleisher Z, Hagin J (1981) Lowering ammonia volatilization losses from urea application by activation of nitrification process. Fert Res 2:101-107

Forster P, Ramaswamy V, Artaxo P, Berntsen T, Betts R, Fahey DW, Haywood J, Lean J, Lowe DC, Myhre G, Nganga J, Prinn R, Raga G, Schulz M, Dorland RV (2007) Changes in atmospheric constituents and in radiative forcing. In: Solomon S et al. (eds) Climate Change 2007: The Physical Science Basis. Contribution of Working Group I to the Fourth Assessment Report of the Intergovernmental Panel on Climate Change. Cambridge University Press, Cambridge, United Kingdom and New York, USA, pp 129-234

Frank S, Beach R, Havlik P, Valin H, Herrero M, Mosnier A, Hasegawa T, Creason J, Ragnauth S, Obersteiner M (2018) Structural change as a key component for agricultural non-CO_2 mitigation efforts. Nat Commun. https://doi.org/10.1038/s41467-018-03489-1

Fu J, Gasche R, Wang N, Lu H, Butterbach-Bahl K, Kiese R (2017) Impacts of climate and management on water balance and nitrogen leaching from montane grassland soils of S-Germany. Environ Pollut 229:119-131

Fujii K, Uemura M, Hayakawa C, Funakawa S, Sukartiningsih, Kosaki T et al (2009) Fluxes of dissolved organic carbon in two tropical forest ecosystems of East Kalimantan, Indonesia. Geoderma 152:127-136

Funakawa S, Yoshida H, Watanabe T, Sugihara S, Kilasara M, Kosaki T (2012) Soil fertility status and its determining factors in Tanzania. In Hernandez-Soriano MC (ed) Soil Health and Land Use Management, IntechOpen, pp 3-16, DOI: 10.5772/29199

Gagnon B, Ziadi N, Rochette P, Chantigny MH, Angers DA (2011) Fertilizer source influenced nitrous oxide emissions from a clay soil under corn. Soil Sci Soc Am J 75:595-604

Galloway JN, Aber JD, Erisman JW, Seitzinger SP, Howarth RW, Cowling EB, Cosby BJ (2003) The nitrogen cascade. Bioscience 53: 341-356

Galloway JN, Townsend AR, Erisman JW, Bekunda M, Cai Z, Freney JR et al. (2008) Transformation of the nitrogen cycle: recent trends, questions, and potential solutions. Science 320:889-892

Gao S, Xu P, Zhou F, Yang H, Zheng C, Cao W et al. (2016) Quantifying nitrogen leaching response to fertilizer additions in China's cropland. Environ Pollut 211:241-251

Gatseva PD, Argirova MD (2008) High-nitrate levels in drinking water may be a risk factor for thyroid dysfunction in children and pregnant women living in rural Bulgarian areas. Int J Hyg Environ Health 211:555-559

Gentile R, Vanlauwe B, Chivenge P, Six J (2008) Interactive effects from combining fertilizer and organic residue inputs on nitrogen transformations. Soil Biol Biochem 40: 2375-2384

Gentile R, Vanlauwe B, van Kessel C, Six J (2009) Managing N availability and losses by combining fertilizer-N with different quality residues in Kenya. Agric Ecosyst Environ 131:308-314

Gentile R, Vanlauwe B, Chivenge P, Six J (2011) Trade-offs between the short- and long-term effects of residue quality on soil C and N dynamics. Plant Soil 338:159-169

Gibbs HK, Ruesch AS, Achard F, Clayton MK, Holmgren P, Ramankutty N, Foley JA (2010) Tropical forests were the primary sources of new agricultural land in the 1980s and 1990s. Proc Natl Acad Sci USA 107:16732-16737

Goss MJ, Ehlers W (2009) The role of lysimeters in the development of our understanding of soil water and nutrient dynamics in ecosystems. Soil Use Manage 25:213-223

Gu J, Zheng X, Wang Y, Ding W, Zhu B, Chen X, Wang Y, Zhao Z, Shi Y, Zhu J (2007) Regulatory effects of soil properties on background N_2O emissions from agricultural soils in China. Plant Soil 295:53-65

Gu J, Zheng X, Zhang W (2009) Background nitrous oxide emissions from croplands in China in the year 2000. Plant Soil 320:307-320

Gutlein A, Gerschlauer F, Kikoti I, Kiese R (2018) Impacts of climate and land use on N_2O and CH_4 fluxes from tropical ecosystems in the Mt. Kilimanjaro region, Tanzania. Glob Chang Biol 24:1239-1255

Haden VR, Xiang J, Peng S, Ketterings QM, Hobbs P, Duxbury JM (2011) Ammonia toxicity in aerobic rice: use of soil properties to predict ammonia volatilization following urea application and the adverse effects on germination. Eur J Soil Sci 62:551-559

Han D, Currell MJ, Cao G (2016) Deep challenges for China's war on water pollution. Environ Pollut 218:1222-1233

Hartemink AE, Buresh RJ, van Bodegom PM, Braun AR, Jama B, Janssen BH (2000) Inorganic nitrogen dynamics in fallows and maize on an Oxisol and Alfisol in the highlands of Kenya. Geoderma 98:11-33

Hartmann TE, Yue S, Schulz R, He X, Chen X, Zhang F, Muller T (2015) Yield and N use efficiency of a maize–wheat cropping system as affected by different fertilizer management strategies in a farmer's field of the North China Plain. Field Crop Res 174: 30-39

Hayakawa A, Akiyama H, Sudo S, Yagi K (2009) N_2O and NO emissions from an Andisol field as influenced by pelleted poultry manure. Soil Biol Biochem 41:521-529

Hazell P, Wood S (2008) Drivers of change in global agriculture. Philos Trans R Soc Lond B Biol Sci 363:495-515

He ZL, Alva AK, Calvert DV, Banks DJ (1999) Ammonia volatilization from different fertilizer sources and effects of temperature and soil pH. Soil Sci 164:750-758

Henriksen TM, Breland TA (1999a) Evaluation of criteria for describing crop residue degradability in a model of carbon and nitrogen turnover in soil. Soil Biol Biochem 31:1135-1149

Henriksen TM, Breland TA (1999b) Nitrogen availability effects on carbon mineralization, fungal and bacterial growth, and enzyme activities during decomposition of wheat straw in soil. Soil Biol Biochem 31:1121-1134

Hickman JE, Palm CA, Mutuo P, Melillo JM, Tang J (2014) Nitrous oxide (N_2O) emissions in response to increasing fertilizer addition in maize (Zea mays L.) agriculture in western Kenya. Nutr Cycl Agroecosys 100:177-187

Hickman JE, Tully KL, Groffman PM, Diru W, Palm CA (2015) A potential tipping point in tropical agriculture: Avoiding rapid increases in nitrous oxide fluxes from agricultural intensification in Kenya. J Geophys Res-Biogeo 120:938-951

Hoben JP, Gehl RJ, Millar N, Grace PR, Robertson GP (2011) Nonlinear nitrous oxide (N_2O) response to nitrogen fertilizer in on-farm corn crops of the US Midwest. Global Change Biol 17:1140-1152

Holcomb JC, Sullivan DM, Horneck DA, Clough GH (2011) Effect of irrigation rate on ammonia volatilization. Soil Sci Soc Am J 75:2341-2347

Howarth RW, Marino R (2006) Nitrogen as the limiting nutrient for eutrophication in coastal marine ecosystems: Evolving views over three decades. Limnol Oceanogr 51:364-376

IFA (2017) International Fertilizer Association Database: http://ifadata.fertilizer.org/ucSearch.aspx. Accessed 20 June 2017

IPCC (2006) 2006 IPCC Guidelines for National Greenhouse Gas Inventories. IGES, Kanagawa, Japan

Iqbal A, Garnier P, Lashermes G, Recous S (2013) A new equation to simulate the contact between soil and maize residues of different sizes during their decomposition. Biol Fert Soils 50:645-655

Ishiguro M, Song KC, Yuita K (1992) Ion transport in an allophanic Andisol under the influence of variable charge. Soil Sci Soc Am J 56: 1789-1793

Jalloh A, Roy-Macauley H, Sereme P (2012) Major agro-ecosystems of West and Central Africa: brief description, species richness, management, environmental limitations and concerns. Agric Ecosyst Environ 157:5-16

Juma NG (1993) Interrelationships between soil structure/texture, soil biota/soil organic matter and crop production. Geoderma 57:3-13

Jiang Y, Deng A, Bloszies S, Huang S, Zhang W (2017) Nonlinear response of soil ammonia emissions to fertilizer nitrogen. Biol Fert Soils 53:269-274

Kahimba F, Ishengoma EK, Tarimo AKPR (2015) Managing water: low-cost drip irrigation systems for smallholder farmers in Tanzania. In: Nicol A, Langan S, Victor M Gonsalves J (eds) Water-smart agriculture in East Africa. Colombo, Sri Lanka: IWMI and CGIAR research program on WLE; Kampala, Uganda: GWI EA, pp 165-171

Kamukondiwa W, Bergström L (1994) Nitrate leaching in field lysimeters at an agricultural site in Zimbabwe. Soil Use Manage 10: 118-124

Kandeler E, Gerber H (1988) Short-term assay of soil urease activity using colorimetric determination of ammonium. Biol Fert Soils 6:68-72

Katou H, Clothier BE, Green SR (1996) Anion transport involving competitive adsorption during transient water flow in an Andisol. Soil Sci Soc Am J 60: 1368-1375

Kehoe L, Romero-Munoz A, Polaina E, Estes L, Kreft H, Kuemmerle T (2017) Biodiversity at risk under future cropland expansion and intensification. Nat Ecol Evol 1:1129-1135

Keller M, Weitz AM, Bryan B, Rivera MM, Silver WL (2000) Soil-atmosphere nitrogen oxide fluxes: effects of root disturbance. J Geophys Res-Atmos 105:17693-17698

Khalil K, Mary B, Renault P (2004) Nitrous oxide production by nitrification and denitrification in soil aggregates as affected by O_2 concentration. Soil Biol Biochem 36:687-699

Kihara J, Nziguheba G, Zingore S et al. (2016) Understanding variability in crop response to fertilizer and amendments in sub-Saharan Africa. Agric Ecosyst Environ 229: 1-12

Kim D-G, Giltrap D, Hernandez-Ramirez G (2013a) Background nitrous oxide emissions in agricultural and natural lands: a meta-analysis. Plant Soil 373:17-30

Kim D-G, Hernandez-Ramirez G, Giltrap D (2013b) Linear and nonlinear dependency of direct nitrous oxide emissions on fertilizer nitrogen input: a meta-analysis. Agric Ecosyst Environ 168:53-65

Kim D-G, Thomas AD, Pelster D, Rosenstock TS, Sanz-Cobena A (2016) Greenhouse gas emissions from natural ecosystems and agricultural lands in sub-Saharan Africa: synthesis of available data and suggestions for further research. Biogeosciences 13:4789-4809

Kim GW, Das S, Hwang HY, Kim PJ (2017) Nitrous oxide emissions from soils amended by cover-crops and under plastic film mulching: Fluxes, emission factors and yield-scaled emissions. Atmos Environ 152:377-388

Kimani SK, Nandwa SM, Mugendi DN, Obanyi SN, Ojiem J, Murwira HK, Bationo A (2003) Principles of integrated soil fertility management. In: Gichuri MP et al. (eds) Soil fertility management in Africa: a regional perspective. Academy Science Publishers, Nairobi, pp 51-71

Kimaro AA, Mpanda M, Rioux J, Aynekulu E, Shaba S, Thiong'o M, Mutuo P, Abwanda S, Shepherd K, Neufeldt H, Rosenstock TS (2016) Is conservation agriculture 'climate-smart' for maize farmers in the highlands of Tanzania? Nutr Cycl Agroecosys 105:217-228

Kimetu JM, Mugendi DN, Bationo A, Palm CA, Mutuo PK, Kihara J et al. (2006) Partial balance of nitrogen in a maize cropping system in humic nitisol of Central Kenya. Nutr Cycl Agroecosys 76:261-270

Kissel D., Cabrera ML, Vaio N, Craig JR, Rema JA, Morris LA (2004) Rainfall timing and ammonia loss from urea in a loblolly pine plantation. Soil Sci Soc Am J 68: 1744-1750

Kramer SB, Reganold JP, Glover JD, Bohannan BJ, Mooney HA (2006) Reduced nitrate leaching and enhanced denitrifier activity and efficiency in organically fertilized soils. Proc Natl Acad Sci USA 103:4522-4527

Kravchenko AN, Toosi ER, Guber AK, Ostrom NE, Yu J, Azeem K, Rivers ML, Robertson GP (2017) Hotspots of soil N_2O emission enhanced through water absorption by plant residue. Nat Geosci 10:496-500

Kumar K, Goh KM (1999) Crop residues and management practices: effects on soil quality, soil nitrogen dynamics, crop yield, and nitrogen recovery. In: Donald LS (ed) Advances in Agronomy, vol 68. Academic Press, Cambridge, pp 197-319

Ladha JK, Pathak H, J. Krupnik T, Six J, van Kessel C (2005) Efficiency of fertilizer nitrogen in cereal production: retrospects and prospects. In: Donald LS (ed) Advances in Agronomy vol. 87:85-156

Lehmann J, Schroth G (2003) Nutrient leaching. In: Schroth G, Sinclair EL (eds) Trees, crops, and soil fertility: concepts and research methods. CAB International, Wallingford, UK, pp 151-166

Lelieveld J, Evans JS, Fnais M, Giannadaki D, Pozzer A (2015) The contribution of outdoor air pollution sources to premature mortality on a global scale. Nature 525:367-371

Li X, Hu F, Shi W (2013) Plant material addition affects soil nitrous oxide production differently between aerobic and oxygen-limited conditions. Appl Soil Ecol 64:91-98

Li X, Sørensen P, Olesen JE, Petersen SO (2016) Evidence for denitrification as main source of N_2O emission from residue-amended soil. Soil Biol Biochem 92:153-160

Liu C, Wang K, Zheng X (2012) Responses of N_2O and CH_4 fluxes to fertilizer nitrogen addition rates in an irrigated wheat-maize cropping system in northern China. Biogeosciences 9:839-850

Liu J, Zhu L, Luo S, Bu L, Chen X, Yue S, Li S (2014) Response of nitrous oxide emission to soil mulching and nitrogen fertilization in semi-arid farmland. Agric Ecosyst Environ 188:20-28

Loecke TD, Robertson GP (2009) Soil resource heterogeneity in terms of litter aggregation promotes nitrous oxide fluxes and slows decomposition. Soil Biol Biochem 41:228-235

Lompo DJ-P, Sangaré SAK, Compaoré E, Papoada Sedogo M, Predotova M, Schlecht E, Buerkert A (2012) Gaseous emissions of nitrogen and carbon from urban vegetable gardens in Bobo-Dioulasso, Burkina Faso. J Plant Nutr Soil Sci 175:846-853

Lyimo N (2005) Improving farmers access to and management of disease resistant maize cultivars in the Southern Highlands of Tanzania. Uyole Agricultural Research Institute, Tanzania. https://www.gov.uk/dfid-research-outputs/improving-farmers-access-to-and-management-of-disease-resistant-maize-cultivars-in-the-southern-highlands-of-tanzania-final-technical-report. Accessed 28 April 2018

Lyimo S, Mduruma Z, Groote HD (2014) The use of improved maize varieties in Tanzania. Afr J Agric Res 9: 643-657

Ma BL, Wu TY, Tremblay N, Deen W, McLaughlin NB, Morrison MJ, Stewart G (2010) On-farm assessment of the amount and timing of nitrogen fertilizer on ammonia volatilization. Agron J 102:134-144

Ma BL, Wu TY, Tremblay N, Deen W, Morrison MJ, McLaughlin NB, Gregorich EG, Stewart G (2010) Nitrous oxide fluxes from corn fields: on-farm assessment of the amount and timing of nitrogen fertilizer. Global Change Biol 16:156-170

Mafongoya PL, Bationo A, Kihara J., Waswa BS (2006) Appropriate technologies to replenish soil fertility in southern Africa. Nutr Cycl Agroecosys 76: 137-151

Mapanda F, Wuta M, Nyamangara J, Rees RM (2011) Effects of organic and mineral fertilizer nitrogen on greenhouse gas emissions and plant-captured carbon under maize cropping in Zimbabwe. Plant Soil 343:67-81

Mapanda F, Wuta M, Nyamangara J, Rees RM (2012a) Nitrogen leaching and indirect nitrous oxide emissions from fertilized croplands in Zimbabwe. Nutr Cycl Agroecosys 94:85-96

Mapanda F, Wuta M, Nyamangara J, Rees RM, Kitzler B (2012b) Greenhouse gas emissions from Savanna (Miombo) woodlands: responses to clearing and cropping. African Crop Science Journal 20: 385-400

Maroko JB, Buresh RJ, Smithson PC (1998) Soil nitrogen availability as affected by fallow-maize systems on two soils in Kenya. Biol Fert Soils 26:229-234

Masaka J, Nyamangara J, Wuta M (2014) Nitrous oxide emissions from wetland soil amended with inorganic and organic fertilizers. Arch of Agron Soil Sci 60:1363-1387

Masaka J, Nyamangara J, Wuta M (2016) Nitrous oxide emissions from wetland soil amended with two types of cattle manure. International Journal of Recycling of Organic Waste in Agriculture 5:125-140

Masvaya EN, Nyamangara J, Descheemaeker K, Giller KE (2017) Tillage, mulch and fertiliser impacts on soil nitrogen availability and maize production in semi-arid Zimbabwe. Soil Tillage Res 168:125-132

McSwiney CP, Robertson GP (2005) Nonlinear response of N_2O flux to incremental fertilizer addition in a continuous maize (Zea mays L.) cropping system. Global Change Biol 11:1712-1719

Millar N, Ndufa JK, Cadisch G, Baggs EM (2004) Nitrous oxide emissions following incorporation of improved-fallow residues in the humid tropics. Global Biogeochem Cy. https://doi.org/10.1029/2003GB002114

Mtambanengwe F, Mapfumo P (2006) Effects of organic resource quality on soil profile N dynamics and maize yields on sandy soils in Zimbabwe. Plant Soil 281:173-191

Mueller ND, Gerber JS, Johnston M, Ray DK, Ramankutty N, Foley JA (2012) Closing yield gaps through nutrient and water management. Nature 490:254-257

Muhammad W, Vaughan SM, Dalal RC, Menzies NW (2011) Crop residues and fertilizer nitrogen influence residue decomposition and nitrous oxide emission from a Vertisol. Biol Fertil Soils 47:15-23

Mungai LM, Snapp S, Messina JP, Chikowo R, Smith A, Anders E, Richardson RB, Li G (2016) Smallholder farms and the potential for sustainable intensification. Front Plant Sci 7:1720

Nicolardot B, Recous S, Mary B (2001) Simulation of C and N mineralisation during crop residue decomposition: A simple dynamic model based on the C:N ratio of the residues. Plant Soil 228:83-103

Njoroge R, Otinga AN, Okalebo JR, Pepela M, Merckx R (2017) Occurrence of poorly responsive soils in western Kenya and associated nutrient imbalances in maize (Zea mays L.). Field Crop Res 210: 162-174

Nyamangara J, Bergstrom LF, Piha MI, Giller KE (2003) Fertilizer use efficiency and nitrate leaching in a tropical sandy soil. J Environ Qual 32:599-606

Nziguheba G, Palm CA, Berhe T, Denning G, Dicko A, Diouf O, Diru W, Flor R, Frimpong F, Harawa R, Kaya B, Manumbu E, McArthur J, Mutuo P, Ndiaye M, Niang A, Nkhoma P, Nyadzi G, Sachs J, Sullivan C, Teklu G, Tobe L, Sanchez PA (2010) The African Green Revolution: Results from the Millennium Villages Project. In: Donald LS (ed) Advances in Agronomy, vol 109. Academic Press, London, pp 75-115

Ocio JA, Brookes PC, Jenkinson DS (1991) Field incorporation of straw and its effects on soil microbial biomass and soil inorganic-N. Soil Biol Biochem 23:171-176

Ortiz-Gonzalo D, de Neergaard A, Vaast P, Suarez-Villanueva V, Oelofse M, Rosenstock TS (2018) Multi-scale measurements show limited soil greenhouse gas emissions in Kenyan smallholder coffee-dairy systems. Sci Total Environ 626:328-339

Outram FN, Cooper RJ, Sunnenberg G, Hiscock KM, Lovett AA (2016) Antecedent conditions, hydrological connectivity and anthropogenic inputs: Factors affecting nitrate and phosphorus transfers to agricultural headwater streams. Sci Total Environ 545-546:184-199

Padilla FM, Gallardo M, Manzano-Agugliaro F (2018) Global trends in nitrate leaching research in the 1960-2017 period. Sci Total Environ 643:400-413

Palm C, Neill C, Lefebvre P, Tully K (2017) Targeting Sustainable Intensification of Maize-Based Agriculture in East Africa. Trop Conserv Sci 10:1-4

Palm CA, Gachengo CN, Delve RJ, Cadisch G, Giller KE (2001) Organic inputs for soil fertility management in tropical agroecosystems: application of an organic resource database. Agric Ecosyst Environ 83:27-42

Pan B, Lam SK, Mosier A, Luo Y, Chen D (2016) Ammonia volatilization from synthetic fertilizers and its mitigation strategies: A global synthesis. Agri Ecosyst Environ 232:283-289

Pelster D, Rufino M, Rosenstock T, Mango J, Saiz G, Diaz-Pines E, Baldi G, Butterbach-Bahl K (2017) Smallholder farms in eastern African tropical highlands have low soil greenhouse gas fluxes. Biogeosciences 14:187-202

Philippot L, Hallin S, Schloter M (2007) Ecology of denitrifying prokaryotes in agricultural soil. In: Donald LS (ed) Advances in Agronomy, vol 96. Academic Press, pp 249-305.

Postel S, Polak P, Gonzales F, Keller J (2001) Drip irrigation for small farmers: a new initiative to alleviate hunger and poverty. Water International 26:3-13

Predotova M, Gebauer J, Diogo RVC, Schlecht E, Buerkert A (2010) Emissions of ammonia, nitrous oxide and carbon dioxide from urban gardens in Niamey, Niger. Field Crops Res 115:1-8

Qin B, Zhu G, Gao G, Zhang Y, Li W, Paerl HW et al (2010) A drinking water crisis in Lake Taihu, China: linkage to climatic variability and lake management. Environ manage 45:105-112

Rasouli S, Whalen JK, Madramootoo CA (2014) Review: Reducing residual soil nitrogen losses from agroecosystems for surface water protection in Quebec and Ontario, Canada: Best management practices, policies and perspectives. Can J Soil Sci 94: 109-127

Ravishankara AR, Daniel JS, Portmann RW (2009) Nitrous oxide (N_2O): the dominant ozone-depleting substance emitted in the 21st century. Science 326:123-125

Reay DS, Davidson EA, Smith KA, Smith P, Melillo JM, Dentener F, Crutzen PJ (2012) Global agriculture and nitrous oxide emissions. Nat Clim Change 2:410-416

Recous S, Robin D, Darwis D, Mary B (1995) Soil inorganic N availability: Effect on maize residue decomposition. Soil Biol Biochem 27:1529-1538

Reddy DD, Sharma KL (2000) Effect of amending urea fertilizer with chemical additives on ammonia volatilization loss and nitrogen-use efficiency. Biol Fert Soils 32:24-27

Rees RM, Wuta M, Furley PA, Li C (2006) Nitrous oxide fluxes from savanna (miombo) woodlands in Zimbabwe. J Biogeogr 33:424-437

Rimski-Korsakov H, Rubio G, Lavado RS (2012) Fate of the nitrogen from fertilizers in field-grown maize. Nutr Cycl Agroecosys 93:253-263

Robertson GP, Vitousek PM (2009) Nitrogen in agriculture: balancing the cost of an essential resource. Annu Rev Env Resour 34:97-125

Rochette P, Angers DA, Chantigny MH, Gasser M-O, MacDonald JD, Pelster DE, Bertrand N (2013a) Ammonia volatilization and nitrogen retention: How deep to incorporate urea? J Environ Qual 42:1635-1642

Rochette P, Angers DA, Chantigny MH, Gasser M-O, MacDonald JD, Pelster DE, Bertrand N (2013b) NH3 volatilization, soil concentration and soil pH following subsurface banding of urea at increasing rates. Can J Soil Sci 93:261-268

Rosenstock TS, Mpanda M, Pelster DE, Butterbach-Bahl K, Rufino MC, Thiong'o M, Mutuo P, Abwanda S, Rioux J, Kimaro AA, Neufeldt H (2016) Greenhouse gas fluxes from agricultural soils of Kenya and Tanzania. J Geophys Res-Biogeo 121:1568-1580

Rowhani P, Lobell DB, Linderman M, Ramankutty N (2011) Climate variability and crop production in Tanzania. Agr Forest Meteorol 151: 449-460

Russo TA, Tully K, Palm C, Neill C (2017) Leaching losses from Kenyan maize cropland receiving different rates of nitrogen fertilizer. Nutr Cycl Agroecosys 108:195-209

Sahrawat KL (1984) Effects of temperature and moisture on urease activity in semi-arid tropical soils. Plant Soil 78:401-408

Sakala WD, Cadisch G, Giller KE (2000) Interactions between residues of maize and pigeonpea and mineral N fertilizers during decomposition and N mineralization. Soil Biol Biochem 32:679-688

Sakurai K, Ohdate Y, Kyuma K (1989) Potentiometric automatic titration (PAT) method to evaluate zero point of charge (ZPC) of variable charge soils. Soil Sci Plant Nutr 35:89-100

Sanchez-Martín L, Meijide A, Garcia-Torres L, Vallejo A (2010) Combination of drip irrigation and organic fertilizer for mitigating emissions of nitrogen oxides in semiarid climate. Agri Ecosyst Environ 137:99-107

Sanchez P, Palm C, Sachs J, Denning G, Flor R, Harawa R, Jama B, Kiflemariam T, Konecky B, Kozar R, Lelerai E, Malik A, Modi V, Mutuo P, Niang A, Okoth H, Place F, Sachs SE, Said A, Siriri D, Teklehaimanot A, Wang K, Wangila J, Zamba C (2007) The African Millennium Villages. P Natl Acad Sci USA 104: 16775-16780

Sanchez PA (2002) Soil fertility and hunger in Africa. Science 295:2019-2020

Sanchez PA (2015) En route to plentiful food production in Africa. Nat Plants 1:14014

Sanchez PA, Denning GL, Nziguheba G (2009) The African Green Revolution moves forward. Food Sec 1:37-44

Scudlark JR, Jennings JA, Roadman MJ, Savidge KB, Ullman WJ (2005) Atmospheric nitrogen inputs to the Delaware Inland Bays: the role of ammonia. Environ Pollut 135:433-443

Sey BK, Manceur AM, Whalen JK, Gregorich EG, Rochette P (2009) Root-derived respiration and nitrous oxide production as affected by crop phenology and nitrogen fertilization. Plant Soil 326:369-379

Shibata M, Sugihara S, Mvondo-Ze AD, Araki S, Funakawa S (2017) Nitrogen flux patterns through Oxisols and Ultisols in tropical forests of Cameroon, Central Africa. Soil Sci Plant Nutr 63:306-317

Shiferaw B, Prasanna BM, Hellin J, Bänziger M (2011) Crops that feed the world 6. Past successes and future challenges to the role played by maize in global food security. Food Sec 3: 307-327

Shinjo H, Kato A, Fujii K, Mori K, Funakawa S, Kosaki T (2006) Carbon dioxide emission derived from soil organic matter decomposition and root respiration in Japanese forests under different ecological conditions. Soil Sci Plant Nutr 52:233-242

Sigunga DO, Janssen BH, Oenema O (2002) Ammonia volatilization from vertisols. Eur J Soil Sci 53:195-202

Sileshi GW, Nhamo N, Mafongoya PL, Tanimu J (2016) Stoichiometry of animal manure and implications for nutrient cycling and agriculture in sub-Saharan Africa. Nutr Cycl Agroecosys 107: 91-105

Singh R, Nye PH (1984) The effect of soil pH and high urea concentrations on urease activity in soil. J Soil Sci 35:519-527

Smith MS, Tiedje JM (1979) The effect of roots on soil denitrification. Soil Sci Soc Am J 43:951-955

Smith VH, Tilman GD, Nekola JC (1999) Eutrophication: impacts of excess nutrient inputs on freshwater, marine, and terrestrial ecosystems. Environ Pollut 100:179-196

Soares JR, Cantarella H, Menegale MLdC (2012) Ammonia volatilization losses from surface-applied urea with urease and nitrification inhibitors. Soil Biol Biochem 52:82-89

Soil Survey Staff (2010) Keys to Soil Taxonomy. 11th ed. United States Department of Agriculture Natural Resources Conservation Service, Washington, DC.

Sommer SG, Schjoerring JK, Denmead OT (2004) Ammonia emission from mineral fertilizers and fertilized crops. In: Donald LS (ed) Advances in Agronomy, vol 82. Academic Press, London, pp 557-622

Stevenson JR, Villoria N, Byerlee D, Kelley T, Maredia M (2013) Green Revolution research saved an estimated 18 to 27 million hectares from being brought into agricultural production. Proc Natl Acad Sci USA 110:8363-8368

Subedi R, Kammann C, Pelissetti S, Taupe N, Bertora C, Monaco S, Grignani C (2015) Does soil amended with biochar and hydrochar reduce ammonia emissions following the application of pig slurry? Eur J Soil Sci 66:1044-1053

Sugihara S, Funakawa S, Kilasara M, Kosaki T (2010) Effect of land management and soil texture on seasonal variations in soil microbial biomass in dry tropical agroecosystems in Tanzania. Appl Soil Ecol 44:80-88

Sugihara S, Funakawa S, Kilasara M, Kosaki T (2012a) Effect of land management on soil microbial N supply to crop N uptake in a dry tropical cropland in Tanzania. Agric Ecosyst Environ 146:209-219

Sugihara S, Funakawa S, Kilasara M, Kosaki T (2012b) Effects of land management on CO_2 flux and soil C stock in two Tanzanian croplands with contrasting soil texture. Soil Biol Biochem 46:1-9

Sutton MA, Oenema O, Erisman JW, Leip A, Grinsven Hv, Winiwarter W (2011) Too much of a good thing. Nature 472:159-161

Svoboda N, Taube F, Wienforth B, Kluß C, Kage H, Herrmann A (2013) Nitrogen leaching losses after biogas residue application to maize. Soil Tillage Res 130:69-80

Tamene L, Mponela P, Ndengu G, Kihara J (2015) Assessment of maize yield gap and major determinant factors between smallholder farmers in the Dedza district of Malawi. Nutr Cycl Agroecosys 105: 291-308

Tian D, Niu S (2015) A global analysis of soil acidification caused by nitrogen addition. Environ Res Lett 10 024019

Tian G, Cai Z, Cao J, Li X (2001) Factors affecting ammonia volatilisation from a rice–wheat rotation system. Chemosphere 42:123-129

Tittonell P, Muriuki A, Klapwijk CJ, Shepherd KD, Coe R, Vanlauwe B (2013) Soil heterogeneity and soil fertility gradients in smallholder farms of the East African highlands. Soil Sci Soc Am J 77:525-538

Tittonell P, Zingore S, van Wijk MT, Corbeels M, Giller KE (2007) Nutrient use efficiencies and crop responses to N, P and manure applications in Zimbabwean soils: Exploring management strategies across soil fertility gradients. Field Crop Res 100:348-368

Trinsoutrot I, Recous S, Bentz B, Line`res M, Che`neby D, Nicolardot B (2000) Biochemical quality of crop residues and carbon and nitrogen mineralization kinetics under nonlimiting nitrogen conditions. Soil Sci Soc Am J 64:918-926

Tully KL, Hickman J, McKenna M, Neil C, Palm CA (2016) Effects of fertilizer on inorganic soil N in East Africa maize systems: vertical distributions and temporal dynamics. Ecol Appl 26:1907-1919

Tully KL, Wood SA, Lawrence D (2013) Fertilizer type and species composition affect leachate nutrient concentrations in coffee agroecosystems. Agroforest Syst 87:1083-1100

United Nations, Department of Economic and Social Affairs, Population Division (2017) World Population Prospects: The 2017 Revision, Key Findings and Advance Tables. Working Paper No. ESA/P/WP/248

Van Groenigen JW, Velthof GL, Oenema O, Van Groenigen KJ, Van Kessel C (2010) Towards an agronomic assessment of N_2O emissions: a case study for arable crops. Eur J Soil Sci 61:903-913

van Ittersum MK, van Bussel LG, Wolf J, Grassini P, van Wart J, Guilpart N, Claessens L, de Groot H, Wiebe K, Mason-D'Croz D, Yang H, Boogaard H, van Oort PA, van Loon MP, Saito K, Adimo O, Adjei-Nsiah S, Agali A, Bala A, Chikowo R, Kaizzi K, Kouressy M, Makoi JH, Ouattara K, Tesfaye K, Cassman KG (2016) Can sub-Saharan Africa feed itself? Proc Natl Acad Sci USA 113:14964-14969

van Kessel C, Clough T, van Groenigen JW (2009) Dissolved organic nitrogen: an overlooked pathway of nitrogen loss from agricultural systems? J Environ Qual 38:393-401

Vanlauwe B, Coyne D, Gockowski J, Hauser S, Huising J, Masso C, Nziguheba G, Schut M, Van Asten P (2014a) Sustainable intensification and the African smallholder farmer. Curr Opin Env Sust 8:15-22

Vanlauwe B, Descheemaeker K, Giller KE, Huising J, Merckx R, Nziguheba G, Wendt J, Zingore S (2015) Integrated soil fertility management in sub-Saharan Africa: unravelling local adaptation. Soil 1: 491-508

Vanlauwe B, Diels J, Aihou K, Iwuafor ENO, Lyasse O, Sanginga N et al. (2002) Direct interactions between N fertilizer and organic matter: evidence from trials with ^{15}N-labelled fertilizer. In: Vanlauwe B, Diels J, Sanginga N, Merckx R (eds) Integrated Plant Nutrient Management in Sub-Saharan Africa: from Concept to Practice. CAB International, New York, pp 173-184

Vanlauwe B, Kihara J, Chivenge P, Pypers P, Coe R, Six J (2011) Agronomic use efficiency of N fertilizer in maize-based systems in sub-Saharan Africa within the context of integrated soil fertility management. Plant Soil 339:35-50

Vanlauwe B, Wendt J, Diels J (2001) Combined application of organic matter and fertilizer. In: Tian G, Ishida F, Keatinge D (eds) Sustaining Soil Fertility in West Africa. Soil Science Society of America and American Society of Agronomy, Madison, WI, pp 247-279

Vanlauwe B, Wendt J, Giller KE, Corbeels M, Gerard B, Nolte C (2014b) A fourth principle is required to define Conservation Agriculture in sub-Saharan Africa: The appropriate use of fertilizer to enhance crop productivity. Field Crop Res 155:10-13

Vitousek PM, Naylor R, Crews T, David MB, Drinkwater LE, Holland E, Johnes PJ, Katzenberger J, Martinelli LA, Matson PA, Nziguheba G, Ojima D, Palm CA, Robertson GP, Sanchez PA, Townsend AR, Zhang FS (2009) Nutrient imbalances in agricultural development. Science 324:1519-1520

Wang JY, Jia JX, Xiong ZQ, Khalil MAK, Xing GX (2011) Water regime–nitrogen fertilizer–straw incorporation interaction: Field study on nitrous oxide emissions from a rice agroecosystem in Nanjing, China. Agric Ecosyst Environ 141:437-446

Wang M, Wang L, Cui Z, Chen X, Xie J, Hou Y (2017) Closing the yield gap and achieving high N use efficiency and low apparent N losses. Field Crop Res 209: 39-46

Wang Q, Cameron K, Buchan G, Zhao L, Zhang EH, Smith N et al. (2012) Comparison of lysimeters and porous ceramic cups for measuring nitrate leaching in different soil types. New Zeal J Agr Res 55:333-345

Wang YY, Cheng YH, Chen KE, Tsay YF (2018) Nitrate Transport, Signaling, and Use Efficiency. Annu Rev Plant Biol. 69:27.1-27.38

Wanyama I, Pelster DE, Arias-Navarro C, Butterbach-Bahl K, Verchot LV, Rufino MC (2018) Management intensity controls soil N_2O fluxes in an Afromontane ecosystem. Sci Total Environ 624:769-780

Water Quality Association (2014) Nitrate/nitrite fact sheet. https://www.wqa.org/Portals/0/Technical/Technical%20Fact%20Sheets/2014_NitrateNitrite.pdf. Accessed 20 April 2018

Watson CJ, Kilpatrick DJ (1991) The effect of urea pellet size and rate of application on ammonia volatilization and soil-nitrogen dynamics. Fert Res 28:163-172

Werner C, Kiese R, Butterbach-Bahl K (2007) Soil-atmosphere exchange of N_2O, CH_4, and CO_2 and controlling environmental factors for tropical rain forest sites in western Kenya. J Geophys Res-Atmos. https://doi.org/10.1029/2006JD007388

Wetselaar R (1961) Nitrate distribution in tropical soils. Plant Soil 15: 110-120

Whitehead DC, Raistrick N (1993) The volatilization of ammonia from cattle urine applied to soils as influenced by soil properties. Plant Soil 148:43-51

Wortmann CS, Milner M, Kaizzi KC, Nouri M, Cyamweshi AR, Dicko MK, Kibunja CN, Macharia M, Maria R, Nalivata PC, Demissie N, Nkonde D, Ouattara K, Senkoro CJ, Tarfa BD, Tetteh FM (2017) Maize-nutrient response information applied across Sub-Saharan Africa. Nutr Cycl Agroecosys 107: 175-186

Wrage-Mönnig N, Horn MA, Well R, Müller C, Velthof G, Oenema O (2018) The role of nitrifier denitrification in the production of nitrous oxide revisited. Soil Biol Biochem 123:A3-A16

Wu F, Jia Z, Wang S, Chang SX, Startsev A (2012) Contrasting effects of wheat straw and its biochar on greenhouse gas emissions and enzyme activities in a Chernozemic soil. Biol Fert Soils 49:555-565

Xing GX, Zhu ZL (2000) An assessment of N loss from agricultural fields to the environment in China. Nutr Cycl Agroecosys 57:67-73

Xu G, Fan X, Miller AJ (2012) Plant nitrogen assimilation and use efficiency. Annu Rev Plant Biol 63:153-182

Yang X, Lu Y, Ding Y, Yin X, Raza S, Tong Y (2017) Optimising nitrogen fertilisation: A key to improving nitrogen-use efficiency and minimising nitrate leaching losses in an intensive wheat/maize rotation (2008–2014). Field Crop Res 206:1-10

Yao Y, Zhang M, Tian Y, Zhao M, Zhang B, Zhao M, Zeng K, Yin B (2018) Urea deep placement for minimizing NH_3 loss in an intensive rice cropping system. Field Crops Res 218:254-266

Zaman M, Nguyen ML, Blennerhassett JD, Quin BF (2008) Reducing NH_3, N_2O and NO_3^--N losses from a pasture soil with urease or nitrification inhibitors and elemental S-amended nitrogenous fertilizers. Biol Fert Soils 44: 693-705

Zantua MI, Bremner JM (1975) Preservation of soil samples for assay of urease activity. Soil Biol Biochem 7: 297-299

Zhang X, Davidson EA, Mauzerall DL, Searchinger TD, Dumas P, Shen Y (2015) Managing nitrogen for sustainable development. Nature 528:51-59

Zhao X, Nafziger ED, Pittelkow CM (2017) Nitrogen rate strategies for reducing yield-scaled nitrous oxide emissions in maize. Environ Res Lett. https://doi.org/10.1088/1748-9326/aa9007

Zheng J, Kilasara MM, Mmari WN, Funakawa S (2018a) Ammonia volatilization following urea application at maize fields in the East African highlands with different soil properties. Biol Fert Soils 54:411-422

Zheng J, Mmari WN, Nishigaki T, Kilasara MM, Funakawa S (2018b) Nitrogen availability to maize as affected by fertilizer application and soil type in the Tanzanian highlands. Nutr Cycl Agroecosys. https://doi.org/10.1007/s10705-018-9939-1

Zhou Y, Berruti F, Greenhalf C, Henry HAL (2017) Combined effects of biochar amendment, leguminous cover crop addition and snow removal on nitrogen leaching losses and nitrogen retention over winter and subsequent yield of a test crop (Eruca sativa L.). Soil Biol Biochem 114:220-228

Zhou Y, Zhang Y, Tian D, Mu Y (2017) The influence of straw returning on N_2O emissions from a maize-wheat field in the North China Plain. Sci Total Environ 584-585:935-941

Zingore S, Delve RJ, Nyamangara J, Giller KE (2007) Multiple benefits of manure: The key to maintenance of soil fertility and restoration of depleted sandy soils on African smallholder farms. Nutr Cycl Agroecosys 80: 267-282

Zomer RJ, Bossio DA, Sommer R, Verchot LV (2017) Global Sequestration Potential of Increased Organic Carbon in Cropland Soils. Sci Rep. https://doi.org/10.1038/s41598-017-15794-8

CURRICULUM VITAE

Jinsen Zheng

Born in 1990

jinsenzheng@gmail.com

❖ EDUCATION

- M.Sc. (2015) & Ph.D. (2019 expected) in Agriculture
    - Division of Environmental Science & Technology, Kyoto University, Japan
    - Program for Leading Graduate Schools (MEXT); GSS program at Kyoto University
    - G30 project
- B.Sc. in Physical Geography (2012)
    - School of Geographic and Oceanographic Sciences, Nanjing University, China
    - Short-term exchange (2010.08–2011.01) at Linkoping University, Sweden

❖ EMPLOYMENT

- Research assistant (2012.07–2013.03) at Nanjing Institute of Geography and Limnology, Chinese Academy of Sciences, China
- Research fellow (2018.03–present) at Graduate School of Global Environmental Studies, Kyoto University, Japan

❖ PUBLICATIONS

- **Zheng J**, Qu Y, Kilasara MM, Mmari WN, Funakawa S (In preparation) Nitrate leaching from critical root zone of maize in two tropical highlands of Tanzania: effects of fertilizer-nitrogen rate and straw incorporation
- **Zheng J**, Qu Y, Kilasara MM, Mmari WN, Funakawa S (In preparation) Soil-atmosphere exchange of nitrous oxide in two Tanzanian croplands: effects of nitrogen and straw management
- **Zheng J**, Kilasara MM, Mmari WN, Funakawa S (2018) Ammonia volatilization following urea application at maize fields in the East African highlands with different soil properties. *Biol Fert Soils* 54:411-422
- **Zheng J**, Mmari WN, Nishigaki T, Kilasara MM, Funakawa S (2018) Nitrogen availability to maize as affected by fertilizer application and soil type in the Tanzanian highlands. *Nutr Cycl Agroecosys*. https://doi.org/10.1007/s10705-018-9939-1 (in press)
- Li Q, Zhu Q, **Zheng J**, Liao K, Yang G, 2015. Soil moisture response to rainfall in forestland and vegetable plot in Taihu Lake Basin, China. *Chin Geogr Sci* 25:426–437
- Liao K, Xua F, **Zheng J**, Zhu Q, Yang G, 2014. Using different multimodel ensemble approaches to simulate soil moisture in a forest site with six traditional pedotransfer functions. *Environ Modell Softw* 57:27–32